

Confronting the instanton calculus in Yang-
Mills theories to the lattice

MORI SHINGO

Doctor of Philosophy

Department of Particle and Nuclear Physics
School of High Energy Accelerator Science
SOKENDAI (The Graduate University for
Advanced Studies)

Confronting the instanton calculus in Yang-Mills theories to the lattice

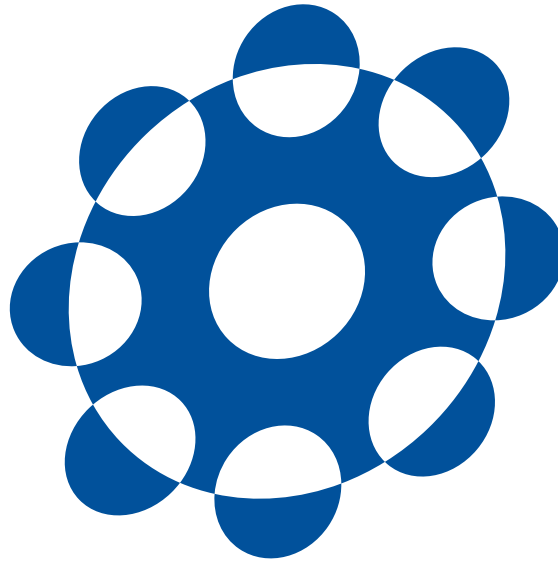
by

Shingo Mori

Dissertation

submitted to the Department of Particle and Nuclear Physics
in partial fulfillment of the requirements for the degree of

Doctor of Philosophy



SOKENDAI (The Graduate University for Advanced Studies)

December 8, 2017

Acknowledgments

I would like to thank my supervisors Ryuichiro Kitano and Norikazu Yamada for their scientific guidance, encouragement, and ideas that were invaluable for writing this thesis. I appreciate their kindness to have the study meeting about the “Abc’s of Instanton” [1]. Ryuichiro introduces me the nice project about the instanton and the lattice calculation. I always ask Norikazu many questions about the lattice calculation, e.g., the meaning of the parameters used in the HMC process, which are indispensable for me to perform the numerical simulation.

As well as them, I would like to acknowledge Julien Frison for the years-long collaboration and providing me a set of useful code for calculating the QCD topology on the lattice. I would also like to thank Hideo Matsufuru for coding the program of configuration generation in SU(2) Yang-Mills theory by modifying the original Bridge++ code, which provides me a good understanding of the usage of Bridge++ code.

These works are in part based on Bridge++ code (<http://bridge.kek.jp/Lattice-code/>).

I am deeply indebted to Sokendai for the full support to attend the Lattice conference held at Granada in 2017 and have a seminar at UCLouvain.

I would like to thank the many experts for discussing our work or asking the sharp questions or giving me some advice at the conferences: Yusuke Taniguchi, Hiroshi Suzuki, Shinji Ejiri, Shoji Hashimoto, Hidenori Fukaya, Takashi Kaneko, Naoki Yamamoto, Akira Ohnishi.

Apart from the project described in this thesis, Kaoru Hagiwara kindly introduced me the project about the search for the CP-violating Higgs coupling at LHC. He also gave me an opportunity to work using English with Ma Kai, and precious chance to go to Belgium for conveying the seminar and lunch with Michel Herquet, who bought me lasagna and gave me time for talking with me.

Yutaka Sakamura and Toru Goto often go out for dinner with me for the past five

years. I really enjoyed the dinner and talking with them.

Several students of Sokendai sometimes spend holiday with me to go fishing or skiing. I am indebted to Tomomi Sato for introducing me the fishing as a new hobby in summer and always go fishing with me; to Taro Mori for introducing me the skiing as a new winter hobby and always go fishing with me; to Ryuji Motono for inviting me to his house; to Katsumasa Nakayama for discussing the physics.

Abstract

The Standard Model (SM) in the elementary particle physics describes the fundamental physical law in nature and, in principle, provides us infinitely accurate predictions, which are consistent with most of the currently available experimental measurements. The CP is not a symmetry of the SM. The weak interaction has the source of the CP-violating effects, while there is no experimental indication for the CP violation in the electromagnetic interaction and the strong interaction. However, the QCD Lagrangian, in general, includes the CP-violating term $\theta F\tilde{F}$. The neutron electric dipole moment bounds $|\theta| \leq O(10^{-10})$, which mean that CP is a symmetry or an approximate symmetry of QCD. Also, due to the $U(1)_A$ rotation of the quark fields, the θ parameter is related to the phase of the quark mass. Thus the suppression of the CP-violating term is equivalent to the fine-tuning problem in the QCD Lagrangian without any reason, which is called the strong CP problem. There are several ways to solve this problem, which are realized within the SM or require some extension to the SM. The best-motivated solution is to deal with the coupling θ as a dynamical axion field $a(x)$, whose potential has a minimum at $\theta = 0$ due to the non-perturbative topological fluctuation of the gluon fields called the QCD instanton. The axion solution is attractive because it also provides a candidate for the dark matter of the universe through the misalignment mechanism for the axion generation.

The QCD topological susceptibility at high temperature, $\chi_t(T)$, provides an essential input for the estimate of the axion abundance in the present universe. Since the axion potential is induced by the fluctuation of the instanton, its mass is directly related to the topological fluctuation $\chi_t(T)$ which, in the path integral formalism, is dominated by the non-perturbative instanton configuration. The instanton gas approximation to the analytic calculation of $\chi_t(T)$ is applicable in the high-temperature limit and is not justified at the low temperature where the strong coupling is not small, for instance

at the temperature at which the axion starts to oscillate in the early universe. Although the model-independent determination of $\chi_t(T)$ should be possible from the first principles using lattice QCD, the existing method has a statistical disadvantage in the high-temperature region. This is not only because the probability for generating the configuration with non-trivial topological charge in the Monte-Carlo process decreases but also because the auto-correlation time increases. We propose a novel method to calculate the temperature dependence of topological susceptibility at high temperature. We test the feasibility of this method on a small lattice in the quenched approximation, and the results are compared to the prediction of the dilute instanton gas approximation. It is found that the method works well at a very high temperature and the result is consistent with the instanton calculus down to $T \sim 2T_c$ within the statistical uncertainty.

The instanton is the non-perturbative topological fluctuation of the gluon, which is physically essential not only as one of the sources of non-perturbative dynamics in QCD but also the foundation of the solutions for the strong CP problem. In spite of its relevance, the understanding of the role of the instanton based on the QCD Lagrangian is still poor since it is based on the semi-classical approximation and the notorious infrared divergence happens at zero temperature. Only at high temperature, the instanton picture is applicable. In the $SU(N)$ Yang-Mills theory, the topological susceptibility $\chi_t(T)$ at high temperature is numerically consistent with the instanton calculus. However, we need more precise information to conclude the instanton calculus determines non-perturbative dynamics related to the topology. Also, it is still unclear that this picture applies the local observables, by which the information of the instanton density $n(\rho)$ can be extracted. Besides, it is also unclear that how the picture disappears as temperature decreases. To better understand the role played by the instantons behind the QCD topology, we investigate the instanton contribution to the gluonic two-point correlation functions in the $SU(N)$ Yang-Mills theory to explore the distribution of the instanton size. The CP-violating gluonic correlator is an excellent laboratory to investigate the instanton effects in the local observable, since, in the lattice calculation, the instanton contribution would dominate the perturbative contribution. In this work, the pseudoscalar-scalar gluonic correlation functions are calculated on the lattice at various temperatures and compared with the instanton calculus. In the semi-classical instanton calculus, we use the regularized thermal instanton to avoid the singularity at the instanton position in the usual thermal instanton. In the lattice calculation, we

use the gradient flow with large flow time to reduce the quantum fluctuation around the classical solution. Under the procedure, the instanton size is untouched since the gradient flow does not change the classical solution. Then, the instanton-size distribution $n(\rho)$ generated by the Monte-Carlo process survives even after the large flow time. Comparing the numerical and analytic calculation, we find at high temperature the CP-violating correlator calculated on lattice behaves consistently with the semi-classical calculation in the single instanton background. At low temperature, we find the larger size instanton dominate than what the instanton calculus predicts.

Contents

1	Introduction	1
2	The strong CP problem and the axion solution	11
2.1	QCD Lagrangian	11
2.2	The strong CP problem and its solutions	12
2.3	The axion solution	14
3	QCD instanton	19
3.1	The instanton in the quantum mechanics	19
3.1.1	The harmonic-oscillator type potential	22
3.1.2	The double-well type potential	23
3.2	The instanton in the Yang-Mills theory	30
3.2.1	θ vacuum	30
3.2.2	Instanton action	32
3.2.3	BPST instanton	33
3.2.4	The singular solution and 't Hooft ansatz	36
3.2.5	Harrington-Sheperd caloron	40
3.3	Yang-Mills instanton density at zero and finite temperature	42
3.3.1	Background field method	42
3.3.2	Treatment for the collective coordinate	46
3.3.3	The collective coordinates of the Yang-Mills instanton	48
3.3.4	Calculation of the Yang-Mills instanton density	52
3.3.5	Calculation of $J(\gamma)$ in the semi-classical approximation	53
3.3.6	Calculation of $\Gamma^A + \Gamma^{\text{gh}}$	55
3.3.7	Calculation of Γ^F	57

3.3.8	The Yang-Mills instanton density at zero temperature	59
3.3.9	The finite temperature correction	60
3.4	The calculation of the topological susceptibility at finite temperature	61
3.5	The calculation of the gluon correlator at zero temperature	62
3.5.1	The result in SU(2) Yang-Mills theory	62
3.5.2	The result of SU(3) YM theory	64
4	Lattice field theory	69
4.1	gauge actions on lattice	70
4.2	The fermion action and the topology fixing term	73
4.3	The partition functions on lattice	74
5	Topological susceptibility at high temperature on the lattice	77
5.1	Method	77
5.1.1	high temperature limit	81
5.2	test in the quenched approximation	83
5.2.1	lattice setup	83
5.2.2	numerical results	85
5.3	summary and future prospects	87
6	Instanton effects on CP-violating gluonic correlators	93
6.1	Instanton calculus	93
6.2	Simulation setup	101
6.3	Gradient flow with large flow time	102
6.4	CP violating correlation function in the $Q = 1$ sector	104
6.5	Summary and outlook	106
7	Conclusion	107
Appendix A	Appendix	111
A.1	Notations in Minkowski space and Euclidean space	111
A.2	Thermal field theory	113
Bibliography		115

1

Introduction

The Standard Model describes the most of the experimental results consistently and gives in principle infinitely precise predictions. However, it is still far from the ultimate theory of nature. Actually, it is confronting many problems in both theoretical and phenomenological issues. In the Standard Model, QCD is the theory describing the strong interaction among the quarks and the gluons which compose the mesons or the nucleons. QCD involves many interesting physical issues which cannot be controlled by the perturbation, e.g., the confinement/deconfinement transition, the restoration of chiral symmetry and $U(1)_A$ symmetry. In particular, our interests are in the structure of the θ -vacuum of QCD and on the role played by the topological gluon fluctuation so-called instanton. We will focus on the theoretical difficulties in QCD such as the fine-tuning problem, and the poorly understood role of the instanton. As a tool to investigate the non-perturbative regime directly, the numerical simulation based on the lattice gauge theory is powerful and provides us with crucial hints to interpret the dynamics.

The θ -vacuum is a superposition of the degenerate zero-energy states $|n\rangle$ which are characterized by an integer winding number n . The discrete translational symmetry

along the direction of the winding number determines the θ -vacuum as a Bloch state $|\theta\rangle = \sum_n e^{in\theta} |n\rangle$ with a vacuum angle θ . The QCD instanton effects appear as a tunneling path from one zero-energy states with winding number n_i to the other with n_f . The topological charge Q is the difference between the winding numbers, $Q = n_f - n_i$. Thus, the instanton is associated with the construction of the θ -vacuum. Moreover, the instanton effects appear not only in the non-perturbative dynamics in QCD but also in the phenomenology beyond the Standard Model.

Although in the Hamiltonian formalism the physical interpretation of the vacuum angle θ and the instanton is transparent, from the viewpoint of the field theory we usually adopt the Lagrangian formalism based on the path integral. In the Lagrangian formalism, the vacuum angle appears in the QCD Lagrangian as the θ -term, $\theta F_{\mu\nu}^a \tilde{F}_{\mu\nu}^a$. This is the renormalizable and gauge-invariant operator and hence in the construction of the Lagrangian we cannot miss this term. Before the discovery of the instanton, it has been considered that such term does not affect the physics since it can be written as the total derivative, $F_{\mu\nu}^a \tilde{F}_{\mu\nu}^a = \partial_\mu K_\mu$, using the Chern-Simon current K_μ . The instanton makes $F_{\mu\nu}^a \tilde{F}_{\mu\nu}^a$ non-vanishing. In the QCD Lagrangian, θ -term violates the P and CP symmetry other than the case of $\theta = 0$ or π . The existence of the instanton solution suggests that this term may not vanish.

The instanton solution is related to the long-standing puzzle in the Standard Model. As it is well known, neither the P nor CP symmetry is preserved in nature. Although at the level of the classical electromagnetism and special relativity those symmetries are preserved, in more fundamental physics both of them are violated. For example, only the left-handed neutrino is observed in any experiments, which means the maximal P violation in our world. The CP-violation has also been observed in the neutral Kaon system that can be understood now as the effects of the complex phase in the Cabbibo-Kobayashi-Masukawa matrix. The mixing and phase in the CKM matrix appears in the vertex of the weak interaction of the quarks. On the other hand, CP is extremely well preserved under the strong interaction. The current experimental upper bound of the electric dipole moment of the neutron means that QCD Lagrangian has CP symmetry or approximate CP symmetry. This is quite non-trivial and may require an explanation for the physics beyond the Standard Model. Although there is no reason to drop the renormalizable CP violating term, $\theta F_{\mu\nu}^a \tilde{F}_{\mu\nu}^a$, in the QCD Lagrangian, the results of the current experiments put the strong bound, $\theta < \mathcal{O}(10^{-12})$. The experimental constraint is actually put on the $\bar{\theta}$ parameter that is a combination of $\theta + \arg(\det M)$ where M

is the quark mass matrix. It is quite puzzling since the phase in CKM matrix is non-vanishing while $\bar{\theta}$ is suppressed at least by $O(10^{-12})$. This puzzle is called the strong CP problem.

There are two classes of solutions to the strong CP problem either within the framework of the standard model or by introducing the new physics. The first one is the possibility to accept massless up quark so that the θ parameter can be rotated out by a $U(1)_A$ transformation and hence θ is unphysical. The fact that the up quark mass is a non-observable makes the situation confusing. Within the multiplicative renormalization given by the perturbation, once one assumes that the up quark is massless at some scale, it must be massless in any scale. However, the so-called the 't Hooft vertex induced by the instanton effects induces an additive shift to the quark mass. This non-perturbative contribution makes the relation $m_u = 0$ scale dependent. One needs full non-perturbative treatment such as lattice QCD for understanding the possibility. The state of art estimation of the up quark mass by lattice QCD strongly disfavors the massless up quark although there are still active discussion on the possible theoretical uncertainties in the lattice results.

The second solution is to introduce the axion field coupling to $F_{\mu\nu}^a \tilde{F}_{\mu\nu}^a$ [2, 3, 4, 5, 6, 7, 8, 9]. Such a model can be realized by spontaneous breaking of the $U(1)$ Peccei-Quinn symmetry, where the axion appears at low energy as the NG boson. In this hypothesis, the θ parameter is interpreted as a dynamical axion field a/f_a , which automatically selects the CP symmetric vacuum through a non-perturbatively generated potential $\chi_t(1 - \cos a/f_a)$, where χ_t is the topological susceptibility.

The PQ mechanism is attractive because it also provides a candidate for the dark matter of the Universe through the misalignment mechanism for the axion generation [10, 11, 12]. Two ingredients determine the axion abundance of the present Universe: the axion mass as a function of T , $m_a(T)$, and the initial misalignment angle θ' . The square of axion mass is derived by the second derivative of the partition function in terms of the axion field, which is equivalent to the definition of the topological susceptibility. In this manner, the problem of the axion dynamics is converted into the problem of the non-perturbative dynamics in the QCD Lagrangian at finite temperature. Further details about the axion and its abundance are elucidated in chap. 2.

Here, we briefly introduce the instanton solution of the $SU(2)$ Yang-Mills theory. By embedding this solution to $SU(N)$ matrices and applying some gauge rotations, we can construct the instanton solution in the $SU(N)$ gauge group ($N > 2$). The instanton

is the solution of the equation of motion of the Euclidean Yang-Mills action (the Yang-Mills equation).

To obtain the stationary solution which may have a dominant contribution to the partition function, the gauge action should be finite. The necessary condition is to consider gauge fields which have the vanishing energy-momentum tensor at spatial infinity. In other words, at the spatial infinity, the gauge field should take the pure gauge form, $\lim_{|x| \rightarrow \infty} A_\mu(x) = g^{-1}(\vec{e})\partial_\mu g(\vec{e})$, where \vec{e} is the unit vector parallels to the vector \vec{x} and the element of the three-dimensional space S^3 and $g(\vec{e}) \in \text{SU}(2)$. Then this is a mapping from S^3 to the gauge group $\text{SU}(2)$, That is equivalent to a mapping of $S^3 \rightarrow S^3$, which can be divided into a set of homotopy classes. Using the boundary condition at the spatial infinity and the spherically symmetric and regular ansatz, the BPST instanton solution is derived [13]. At finite temperature, the existence of the instanton solution is proved in parallel to the above. The only difference is the topology at the spatial infinity: the finite temperature theory is on $S^3 \times S^1$. The thermal instanton is constructed as a multi-instanton configuration in which the instantons stand in a queue along the imaginary time direction with an equal interval [14]. The instanton is a classical solution of the Euclidean $\text{SU}(N)$ Yang-Mills theory and is known as the BPST instanton [13]. At finite temperatures, i.e., with a compactified time direction, there are known solutions such as the HS caloron for a trivial holonomy [14] and the KvBLL caloron for a non-trivial holonomy [15, 16, 17].

The instanton density, $n(\rho)$, describes the contribution to the partition function from the instanton with a size ρ . It is obtained by an the functional integral associated with the instanton saddle point in the semi-classical approximation. To obtain an expectation value of an operator around one instanton background, we apply the instanton density as a weight. The instanton size ρ is a non-compact collective coordinate and hence integrated over all possible size in the path integral with the weight $n(\rho)$, which leads to the infrared divergence. To obtain a meaningful result, we need to introduce an IR cutoff in the instanton size integration. At zero temperature, the natural way is considering the theory with a finite volume V_4 , in which the instanton size is smaller than the scale $V_4^{1/4}$ [18]. Apart from that, a Higgs field which acquires a vev at high scale introduces the natural cutoff. In this situation, the gauge boson mass introduces a new scale [19] keeping the strong coupling small, which justifies the semi-classical approximation. Unfortunately, in QCD instanton calculation at zero temperature, no such natural cutoff exist. Even if we admit the ad-hoc cutoff by hand,

e.g., the dynamical scale Λ , the coupling constant becomes large, then we can no longer justify the semi-classical approximation.

In the computation based on the BPST instanton, one often encounters the IR divergences in the integration over the instanton size ρ . This problem disappears at finite temperatures; the Debye screening effectively introduces the cutoff on the size of the instantons at $\rho \sim 1/T$, making all physical quantities IR finite. Especially, when the temperature is high enough, the interactions among instantons are expected to be neglected, and the dilute instanton gas approximation (DIGA) seems to work well.

At finite temperature, the temperature introduces a cutoff which is a dynamical consequence of an electric screening [20]. Although the classical instanton action $S_{\text{cl}} = 8\pi^2/g^2$ is independent of the instanton size, the quantum effects produce the cutoff at scale $\rho_{\text{cut}} \sim 1/\pi T$. At high temperature the typical instanton size is small, and hence the overlap or the interaction between the instantons are negligible. To obtain the instanton prediction to the observables in θ -vacuum, we need to sum up the expectation value of the operator in all topological charge sector. However, the multi-instanton solutions at finite temperature are rather complicated, and the calculation of the background field method cannot be done exactly. In the DIGA where the instanton size is much smaller than the typical spacing between the instantons, we can use the unit (anti-)instanton sector as building blocks to represent the sector of general topological charge Q . In this limit, the θ -dependence of the partition function of the finite temperature Yang-Mills gas is calculated as $Z_\theta = \exp(-(1/2)V_4\chi_t(T)(1 - \cos\theta))$, where V_4 is the four-volume [21, 14]. The topological susceptibility $\chi_t(T)$ can also be calculated in this limit. As a consequence its temperature dependence is obtained at the 1-loop level as $T^{-(11N/3-4)}$ for the $SU(N)$ pure Yang-Mills theory and T^{-8} for three-flavor QCD. In the above situation, the instanton configurations and the small quantum fluctuation around them dominate the path integrals. In such a case, the instanton picture makes sense. Further details about the instanton and the semi-classical calculation will be reviewed in chap. 3.

In the estimate of the axion abundance of the Universe, the instanton picture is widely adopted [19]. The relevant temperature range for the axion abundance is $T^* \sim O(1)$ GeV which is about a factor of six higher than the critical temperature for the chiral symmetry breaking $T_c \sim 150$ MeV [22, 20, 23]. However, the instanton calculus hinges on the perturbation theory, and hence the reliability is not very clear around $T \lesssim 1$ GeV. Furthermore, the possibility that, in two-flavor QCD, χ_t behaves like a

step function at $T = T_c$ when the quarks are sufficiently light is discussed based on reasonable assumptions [24, 25] (see also a clarification in Ref. [26]). In such a case, a significant enhancement of the axion abundance is predicted and even excludes the standard axion scenario if the initial misalignment angle is $O(1)$ [27].

To deal with the non-Abelian gauge theory in the non-perturbative regime, the lattice approximation is a powerful approach to evaluate the path integral in the gauge invariant manner. In this method, the observables are approximated by the gauge invariant theory with the finite lattice spacing a and the finite volume V_4 of the Euclidean space-time. In addition, the observables calculated by the path integral in terms of the field configuration is approximated by the ensemble average of the field configuration which is generated by the Monte-Carlo algorithm with a weight of the lattice action. Taking the continuum and the infinite volume limit as well as using an infinite number of the configurations, the numerical simulation of lattice QCD in principle can unambiguously determine the physical quantities such as the topological susceptibility or the gluon correlators. Further details on the lattice action and the configuration generations are reviewed in chap. 4.

The topological susceptibility multiplied by the four-volume $\chi_t V_4$ is by definition written as the variation of the topological charge $\langle Q^2 \rangle$. It is well measured at zero temperature, while at high temperature it becomes statistically challenging. Since the topological susceptibility rapidly decreases as temperature increases, the fluctuation of the topological charge becomes small, and hence the configurations with large $|Q|$ becomes rare. In addition to the smallness of the fluctuation, at high temperature, the change of Q during the update of the configuration also hardly occurs, which requires a much longer interval of trajectories to reduce the auto-correlation between the configurations. Due to these two problems, it is practically challenging to measure the susceptibility at high temperature.

The numerical simulations of the lattice QCD can unambiguously determine $\chi_t(T)$ in principle. The studies of χ_t at high temperature like $\sim 2T_c$ or higher have been begun in the $SU(3)$ Yang-Mills theory [28, 27, 29]. Recently, the full QCD results were reported [30, 31]. Several remarks are as follows. First, the lattice calculations of $\chi_t(T)$ in the $SU(3)$ Yang-Mills theory shows $\chi_t(T) \sim T^{-X}$ with $5.6 \lesssim X \lesssim 7.14$, which is compatible with $X \sim 7$ in the instanton calculus [22, 20, 23]. Secondly, one of the full QCD calculations in Ref. [30] finds $X \sim 3$, which disagrees with $X \sim 8$ in the instanton calculus, while $X \sim 8$ is reported in Ref. [31]. Thirdly, $\langle Q^2 \rangle|_T = \chi_t(T) V_4$ rapidly decreases

with T , where V_4 represents the four-dimensional volume, and importantly existing lattice methods fail when $\chi_t(T)V_4 \ll 1$ ¹. Since $\chi_t(T)V_4 \ll 1$ is realized above a certain temperature, the axion abundance becomes uncertain. Thus, methods overcoming this difficulty are desired.

To be specific, in Ref. [27], where $\chi_t(T)$ is calculated on $16^3 \times 4$ lattices in the quenched approximation with one of the standard methods counting the fermionic zero modes, $\chi_t(T)V_4$ is estimated to be 0.35, 0.09, 0.03 at $T = 1.34 T_c, 1.5 T_c, 1.75 T_c$, respectively, and no reliable estimate is given above $2 T_c$.

In chap. 5, we propose a novel method to measure the temperature dependence of $\chi_t(T)$ which especially works at high temperature. This method enables us to obtain not $\chi_t(T)$ itself but the power behavior $d \ln \chi_t(T)/d \ln T$ by estimating the difference of the gauge action and the chiral condensate between two distinct topological charge sectors. We examined this method on a small lattice in the quenched approximation and compared the results with the prediction from the DIGA.

In the above mentioned study, we have calculated the DIGA of the global observable such as the topological susceptibility. On the other hand, it is still unclear whether the instanton picture also applies to the local observables. By observing the local structure and comparing with DIGA, we will be able to read off information of $n(\rho)$. In ref. [33] and the references therein, the gluonic two-point correlation functions, i.e. $\langle Tq(x)q(0) \rangle$ or $\langle Ts(x)s(0) \rangle$, have been calculated, where $q(x) = (1/4)F_{\mu\nu}^a \tilde{F}_{\mu\nu}^a$ and $s(x) = (g^2/32\pi^2)F_{\mu\nu}^a F_{\mu\nu}^a$ at zero temperature in several phenomenological instanton models. In these models, the instanton density is modified so that the correlator becomes IR finite. The instanton-size ρ dependencies are based on the DIGA or the instanton liquid model. At zero temperature QCD, there are the perturbative contributions to these correlators, which may overwhelm the instanton contribution to the path integral.

Recently, Dine *et. al.* [34] have pointed out that in the SU(2) Yang-Mills theory the 2-pt gluonic correlator in one instanton background is IR finite without introducing the ad-hoc IR cutoff. This is interesting because one of the reasons for the breakdown of the instanton picture at zero temperature is the notorious IR divergence which makes the instanton calculus ill-defined.

On top of that, the CP-violating correlator is free from the perturbative contribution, so that the instanton can provide the leading contribution. If we choose the gluon

¹An interesting proposal to avoid this difficulty is found in Ref. [32].

correlator which does not preserve CP symmetry, the contribution to the path integral is limited to the topologically non-trivial ones. Hence the instanton contribution enhances the path integral. Thus, we expect that the lattice simulation on CP-violating correlator provides us the good laboratory to investigate the instanton picture. We expect that the following points can be clarified. First, it is not clear whether or not the instanton picture applies to the local observable. Second, there might be a special case where the picture makes sense even at zero temperature. If we choose the specific combination of observables and the number of colors and the number of fermions, surprisingly the instanton calculus becomes IR finite even at zero temperature. Third, it is unclear how low temperature the instanton picture applies and how it disappears as decreasing temperature. Although at the high-temperature limit the instanton picture applies to the topological susceptibility in the pure Yang-Mills theory, there is still a tension about how low temperature the instanton picture makes sense.

In chap. 6, we try to clarify the first and third points using the CP-violating gluon correlator $\langle s(x)q(0) \rangle$ in the SU(2) pure Yang-Mills theory at finite temperature. The SU(2) Yang-Mills theory is particularly interesting because the semi-classical estimation of the two-point function $\langle F_{\mu\nu}^a F_{\mu\nu}^a(x) F_{\mu\nu}^b F_{\mu\nu}^b(0) \rangle$ remains IR finite in the ρ integration even at zero temperatures [34]. First, we performed the instanton calculus of this local observable in the one instanton background, where the instanton configuration is transformed into the regular thermal instanton solution from the existing singular one. Then, we carried out the numerical simulation of the lattice using the quenched SU(2) lattice action. The CP-violating gluon correlator is calculated on the lattice at various temperatures, both below and above the critical temperature T_c of the confinement/deconfinement transition. In this numerical analysis, we employ the gradient flow method as not only the smearing of the configurations but also conserving the information of the classical instanton. In order to test the instanton picture at various temperatures, we compared the results of the analytic and numerical calculations.

We organize the thesis as follows. In chap. 2, we will review the axion solution of the Strong CP problem. In chap. 3, some fundamental pieces of the instanton calculus are reviewed. In chap. 4, we will review the lattice gauge theory and the topological charge defined on the lattice and the configuration generation. After the above review parts, in chap. 5 we will show the novel method to obtain the temperature dependence of $\chi_t(T)$ and the numerical test using the lattice simulation of the quenched approximation. In chap. 6, the CP-violating correlator is investigated in order to measure the

instanton size distribution from the numerical result at high temperature.

2

The strong CP problem and the axion solution

We review the topological property of QCD and the strong CP problem. For further reviews see [35, 36, 37, 38, 23].

2.1 QCD Lagrangian

In the four-dimensional Euclidean space, the action of the $SU(N_c)$ gauge theory with N_f -fermion is given as

$$S_{\text{QCD}} = \int d^4x \left[\frac{1}{4g^2} F_{\mu\nu}^a F_{\mu\nu}^a + \frac{i\theta}{64\pi^2} \epsilon_{\mu\nu\alpha\beta} F_{\mu\nu}^a F_{\alpha\beta}^a + \bar{\psi}^\alpha (\not{D} + M)^{\alpha\beta} \psi^\beta \right], \quad (2.1)$$

$$\equiv \int d^4x \mathcal{L}_{\text{QCD}},$$

$$F_{\mu\nu}^a = \partial_\mu A_\nu^a - \partial_\nu A_\mu^a + f^{abc} A_\mu^b A_\nu^c, \quad (2.2)$$

$$D_\mu \psi^\alpha = (\partial_\mu + iA_\mu^a T^a) \psi^\alpha, \quad (2.3)$$

where A_μ^a ($a = 1 \cdots N_c^2 - 1$) is the gauge field and ψ^α is the fermion of the fundamental representation of $SU(N_c)$. The Greek indices $\alpha, \beta (= 1, \cdots, N_f)$ represent the flavor of the quarks. Then the mass matrix M is the $N_f \times N_f$ matrix. The matrix T^a ($a = 1 \cdots N_c^2 - 1$) is the $SU(N_c)$ generator. The anti-symmetric tensor f^{abc} is defined as $[T^a, T^b] = 2f^{abc}T^c$. $\epsilon_{\mu\nu\rho\sigma}$ is also the anti-symmetric tensor with $\epsilon_{1234} = 1$. We adopt the Feynman's slash notation for the covariant derivative

$$\not{D} \equiv D_\mu \gamma_\mu, \quad (2.4)$$

where γ_μ is the gamma matrices in the Euclidean space with relations

$$\{\gamma_\mu, \gamma_\nu\} = 2\delta_{\mu\nu}. \quad (2.5)$$

In section A.1, we will clarify the relations of the four-vector and the gamma matrices in our notation in between the Euclidean space and the Minkowski space.

The partition function of the action with non-zero θ in path integral formalism is written as

$$Z_\theta = \int [dA][d\psi_f][d\bar{\psi}_f] e^{-S_{\text{QCD}}}. \quad (2.6)$$

The expectation value of a physical observable \mathcal{O} in this theory is

$$\langle \mathcal{O} \rangle_\theta = \frac{1}{Z_\theta} \int [dA][d\psi_f][d\bar{\psi}_f] \mathcal{O} e^{-S_{\text{QCD}}}. \quad (2.7)$$

2.2 The strong CP problem and its solutions

The QCD Lagrangian can contain four-dimensional and gauge invariant term, called θ term,

$$\mathcal{L}_\theta = \frac{i\theta}{64\pi^2} \epsilon_{\mu\nu\alpha\beta} F_{\mu\nu}^a F_{\alpha\beta}^a. \quad (2.8)$$

The θ term violates the P and CP symmetries. Due to the existence of the instanton¹ configuration for providing non-zero value of $\text{tr} F\tilde{F}$, this term can non-trivially con-

¹The instanton will be explained in chap. 3

tribute to the path integral.

Suppose we perform a $U(1)_A$ transformation to the quark field q with a mass m_q as $q \rightarrow e^{i\gamma_5\alpha} q$, the mass term changes as

$$m_q \bar{q} q \rightarrow m_q \bar{q} e^{2i\gamma_5\alpha} q + (2\alpha) \frac{i}{64\pi^2} \epsilon_{\mu\nu\alpha\beta} F_{\mu\nu}^a F_{\alpha\beta}^a. \quad (2.9)$$

The last term $\epsilon_{\mu\nu\alpha\beta} F_{\mu\nu}^a F_{\alpha\beta}^a$ comes from the anomalous breaking of the $U(1)_A$ symmetry. Thus, the $U(1)_A$ rotation of the quark fields shifts the θ term. This rotation removes the imaginary part of the quark mass which has another CP violating contribution. In the QCD Lagrangian (eq. 2.1), we can remove the imaginary part of the mass matrix M by the $U(1)_A$ rotation. Then, the θ parameter changes as

$$\theta \rightarrow \bar{\theta} \equiv \theta + \text{Arg det } M. \quad (2.10)$$

Then, all the CP violating effects comes from the parameter $\bar{\theta}$.

If QCD has non-zero $\bar{\theta}$ value, the CP violating observables can be non-vanishing. The neutron electric dipole moment (nEDM) is the most sensitive to the $\bar{\theta}$ parameter as

$$d_n \simeq \frac{e\bar{\theta}m_q}{m_N^2}. \quad (2.11)$$

However, the current experiment to measure the nEDM has not observed the sign of the CP violation and imposes the strong upper bound $|d_n| \leq 0.30 \times 10^{-25} e \text{ cm}$ [39], which corresponds $|\theta| \leq 10^{-10}$.

The small or vanishing $\bar{\theta}$ means that, in the QCD Lagrangian, two independent parameters, i.e., θ and the imaginary part of the quark mass $\text{Arg det } M$, cancel each other. This is the fine-tuning problem, called the strong CP problem.

One possible solution to the strong CP problem within the framework of the standard model is to consider the massless up quark. If the up quark is massless, we can perform a $U(1)_A$ transformation of the up quark field so that the $\bar{\theta}$ parameter is shifted away. However, the lattice calculation by Fodor *et al.* [40] have determined $m_u = 2.27 \text{ MeV}$ in the $\overline{\text{MS}}$ scheme at 2 GeV. This result excludes the $m_u = 0$ solution by more than 24 standard deviations.

However, the condition $m_u = 0$ is not renormalization invariant, because of the

non-perturbative contribution, namely the t' Hooft vertex provides up quark mass for the chiral perturbation.[41, 34, 42, 43] Even if $m_u = 0$ is satisfied at some scale, it is not guaranteed on other scales. Recently, Frison *et al.* [44] propose to use the physical quantity, the topological susceptibility χ_t , instead of a non-observable parameter m_u .

2.3 The axion solution

A solution to the strong CP problem is to apply the Peccei-Quinn mechanism. In this mechanism, we introduce an additional $U(1)_{\text{PQ}}$ symmetry which is spontaneously broken at high energy f_{PQ} . If the quarks respect the symmetry, the transformation by angle α_{PQ} as $q \rightarrow qe^{i\alpha_{\text{PQ}}}$ shifts the $\bar{\theta}$ parameter as

$$\bar{\theta} \rightarrow \bar{\theta} + 2\alpha_{\text{PQ}}. \quad (2.12)$$

Thus, as the $m_u = 0$ solution, we can rotate away the $\bar{\theta}$ parameter and the strong CP problem is gone.

To introduce the anomalous additional $U(1)_{\text{PQ}}$ symmetry, Peccei and Quinn [2] consider the two Higgs doublet model as

$$\begin{aligned} \mathcal{L} = & -\bar{Q}u_R H_u - \bar{Q}d_R H_d - V(H_u, H_d) + \text{h.c.} \\ & - \frac{i\theta}{64\pi^2} \epsilon_{\mu\nu\alpha\beta} F_{\mu\nu}^a F_{\alpha\beta}^a, \end{aligned} \quad (2.13)$$

where $V(H_u, H_d)$ is the Higgs potential and $Q = (u_L, d_L)^T$ is the $SU(2)_L$ -doublet of the left-handed quarks. H_u and H_d is the $SU(2)_L$ -doublet complex scalar fields with the hypercharge $Y = 1/2$ and $Y = -1/2$, respectively. They introduce $U(1)_{\text{PQ}}$ symmetry as

$$H_{u,d} \rightarrow e^{i\alpha} H_{u,d}, \quad (2.14)$$

$$u_R \rightarrow e^{-i\alpha} u_R, \quad (2.15)$$

$$d_R \rightarrow e^{-i\alpha} d_R. \quad (2.16)$$

This is the classical symmetry of the Lagrangian, while at the quantum level $U(1)_{\text{PQ}}$ -QCD anomaly breaks the symmetry. Then, the above rotation by an angle α shifts the

θ term as

$$\bar{\theta} \rightarrow \bar{\theta} - 2N_g\alpha, \quad (2.17)$$

where N_g is the number of the generations of the quarks. By the PQ rotation, $\bar{\theta}$ can be shifted away, so that $\bar{\theta}$ is unphysical.

Under the $U(1)_{\text{PQ}}$ transformation, the angular component of the Higgs fields called the axion field a shifts $a \rightarrow a + \text{const.}$ that corresponds to the Nambu-Goldstone boson of the spontaneous breaking of $U(1)_{\text{PQ}}$ [4, 45]. In the original paper, the $U(1)_{\text{PQ}}$ symmetry is broken at weak scale. We call the resulting axion as the Peccei-Quinn-Weinberg-Wilczek (PQWW) axion,

$$a = \frac{\sqrt{2}v_u v_d}{\sqrt{v_u^2 + v_d^2}} (\arg H_u + \arg H_d), \quad (2.18)$$

$$f_a = \frac{2\sqrt{2}v_u v_d}{\sqrt{v_u^2 + v_d^2}}, \quad (2.19)$$

where v_u and v_d is the VEV of H_u and H_d , respectively. The axion couples to the QCD topological charge, whose couplings are suppressed by the scale f_a due to the axion-gluon-gluon anomalous coupling,

$$\mathcal{L} = \left(\frac{a}{f_a} - \bar{\theta} \right) \frac{i}{64\pi^2} \epsilon_{\mu\nu\alpha\beta} F_{\mu\nu}^a F_{\alpha\beta}^a. \quad (2.20)$$

Such coupling allows the CP-violating parameter $\bar{\theta}$ redefined away via a shift of the axion field, and the non-perturbative effects provides the potential for the CP-conserving vacuum [46],²

$$\frac{\langle a \rangle}{f_a} - \bar{\theta} = 0. \quad (2.21)$$

The coupling f_a is the quantity that enters into the low-energy observables [48]. In general, the light boson has the couplings to the other SM particles through the inter-

² The weak CP violation shifts θ a little, i.e., $\theta \sim O(10^{-7})$ [47].

action Lagrangian,

$$\mathcal{L} = \frac{1}{f_a} J_\mu \partial_\mu a, \quad (2.22)$$

where J_μ is the Nöether current of the PQ symmetry.

The axion mass comes from the second derivative of the effective potential in terms of the axion field, which is calculated as

$$m_a^2 = \frac{\delta^2}{\delta a^2} \ln Z \left[\frac{a}{f_a} \right] \Big|_{a=0} = \frac{1}{f_a^2} \frac{d^2}{d\theta^2} \ln Z[\theta] \Big|_{\theta=0} = \frac{\chi_t}{f_a^2}. \quad (2.23)$$

Thus, the topological susceptibility χ_t is related to the square of the axion mass. At zero temperature, the axion mass is calculated using the chiral perturbation theory [49, 4] as

$$m_a = \frac{N_g \sqrt{m_u m_d} f_\pi}{m_u + m_d} m_\pi \sim O(100) \text{ keV}. \quad (2.24)$$

The axion mass in the large N limit is studied in Ref. [50].

Since the axion interacts with the SM particles in eq. 2.22, the axion should be produced for example in the stars and also in the K meson decays. Soon after the proposal of the PQWW axion, the axion was found to be too heavy for avoiding the existing experimental bounds [51, 52, 53, 54].

If the scale of the PQ symmetry breaking is much higher than the weak scale [6, 7, 8, 9], the axion becomes lighter than the PQWW axion and become acceptable to the experimental bounds. Such a light axion model is called as the invisible axion. For the detail of the invisible axion models, see the reviews [38, 37, 35] and the references therein.

The experimentally allowed region of the parameter space of the axion models is called the axion window,

$$10^9 \text{ GeV} \leq f_a \leq 10^{12} \text{ GeV}. \quad (2.25)$$

The lower bound of the decay constant comes from the astrophysical phenomena. The axion production processes carry away the energy of the stars. The coupling ($1/f_a$) should be small so that the energy loss of the stars is the acceptable amount.

On the other hand, the upper bound of the decay constant denotes the cosmological constraint [10, 11, 12]. During the evolution of the universe, eventually, the axion decouples and starts to oscillate coherently. Unless the coupling $1/f_a$ is large enough, the energy density of the axion exceeds the critical density of the universe. For the further detail, see the reference [55].

The axion can be a candidate for the dark matter in the universe. Here, we discuss that the axion with the acceptable decay constant naturally explains the dark matter abundance. Suppose the axion is produced before the end of the inflation, the initial angle is arbitrarily set in the causally connected regions. Later, the inflation starts and stretches the region, then the misalignment angle prevails. The evolution of the axion energy density is determined by the equation of motion of the coherent axion field,

$$\ddot{a} + 3H(T)\dot{a} = -m_a^2(T)a. \quad (2.26)$$

where $H(T)$ is the Hubble parameter and $m_a(T)$ is the axion mass at a temperature T . The axion mass $m_a(T)$ relates to the topological susceptibility as in eq. 2.23. The energy density $\rho_a(T)$ of the axion at present is determined by the amplitude $a(T_*)$ at which the axion starts to oscillate, i.e., $m_a(T_*) \simeq 3H(T_*)$.

Assuming the temperature dependence of the axion mass is determined by the dilute instanton gas approximation (DIGA)³, it behaves as $m_a(T) \propto T^{-4}$. Using the Hubble parameter $H(T) \sim T^2/M_{\text{Pl}}$, we can obtain T_* as

$$T_* \simeq O(1) \text{ GeV} \cdot \left(\frac{m_a}{10^{-5} \text{ eV}} \right)^{1/6}. \quad (2.27)$$

With the acceptable decay constant $f_a \sim 6 \times 10^{11} \text{ GeV}$, the axion abundance in the present universe becomes

$$\Omega_a \simeq 0.2 \cdot \theta^2 \cdot \left(\frac{m_a}{10^{-5} \text{ eV}} \right)^{-7/6}. \quad (2.28)$$

For the recent detail calculation, see reference [23]. Note that the DIGA is valid in the weak coupling regime, and thus, at the temperature around 1 GeV, DIGA may not apply. Lattice simulation is needed to provide the correct behavior of the topological susceptibility around the critical temperature.

³The DIGA will be precisely explained in chap. 3

For the phenomenological use of $\chi_t(T)$, we need the three-flavor QCD with the physical fermion masses. At present, Borsanyi *et al.* [56] calculates $\chi_t(T)$ at a few GeV in the full QCD with the physical quark masses and obtains results consistent with the DIGA calculation. However, there is still tensions in the temperature dependence of χ_t above the critical temperature. Currently, some groups report the result which is completely inconsistent with the DIGA [57, 30, 25]. It is pointed out by Kitano and Yamada [27] that the drastic drop of the $\chi_t(T)$ above the critical temperature makes the axion abundance significantly larger, which closes the axion window. Recently, Dine *et al.* [58] discuss the impact of the theoretical error in the DIGA to the axion abundance.

3

QCD instanton

In this chapter, we review the instanton calculus and its application to the gluon correlators. Sec. 3.1 and sec. 3.2 are based on ref. [59]. The materials of sec. 3.3.4 are; the Peskin's textbook [60] for the background field method; C.Bernard [61] for the collective coordinate; the seminal paper of 't Hooft' [19] for the instanton density at zero temperature; the paper of Dunne *et al.* [62] for the recent development of the fermion part of the instanton density at zero temperature; the seminal paper of Gross *et al.* [20] for the instanton density at finite temperature. Sec. 3.5 is a review of the works of Forkel [33] and Dine *et al.* [34] for the leading instanton contribution to the gluon correlation function in the SU(3) and SU(2) gauge theory, respectively.

3.1 The instanton in the quantum mechanics

In order to understand the instanton gas picture, we consider the tunneling amplitude in a simple one-dimensional system. Considering the Lagrangian L of a particle with

mass $m = 1$ moving in the potential $V(x)$,

$$L = \frac{1}{2} \left(\frac{dx(t)}{dt} \right)^2 - V(x). \quad (3.1)$$

In the path integral formalism, the transition amplitude from a point $(x_i, -t_0/2)$ to another point $(x_f, t_0/2)$ is sum of all path with the quantum weight $\exp(iS)$

$$\langle x_f | e^{-iHt_0} | x_i \rangle = N \int [dx] e^{iS[x(t)]}, \quad (3.2)$$

where the action is $S = \int_{-t_0/2}^{t_0/2} dt L(x, \dot{x})$ and H is the Hamiltonian and N is the normalization factor. Here, $[dx]$ denotes the integration in terms of all path $x(t)$ which has the boundary condition $x(-t_0/2) = x_i$, $x(t_0/2) = x_f$.

Applying the Wick rotation $t \rightarrow -i\tau$, the amplitude in the real time formalism is converted into one in the Euclidean space time. Inserting the identity operator $1 = \sum_n |n\rangle \langle n|$ and in the long time limit $t_0 = -i\tau_0 \rightarrow \infty$, the l.h.s. of eq. 3.2 is dominated by the lowest energy state $|0\rangle$ with the energy E_0 ,

$$\begin{aligned} \langle x_f | e^{-iHt_0} | x_i \rangle &= \sum_n e^{-iE_n t_0} \langle x_f | n \rangle \langle n | x_i \rangle, \\ &= e^{-E_0 \tau_0} \langle x_f | 0 \rangle \langle 0 | x_i \rangle, \end{aligned} \quad (3.3)$$

where E_n is the energy eigenvalue of the $|n\rangle$. Under the Wick rotation, the action is modified as

$$iS[x(t)] \rightarrow -S_E[x(\tau)] = \int_{-\tau_0/2}^{\tau_0/2} d\tau \left[-\frac{1}{2} \left(\frac{dx(\tau)}{d\tau} \right)^2 - V(x) \right], \quad (3.4)$$

which corresponds to the potential energy with opposite sign $V(x) \rightarrow -V(x)$. If the original Lagrangian has a potential barriers between x_i and x_f , in the Euclidean space time the bump turn into a hollow, then we can find a classical path to go across the potential. Those classical solution is called the instanton and provides the local minimum of the Euclidean action S_E , thus the path integral may be dominated by those classical path. In this case it is valid to approximate the whole path integral by taking into account the contributions from the instanton and small perturbation from the quantum fluctuation around the instanton solution, which is called the semi-classical

approximation.

Hereafter, we will consider the semi-classical approximation in the general action with the potential barrier $V(x)$. Considering the variation of action $S[X(\tau)]$ of the instanton $X(\tau)$ by small fluctuation $\delta x(\tau)$,

$$\begin{aligned}
\delta S &= S[X(\tau) + \delta x(\tau)] - S[X(\tau)] \\
&= \int_{-\tau_0/2}^{\tau_0/2} d\tau \left[\frac{dX(\tau)}{d\tau} \frac{d\delta x(\tau)}{d\tau} + V'(x(\tau))\delta x(\tau) \right. \\
&\quad \left. + \frac{1}{2} \left(\frac{d\delta x(\tau)}{d\tau} \right)^2 + \sum_{n \geq 2} \frac{1}{n!} V^{(n)}(x(\tau)) (\delta x(\tau))^n \right], \\
&= \int_{-\tau_0/2}^{\tau_0/2} d\tau \delta x(\tau) \left[-\frac{d^2 X}{d\tau^2} + \frac{dV(x)}{dx} + O((\delta x(\tau))^2) \right]. \tag{3.5}
\end{aligned}$$

The variational principle provides the equation of motion in terms of the instanton solution $X(\tau)$, as

$$-\frac{d^2 X}{d\tau^2} + \frac{dV(x)}{dx} = 0. \tag{3.6}$$

In order to take into account the contribution from the quantum fluctuation around $X(\tau)$, we will consider the $O((\delta x(\tau))^2)$ contribution,

$$\begin{aligned}
S[X(\tau) + \delta x(\tau)] &= S_0 + \int_{-\tau_0/2}^{\tau_0/2} d\tau \left[\frac{1}{2} \left(\frac{d\delta x(\tau)}{d\tau} \right)^2 + \frac{1}{2!} V''(x(\tau)) (\delta x(\tau))^2 \right. \\
&\quad \left. + O((\delta x(\tau))^3) \right], \\
&\simeq S_0 + \int_{-\tau_0/2}^{\tau_0/2} d\tau \delta x \left[-\frac{1}{2} \frac{d^2}{d\tau^2} \delta x + \frac{1}{2} V''(X) \delta x \right], \tag{3.7}
\end{aligned}$$

where $S_0 = S[X(\tau)]$.

Considering the eigensystem of the differential equation,

$$-\frac{d^2}{d\tau^2} x_n(\tau) + V''(X) x_n(\tau) = \epsilon_n x_n(\tau), \tag{3.8}$$

where ϵ_n is the n -th eigenvalue with the eigenfunction $x_n(\tau)$, where the eigenfunction $\{x_n(\tau)\}$ has the boundary condition $x_n(\pm\tau_0/2) = 0$ and spans the normal orthogonal

base,

$$\int_{-\tau_0/2}^{\tau_0/2} d\tau x_n(\tau)x_m(\tau) = \delta_{nm}. \quad (3.9)$$

Using this base, the arbitrary path $x(\tau)$ is written as

$$x(\tau) = X(\tau) + \sum_n c_n x_n(\tau). \quad (3.10)$$

Substituting $\delta x(\tau) = \sum_n c_n x_n(\tau)$ into eq. 3.7, we obtain

$$S[X(\tau) + \delta x(\tau)] = S_0 + \frac{1}{2} \sum_n \epsilon_n c_n^2. \quad (3.11)$$

After the change of integration variables $[dx] = \prod_n \frac{dc_n}{\sqrt{2\pi}}$, the transition amplitude can be solved by Gaussian integration in terms of c_n and we obtain

$$\langle x_f | e^{-iHt_0} | x_i \rangle = N \int_{-\infty}^{\infty} \prod \frac{dc_n}{\sqrt{2\pi}} \exp\left(S_0 + \frac{1}{2} \sum_n \epsilon_n c_n(\tau)^2\right), \quad (3.12)$$

$$= e^{-S_0} N \prod_n \epsilon_n^{-1/2}, \quad (3.13)$$

$$= e^{-S_0} N \left[\det \left(-\frac{d^2}{d\tau^2} + V''(X(\tau)) \right) \right]^{-1/2}. \quad (3.14)$$

Note that in the system with $\epsilon_0 = 0$ the divergence appeared, then we need to care about the integration in terms of a zero mode c_0 . In this paper such divergence happens in the case of double-well potential in Sec. 3.1.2 and in QCD instanton.

3.1.1 The harmonic-oscillator type potential

Here we consider the transition amplitude of a particle with mass $m = 1$ and the potential $V(x) = m\omega^2 x^2/2$ of the harmonic oscillator. We put the boundary condition $x_i = x_f = 0$. Applying eq. 3.14, the transition amplitude in the Euclidean space time

can be solved as

$$\begin{aligned}\langle 0 | e^{-H\tau_0} | 0 \rangle &= N \left[\det \left(-\frac{d^2}{d\tau^2} + \omega^2 \right) \right]^{-1/2} \\ &= \left[N \left(\prod_{n=1}^{\infty} \frac{\pi^2 n^2}{\tau_0^2} \right)^{-1/2} \right] \prod_{n=1}^{\infty} \left(1 + \frac{\omega^2 \tau_0^2}{n^2 \pi^2} \right)^{-1/2},\end{aligned}\quad (3.15)$$

where we use the fact that the operator $-d^2/d\tau^2 + \omega^2$ has the eigenvalue $\epsilon_n = \pi^2 n^2 / \tau_0^2 + \omega^2$ when $x_n(\pm\tau_0/2) = 0$. Due to the fact that the first factor is the free limit ($\omega \rightarrow 0$), we obtain

$$N \left(\prod_{n=1}^{\infty} \frac{\pi^2 n^2}{\tau_0^2} \right)^{-1/2} = \langle 0 | e^{-\hat{p}^2 \tau_0 / 2} | 0 \rangle = \int_{-\infty}^{\infty} \frac{dp}{2\pi} e^{-\hat{p}^2 \tau_0 / 2} = \frac{1}{\sqrt{2\pi\tau_0}} \quad (3.16)$$

Using the relation,

$$\pi y \prod_{n=1}^{\infty} \left(1 + \frac{y^2}{n^2} \right) = \sinh \pi y, \quad (3.17)$$

we finally obtain

$$\langle 0 | e^{-H\tau_0} | 0 \rangle = \frac{1}{\sqrt{2\pi\tau_0}} \left(\frac{\sinh \omega\tau_0}{\omega\tau_0} \right)^{-1/2} = \left(\frac{\omega}{\pi} \right)^{1/2} (2 \sinh \omega\tau_0)^{-1/2}. \quad (3.18)$$

In the $\tau_0 \rightarrow \infty$ limit we can check the lowest energy state $E_0 = \omega/2$ has the dominant contribution to the amplitude,

$$\lim_{\tau_0 \rightarrow \infty} \langle 0 | e^{-H\tau_0} | 0 \rangle = \left(\frac{\omega}{\tau_0} \right)^{1/2} e^{-\omega\tau_0/2} \left(1 + \frac{1}{2} e^{-2\omega\tau_0} + \dots \right). \quad (3.19)$$

3.1.2 The double-well type potential

In the case of the double-well potential

$$V(x) = \lambda(x^2 - \eta^2)^2, \quad (3.20)$$

the amplitude has naively two contributions. One is from the harmonic oscillation around the bottom of the well $x = \pm\eta$, which has a frequency $\omega^2 = 8\lambda\eta^2$. The other is from the tunneling path from one bottom to the other,

$$X(\tau) = \eta \tanh \frac{\omega(\tau - \tau_c)}{2}, \quad (3.21)$$

which satisfies the boundary condition $X(\pm\infty) = \pm\eta$ and has finite action

$$S_0 \equiv S[X(\tau)] = \int_{-\infty}^{\infty} d\tau \dot{X}^2 = \frac{\omega^3}{12\lambda}. \quad (3.22)$$

It is the time $\tau = \tau_c$ when the transition between bottoms happens, at which the action density $\dot{X}^2(\tau)$ has a peak like a particle localized at $\tau = \tau_c$. This can be considered as a pseudo-particle in the Euclidean space time, which appears for a short time. This is why the tunneling path in the Euclidean space time is named instant-on. Clearly, the action does not depend on the value of τ_c , thus the action or the Lagrangian in this system has a shift symmetry in terms of τ_c .

Hereafter, we consider the tunneling amplitude $\langle -\eta | e^{-H\tau_0} | \eta \rangle$ following the prescription of 't Hooft [19]. Using eq. 3.14, the amplitude becomes

$$\langle -\eta | e^{-H\tau_0} | \eta \rangle = N \left[\det \left(-\frac{d^2}{d\tau^2} + \omega^2 \right) \right]^{-1/2} \left\{ \frac{\det \left[-(d^2/d\tau^2) + V''(X) \right]}{\det \left[-(d^2/d\tau^2) + \omega^2 \right]} \right\}^{-1/2} e^{-S_0}. \quad (3.23)$$

Substituting the instanton solution $X(\tau) = \eta \tanh(\omega\tau/2)$ into the operator $-d^2/d\tau^2 + V''(X)$, the eigenvalue equation eq. 3.8 becomes

$$-\frac{d^2}{d\tau^2} x_n(\tau) + \omega^2 \left(1 - \frac{3}{2} \frac{1}{\cosh^2(\omega\tau/2)} \right) x_n(\tau) = \epsilon_n x_n(\tau). \quad (3.24)$$

The solution of this differential equation is written in the Landau's textbook and has two discrete low energy state and the continuum energy state in the boundary condition $x_n(\pm\infty) = 0$. The two discrete energy eigenvalues are

$$\epsilon_0 = 0 \quad \epsilon_1 = \frac{3}{4}\omega^2. \quad (3.25)$$

The lowest mode of the eigenfunction is

$$x_0(\tau) = \sqrt{\frac{3\omega}{8}} \frac{1}{\cosh^2(\omega\tau)}. \quad (3.26)$$

The zero energy state provides problem because the amplitude has divergence from the determinant $1/\epsilon_0$ in eq. 3.14. However, this can be avoided by introducing so called the collective coordinate in the integral in terms of the zero mode c_0 in eq. 3.12. We will change the integration variable c_0 into τ_c as follows. Considering the path is written as $x(\tau) = X(\tau) + \sum_{n \geq 0} c_n x_n(\tau)$, the shift of $x(\tau)$ by the infinitesimal shift along the zero mode dc_0 is obtained as

$$dx(\tau) = x_0(\tau)dc_0, \quad (3.27)$$

On the other hand, the shift of $x(\tau)$ by the infinitesimal shift in terms of $d\tau_c$ is

$$dx(\tau) = dX(\tau) = \frac{dX(\tau_c)}{d\tau_c} \delta\tau_c = -\sqrt{S_0}x_0(\tau)d\tau_c. \quad (3.28)$$

Then we can relate dc_0 and $d\tau_c$ as

$$dc_0 = \sqrt{S_0}d\tau_c. \quad (3.29)$$

The determinant in eq. 3.23 is modified as integration along the corrective coordinate τ_c ,

$$\begin{aligned} & \left\{ \frac{\det [-(d^2/d\tau^2) + V''(X)]}{\det [-(d^2/d\tau^2) + \omega^2]} \right\}^{-1/2} \\ &= \int_{-\infty}^{\infty} \frac{dc_0}{\sqrt{2\pi}} \exp\left(\frac{1}{2}\epsilon_0 c_0^2\right) \left\{ \frac{\det' [-(d^2/d\tau^2) + V''(X)]}{\det [-(d^2/d\tau^2) + \omega^2]} \right\}^{-1/2}, \\ &= \int_{-\infty}^{\infty} \sqrt{\frac{S_0}{2\pi}} d\tau_c \omega \left\{ \frac{\det' [-(d^2/d\tau^2) + V''(X)]}{\omega^{-2} \det [-(d^2/d\tau^2) + \omega^2]} \right\}^{-1/2}, \end{aligned} \quad (3.30)$$

where \det' denotes the contribution from the discrete first excited state c_1 and the continuum energy spectrum c_n ($n \geq 2$). In the limit $\tau_0 \rightarrow \infty$ we can estimate the

amplitude. The ratio of the determinant is factorized into the contribution from the c_1 integral and the c_n ($n \geq 2$) integral.

$$\begin{aligned} \frac{\det' \left[-(d^2/d\tau^2) + V''(X) \right]}{\omega^{-2} \det \left[-(d^2/d\tau^2) + \omega^2 \right]} &= \left[\frac{\epsilon_1^{\text{d.w.}}}{\omega^{-2} \epsilon_0^{\text{h.o.}} \epsilon_1^{\text{h.o.}}} \right] \left[\prod_{n=2}^{\infty} \frac{\epsilon_n^{\text{d.w.}}}{\epsilon_n^{\text{h.o.}}} \right], \\ &\equiv \Phi_1 \Phi_{\text{cont.}}, \end{aligned} \quad (3.31)$$

where the indices d.w. and h.o. denote the energy spectrum of the double-well type potential and the harmonic-oscillator type potential, respectively. The first factor is easily obtained as

$$\Phi_1 = \frac{\frac{3}{4}\omega^2}{\omega^{-2}\omega^2 \left(\frac{\pi^2}{\tau_0^2} + \omega^2 \right)} \xrightarrow{\tau_0 \rightarrow \infty} \frac{3}{4}. \quad (3.32)$$

We have already know $\epsilon_n^{\text{h.o.}} = \pi^2 n^2 / \tau_0^2 + \omega^2$. As we have already mentioned, in the energy region $\epsilon \geq \omega^2$, the eigenfunction of eq. 3.24 have the continuum energy spectrum for ϵ_n ($n \geq 2$), which is characterized by the momentum of particle $p \in (0, \infty)$ as ϵ_p which has the dispersion relation $p = \sqrt{\epsilon_p - \omega^2}$. Likewise, the eigenfunction $x_n(\tau)$ ($n \geq 2$) is also labeled by p as $x_p(\tau)$. Since the potential in eigenvalue equation eq. 3.24 is bounded as

$$\omega^2 \left(1 - \frac{3}{2} \frac{1}{\cosh^2(\omega\tau/2)} \right) \leq \omega^2, \quad (3.33)$$

we don't need to consider the reflection wave. Then, at the boundary $\tau = \pm\tau_0/2$, the plane wave solution of eq. 3.24 with momentum p is written as

$$x_p(+\tau_0/2) = e^{ip\tau}, \quad x_p(-\tau_0/2) = e^{ip\tau + i\delta_p}, \quad (3.34)$$

where δ_p denotes the phase shift by the potential of eq. 3.24.

$$e^{i\delta_p} = \frac{1 + (ip/\omega)}{1 - (ip/\omega)} \frac{1 + (2ip/\omega)}{1 - (2ip/\omega)}. \quad (3.35)$$

The general solution $Ax_p(\tau) + Bx_p(-\tau)$ has non-trivial solution, when

$$p\tau_0 - \delta_p = n\pi \quad (n \geq 2). \quad (3.36)$$

We will denote the n -th solution as \tilde{p}_n , then we obtain $\epsilon_n^{\text{d.w.}} = \omega^2 + \tilde{p}_n^2$. Likewise the double-well type potential we can obtain $\epsilon_n^{\text{h.o.}} = \omega^2 + p_n^2$, where $p_n = \pi n / \tau_0$.

Using the above result, the ratio of the determinant for n -th ($n \geq 2$) eigenvalue can be written as

$$\Phi_{\text{cont.}} = \prod_{n=1}^{\infty} \frac{\omega^2 + \tilde{p}_n^2}{\omega^2 + p_n^2}. \quad (3.37)$$

The infinite product is calculated as follows.

$$\prod_{n=1}^{\infty} \frac{\omega^2 + \tilde{p}_n^2}{\omega^2 + p_n^2} = \exp\left(\sum_n \ln \frac{\omega^2 + \tilde{p}_n^2}{\omega^2 + p_n^2}\right), \quad (3.38)$$

$$= \exp\left(\sum_n \ln \left(1 + \frac{2p_n(\tilde{p}_n - p_n)}{\omega^2 + p_n^2} + \frac{(\tilde{p}_n - p_n)^2}{\omega^2 + p_n^2}\right)\right), \quad (3.39)$$

$$= \exp\sum_n \left(\frac{2p_n(\tilde{p}_n - p_n)}{\omega^2 + p_n^2} + \mathcal{O}\left(\frac{(\tilde{p}_n - p_n)^2}{\omega^2 + p_n^2}\right)\right), \quad (3.40)$$

In the large n the difference between \tilde{p}_n and p_n becomes negligible, thus we can use the approximation as below.

$$\approx \exp\left(\int_0^{\infty} \frac{dp}{\pi} \frac{\delta_p \cdot 2p}{p^2 + \omega^2}\right), \quad (3.41)$$

$$= \exp\left(\int_0^{\infty} \frac{dp}{\pi} \frac{d}{dp} \left(\ln \left[\frac{p^2 + \omega^2}{\omega^2}\right]\right) \cdot \delta_p\right), \quad (3.42)$$

$$= \exp\left(-\int_0^{\infty} \frac{dp}{\pi} \ln \left[\frac{p^2 + \omega^2}{\omega^2}\right] \cdot \frac{d}{dp} \delta_p\right). \quad (3.43)$$

The derivative of δ_p is calculated as

$$\frac{d\delta_p}{dp} = -i \frac{d}{dp} \left[\ln \left(1 + i \frac{p}{\omega} \right) - \ln \left(1 - i \frac{p}{\omega} \right) + \ln \left(1 + i \frac{2p}{\omega} \right) - \ln \left(1 - i \frac{2p}{\omega} \right) \right], \quad (3.44)$$

$$= -i \left[\frac{i(1/\omega)}{1 + i(p/\omega)} - \frac{i(-1/\omega)}{1 - i(p/\omega)} + \frac{i(2/\omega)}{1 + i(2p/\omega)} - \frac{i(-2/\omega)}{1 - i(2p/\omega)} \right], \quad (3.45)$$

$$= \frac{2}{\omega} \left[\frac{1}{1 + p^2/\omega^2} + \frac{2}{1 + 4p^2/\omega^2} \right]. \quad (3.46)$$

Using the variable $y = p/\omega$, eventually we obtain

$$\begin{aligned} \prod_{n=1}^{\infty} \frac{\omega^2 + \tilde{p}_n^2}{\omega^2 + p_n^2} &= \exp \left(- \int_0^{\infty} \frac{\omega dy}{\pi} \ln(1 + y^2) \frac{2}{\omega} \left[\frac{1}{1 + y^2} + \frac{2}{1 + 4y^2} \right] \right), \\ &= \exp \left(- \frac{2}{\pi} \cdot \pi \ln(3) \right) = \frac{1}{9}. \end{aligned} \quad (3.47)$$

Thus the instanton contribution to the transition amplitude is calculated as

$$\begin{aligned} &\langle -\eta | e^{-H\tau_0} | \eta \rangle \\ &= N \left[\det \left(-\frac{d^2}{d\tau^2} + \omega^2 \right) \right]^{-1/2} \left\{ \frac{\det \left[-(d^2/d\tau^2) + V''(X) \right]}{\det \left[-(d^2/d\tau^2) + \omega^2 \right]} \right\}^{-1/2} e^{-S_0}, \\ &\approx \left(\sqrt{\frac{\omega}{\pi}} e^{-\omega\tau_0/2} \right) \cdot \left(\frac{1}{12} \right)^{-1/2} \cdot \sqrt{\frac{S_0}{2\pi}} \omega e^{-S_0} \int_{-\infty}^{\infty} \omega d\tau_c, \end{aligned} \quad (3.48)$$

$$= \left(\sqrt{\frac{\omega}{\pi}} e^{-\omega\tau_0/2} \right) \left(\sqrt{\frac{6}{\pi}} \sqrt{S_0} e^{-S_0} \right) \int_{-\infty}^{\infty} \omega d\tau_c. \quad (3.49)$$

The above result is valid when

$$\sqrt{S_0} e^{-S_0} \omega \tau_0 \ll 1. \quad (3.50)$$

However, if τ_0 become larger, we must take into account the contribution of the multi-instanton. In this analysis, we have regularized the ultra-violet mode in the determinant of the operator

$$-\frac{d^2}{d\tau^2} + \omega^2 \left(1 - \frac{3}{2} \frac{1}{\cosh^2(\omega\tau/2)} \right) \quad (3.51)$$

by the determinant of the operator $-\frac{d^2}{d\tau^2} + \omega^2$. The divergence coming from the zero mode c_0 is translated into the integration of the collective coordinates and factored out as the volume integral. The similar treatments for these two regularization for both ultraviolet and infrared divergence are adopted in the calculation of the QCD instanton. The second factor $\sqrt{6S_0/\pi}e^{-S_0}$ is called the instanton density or the instanton measure, which originates from the change of variables in the zero mode integration.

Hereafter we introduce the dilute instanton gas approximation. In order to calculate the energy eigenvalue of the ground state and the first excited state in the problem of double-well type potential, we need to take the limit $\tau_0 \rightarrow \infty$ and consider the contribution from the multi-instanton.

Assuming the $n/2$ instantons and $n/2$ anti-instantons have center at $\tau = \tau_1, \tau_2, \dots, \tau_n$, respectively, which satisfy

$$-\frac{\tau_0}{2} < \tau_1 < \tau_2 < \dots < \tau_n < \frac{\tau_0}{2}. \quad (3.52)$$

We also assume the typical length between each (anti)-instantons is enough large $|\tau_i - \tau_j| \gg \omega^{-1}$ to ignore the overlap of each pseudo-particles. In this case the classical action becomes nS_0 , where S_0 is the one (anti)-instanton contribution. Then the amplitude becomes

$$\begin{aligned} & \left(\sqrt{\frac{\omega}{\pi}} e^{-\omega\tau_0/2} \right) \left(\sqrt{\frac{6}{\pi}} \sqrt{S_0} e^{-S_0} \right) \int_{-\infty}^{\infty} \omega d\tau_c, \\ \rightarrow & \left(\sqrt{\frac{\omega}{\pi}} e^{-\omega\tau_0/2} \right) \left(\sqrt{\frac{6}{\pi}} \sqrt{S_0} e^{-S_0} \right)^n \prod_{i=1}^n \left(\int_{-\infty}^{\infty} \omega d\tau_i \right), \\ = & \sqrt{\frac{\omega}{\pi}} e^{-\omega\tau_0/2} d^n \int_{-\tau_0/2}^{\tau_0/2} \omega d\tau_n \int_{-\tau_0/2}^{\tau_n} \omega d\tau_{n-1} \dots \int_{-\tau_0/2}^{\tau_2} \omega d\tau_1, \\ = & \sqrt{\frac{\omega}{\pi}} e^{-\omega\tau_0/2} d^n \frac{(\omega\tau_0)^n}{n!}, \end{aligned} \quad (3.53)$$

where $d = \sqrt{\frac{6}{\pi}} \sqrt{S_0} e^{-S_0}$ is the instanton density.

Considering the sum of all possible n , we obtain the amplitudes $\langle -\eta | e^{-H\tau_0} | \eta \rangle$ and

$\langle \eta | e^{-H\tau_0} | \eta \rangle$ as below.

$$\langle -\eta | e^{-H\tau_0} | \eta \rangle = \sum_{n=1,3,\dots} \sqrt{\frac{\omega}{\pi}} e^{-\omega\tau_0/2} d^n \frac{(\omega\tau_0)^n}{n!} = \sqrt{\frac{\omega}{\pi}} e^{-\omega\tau_0/2} \sinh(\omega\tau_0 d), \quad (3.54)$$

$$\langle \eta | e^{-H\tau_0} | \eta \rangle = \sum_{n=0,2,\dots} \sqrt{\frac{\omega}{\pi}} e^{-\omega\tau_0/2} d^n \frac{(\omega\tau_0)^n}{n!} = \sqrt{\frac{\omega}{\pi}} e^{-\omega\tau_0/2} \cosh(\omega\tau_0 d). \quad (3.55)$$

We obtain the energy spectrum of the ground state and the first excited state from the exponent of

$$\langle -\eta | e^{-H\tau_0} | \eta \rangle = \sqrt{\frac{\omega}{\pi}} \frac{1}{2} \left(e^{-(\omega/2 - \omega d)\tau_0} + e^{-(\omega/2 + \omega d)\tau_0} \right), \quad (3.56)$$

which provides us following two energy eigenvalue as

$$\begin{aligned} \frac{\omega}{2} \mp \omega d &= \frac{\omega}{2} \mp \omega \sqrt{\frac{6}{\pi}} \sqrt{S_0} e^{-S_0}, \\ &= \frac{\omega}{2} \mp \omega \sqrt{\frac{6}{\pi}} \sqrt{\frac{\omega^3}{12\lambda}} e^{-\omega^3/12\lambda}, \\ &= \frac{\omega}{2} \mp \sqrt{\frac{2\omega^3}{\pi\lambda}} e^{-\omega^3/12\lambda} \frac{\omega}{2}. \end{aligned} \quad (3.57)$$

If there were not the instanton contribution, these two energy eigenvalues were degenerated and consistent with the vacuum energy of the harmonic-oscillator system, $\epsilon = \omega/2$. This happens in the limit $\omega^3 \gg \lambda$, where the height of the barrier becomes infinitely large and the tunneling rate becomes negligible.

In the above calculation of the multi-instanton, we have only assumed that the (anti-)instantons are well separated and there are no interactions between (anti-)instantons, which is called the dilute instanton gas.

3.2 The instanton in the Yang-Mills theory

3.2.1 θ vacuum

The vacuum of the non-Abelian gauge field is labeled by the winding number n , which is called the n -vacuum $|n\rangle$. Considering the transition amplitude between two distinct

n -vacua, $|n\rangle$, $|m\rangle$ ($n \neq m$),

$$\text{out} \langle n | m \rangle_{\text{in}} = Z_Q, \quad Q = n - m, \quad (3.58)$$

this amplitude is always non-zero because of the instanton effects. Thus, the n -vacua is not a vacuum of the non-abelian gauge theory.

The quantum vacuum of the non-abelian gauge theory is called the θ -vacuum. The θ -vacuum is the eigenstate of the operator which is commutable with the Hamiltonian, since the θ -vacuum is independent of the time. Using the fact that the Hamiltonian is gauge invariant, the gauge invariant operator T_m labeled by the winding number m satisfies the relations:

$$[T_m, H] = 0, \quad (3.59)$$

$$T_m |n\rangle = |n + m\rangle. \quad (3.60)$$

The θ -vacuum is defined as a superposition of the eigenstate of the operator $\{T_m\}_{m \in \mathbb{Z}}$.

$$|\theta\rangle = \sum_{n \in \mathbb{Z}} e^{in\theta} |n\rangle, \quad \theta \in \mathbb{R}/2\pi, \quad (3.61)$$

where the parameter of the vacuum θ is called the vacuum angle.

Here we mention several properties of the θ -vacuum. The superposition of the vacua with distinct vacuum angles is zero as follows:

$$\begin{aligned} \text{out} \langle \theta' | \theta \rangle_{\text{in}} &= \sum_{n,m} e^{-im\theta'} e^{in\theta} \text{out} \langle m | n \rangle_{\text{in}} \\ &= \sum_{Q,k} e^{i(\theta'+\theta)Q/2} e^{i(\theta'-\theta)k/2} \text{out} \langle Q | 0 \rangle_{\text{in}} \\ &= \delta(\theta' - \theta) \sum_Q e^{i\theta Q} \text{out} \langle Q | 0 \rangle_{\text{in}}. \end{aligned} \quad (3.62)$$

We can check that the vacuum $|\theta\rangle$ is an eigenstate of operator T_m as follows:

$$\begin{aligned}
T_m |\theta\rangle &= \sum_n e^{in\theta} |n+m\rangle \\
&= \sum_{n'} e^{i(n'-m)\theta} |n'\rangle \\
&= e^{-im\theta} |\theta\rangle.
\end{aligned} \tag{3.63}$$

Considering the transition amplitude between the θ -vacua, the vacuum angle comes into the θ term in the Lagrangian.

$$\begin{aligned}
{}_{\text{out}}\langle\theta|\theta\rangle_{\text{in}} &\propto \sum_Q e^{i\theta Q} {}_{\text{out}}\langle Q|0\rangle_{\text{in}} \\
&= \sum_Q \int_{\in Q} [dA_\mu] e^{i\theta Q} \exp \left[\int d^4x \frac{1}{4g^2} F_{\mu\nu}^a F_{\mu\nu}^a \right] \\
&= \sum_Q \int_{\in Q} [dA_\mu] \exp \left[\int d^4x \left(\frac{1}{4g^2} F_{\mu\nu}^a F_{\mu\nu}^a - i \frac{\theta}{32\pi^2} F_{\mu\nu}^a \tilde{F}_{\mu\nu}^a \right) \right],
\end{aligned} \tag{3.64}$$

where the subscript $\in Q$ denotes that the path integral is constrained to the paths with the topological charge Q defined as

$$Q = \int d^4x \frac{1}{32\pi^2} F_{\mu\nu}^a \tilde{F}_{\mu\nu}^a. \tag{3.65}$$

3.2.2 Instanton action

Regardless the explicit form of the instanton solution, the instanton action can be calculated as follows.

$$S = \int d^4x \frac{1}{4} F_{\mu\nu}^a F_{\mu\nu}^a, \tag{3.66}$$

$$= \int d^4x \left[\frac{1}{4} F_{\mu\nu}^a \tilde{F}_{\mu\nu}^a + \frac{1}{8} (F_{\mu\nu}^a - \tilde{F}_{\mu\nu}^a)^2 \right], \tag{3.67}$$

$$= Q \frac{8\pi^2}{g^2} + \frac{1}{8} \int d^4x (F_{\mu\nu}^a - \tilde{F}_{\mu\nu}^a)^2. \tag{3.68}$$

Apparently the action becomes minimum when $F_{\mu\nu}^a = \tilde{F}_{\mu\nu}^a$, which is called the self-duality equation. As a result, the Q -instanton solution S_Q is $8\pi^2 Q/g^2$.

In terms of the configuration with negative topological charge, the replacement of the spatial coordinates $x_{1,2,3} \rightarrow -x_{1,2,3}$ changes the topological charge $Q \rightarrow -Q$. In this case,

$$S = -Q \frac{8\pi^2}{g^2} + \frac{1}{8} \int d^4x (F_{\mu\nu}^a + \tilde{F}_{\mu\nu}^a)^2. \quad (3.69)$$

The minimum of action is realized by the anti-self-duality equation $F_{\mu\nu}^a = -\tilde{F}_{\mu\nu}^a$ as $S_Q = (8\pi^2/g^2)|Q|$.

Those equation are equivalent to the equation of motion of $F_{\mu\nu}^a$.

$$\begin{aligned} D_\mu F_{\mu\nu} &= \pm D_\mu \tilde{F}_{\mu\nu}, \\ &= \pm \frac{1}{2} \epsilon_{\mu\nu\gamma\delta} D_\mu F_{\gamma\delta}, \\ &= \pm \frac{1}{6} \epsilon_{\mu\nu\gamma\delta} (D_\mu F_{\gamma\delta} + D_\gamma F_{\delta\mu} + D_\delta F_{\mu\gamma}), \\ &= 0, \end{aligned} \quad (3.70)$$

where in the last equality we use the Bianchi identity,

$$D_\mu F_{\gamma\delta} + D_\delta F_{\mu\gamma} + D_\gamma F_{\delta\mu} = 0. \quad (3.71)$$

3.2.3 BPST instanton

In the $SU(2)$ Yang-Mills theory in Euclidean space, what we are interested in is the gauge configuration which keeps the action finite in the integration of $F_{\mu\nu}^a F_{\mu\nu}^a$ in the whole region. The sufficient condition but not the necessary condition is to consider the pure gauge at infinity $x \rightarrow \infty$, which satisfy $F_{\mu\nu}^a = 0$.

$$\lim_{x \rightarrow \infty} A_\mu(x) = iS \partial_\mu S^\dagger, \quad (3.72)$$

where S is the unitary unimodular matrix. Considering the matrix S such as

$$S = \frac{i\tau_\mu^+ x_\mu}{\sqrt{x^2}}. \quad (3.73)$$

Since S is the mapping from S_3 sphere to the gauge group $SU(2)$ with one-to-one correspondence, $A_\mu = iS \partial_\mu S^\dagger$ has the topological charge $Q = 1$. Using matrix S , the matrices

corresponding to the topological charge n is

$$S_n = (S)^n, \quad n \in \mathbb{Z}. \quad (3.74)$$

The topological charge n of the gauge configuration is determined only by the information of the spatial infinity. Apparently, the integral of the $F_{\mu\nu}^a F_{\mu\nu}^a$, which is proportional to n , can be expressed by the surface integral as follows.

$$\begin{aligned} n &= \frac{1}{32\pi^2} \int d^4x F_{\mu\nu}^a \tilde{F}_{\mu\nu}^a, \\ &= \frac{1}{32\pi^2} \int d^4x \frac{1}{2} \epsilon_{\mu\nu\alpha\beta} \left[4\partial_\mu A_\nu^a \partial_\alpha A_\beta^a + 4\partial_\mu A_\nu^a \epsilon^{abc} A_\alpha^b A_\beta^c \right. \\ &\quad \left. + (\delta^{bb'} \delta^{cc'} - \delta^{bc'} \delta^{b'c}) A_\mu^a A_\nu^b A_\alpha^{b'} A_\beta^{c'} \right] \\ &= \frac{1}{32\pi^2} \int d^4x \partial_\mu 2\epsilon_{\mu\nu\alpha\beta} \left(A_\nu^a \partial_\alpha A_\beta^a + \frac{1}{3} \epsilon^{abc} A_\nu^a A_\alpha^b A_\beta^c \right) \end{aligned} \quad (3.75)$$

$$\equiv \frac{1}{32\pi^2} \int d^4x \partial_\mu K_\mu, \quad (3.76)$$

where $\tilde{F}_{\mu\nu}^a = (1/2)\epsilon_{\mu\nu\alpha\beta} F_{\alpha\beta}^a$ and $\epsilon_{1234} = 1$, and K_μ is called the Chern-Simon current.

$$\begin{aligned} n &= i \frac{1}{24\pi^2} \int \text{Tr} \epsilon_{\mu\nu\rho\sigma} A_\nu A_\rho A_\sigma dS_\mu, \\ &= i \frac{1}{24\pi^2} \int_{S^3} \text{Tr} \epsilon_{\mu\nu\rho\sigma} (S \partial_\nu S^\dagger) (S \partial_\rho S^\dagger) (S \partial_\sigma S^\dagger) dS_\mu \end{aligned} \quad (3.77)$$

The explicit form of the pure gauge is written as

$$iS \partial_\mu S^\dagger = \frac{1}{x^2} \eta_{a\mu\nu} x_\nu \tau^a, \quad (3.78)$$

where $\eta_{a\mu\nu}$ is called 't Hooft symbols and given by

$$\eta_{a\mu\nu} = \begin{cases} \epsilon_{a\mu\nu}, & \mu, \nu = 1, 2, 3, \\ -\delta_{a\nu}, & \mu = 4, \\ \delta_{a\mu}, & \nu = 4, \\ 0, & \mu = \nu = 4. \end{cases}$$

The symbols $\bar{\eta}_{\mu\nu}$ differ from η by a change in the sign in front of δ . The surface integral in the region S^3 in eq. 3.77 is spherically symmetric and independent of the radius x and direction. Then, it is enough to calculate the integrand at one point, for example the north pole of the unit sphere ($x^4 = 1$, $\vec{x} = \vec{0}$), then multiply the four dimensional solid angle $\Omega_4 = 2\pi^2$. Thus, we can obtain

$$\frac{1}{24\pi^2} \Omega_4 \text{Tr}(\tau^a \tau^b \tau^b) \eta_{ai4} \eta_{bj4} \eta_{ck4} \epsilon_{ijk} = 1. \quad (3.79)$$

Assuming the isotropy of the instanton configuration the boundary condition to be a pure gauge form at spatial infinity, the instanton configuration of the general radius x is written using the ansatz,

$$A_\mu = \frac{f(x^2)}{x^2} \eta_{\mu\nu} x_\nu \tau^a. \quad (3.80)$$

The function $f(x^2)$ has boundary conditions $\lim_{x^2 \rightarrow \infty} f(x^2) = 1$ to make A_μ the pure gauge form at infinity and $\lim_{x^2 \rightarrow 0} f(x^2) = \text{const.} \times x^2$ so that $A_\mu(x)$ is regular at the origin.

The function $f(x^2)$ also appears in the field strength $F_{\mu\nu}^a$ and its dual $\tilde{F}_{\mu\nu}^a$ as follows.

$$\begin{aligned} F_{\mu\nu}^a &= \partial_\mu A_\nu^a - \partial_\nu A_\mu^a + f^{abc} A_\mu^b A_\nu^c, \\ &= 2\eta_{a\nu\sigma} \left(\frac{\delta_{\mu\alpha}}{x^2} f - 2x_\mu \frac{x_\sigma}{x^4} f + \frac{x_\sigma}{x^2} 2x_\mu f' \right) \\ &\quad - 2\eta_{a\mu\sigma} \left(\frac{\delta_{\nu\sigma}}{x^2} f - 2x_\nu \frac{x_\sigma}{x^4} f + \frac{x_\sigma}{x^2} 2x_\nu f' \right) + 4f^{abc} \eta_{b\mu\sigma} \eta_{c\nu\lambda} \frac{x_\sigma x_\lambda}{x^4} f^2, \\ &= 4 \left[\frac{f}{x^2} \eta_{a\nu\mu} - \frac{f}{x^4} (x_\mu \eta_{a\nu\sigma} x_\sigma - x_\nu \eta_{a\mu\sigma} x_\sigma) + \frac{f'}{x^2} (x_\mu \eta_{a\nu\sigma} x_\sigma - x_\nu \eta_{a\mu\sigma} x_\sigma) \right. \\ &\quad \left. + (\delta_{\mu\nu} \eta_{a\sigma\lambda} - \delta_{\mu\lambda} \eta_{a\sigma\nu} - \delta_{\sigma\nu} \eta_{a\mu\lambda} + \delta_{\sigma\lambda} \eta_{a\mu\nu}) \right], \\ &= -4 \left[\frac{f(f-1)}{x^2} \eta_{a\mu\nu} + \frac{x_\mu \eta_{a\nu\sigma} x_\sigma - x_\nu \eta_{a\mu\sigma} x_\sigma}{x^4} (f(1-f) - x^2 f') \right]. \end{aligned} \quad (3.81)$$

$$\begin{aligned}
\tilde{F}_{\mu\nu}^a &= \frac{1}{2}\epsilon_{\mu\nu\alpha\beta}F_{\alpha\beta}^a, \\
&= -\frac{4}{g}\left[\frac{f(f-1)}{x^2}\eta_{a\mu\nu} + \frac{1}{2x^4}\left\{-x_\mu\eta_{a\nu\alpha}x_\alpha + x_\nu\eta_{a\mu\alpha}x_\alpha - x^2\eta_{a\mu\nu} + (\alpha \leftrightarrow \beta)\right\}\right. \\
&\quad \left.\times (f(1-f) - x^2f')\right], \\
&= -\frac{4}{g}\left[\frac{f(f-1)}{x^2}\eta_{a\mu\nu} - \frac{1}{x^2}(x_\mu\eta_{a\nu\alpha}x_\alpha - x_\nu\eta_{a\mu\alpha}x_\alpha)(f(1-f) - x^2f')\right. \\
&\quad \left.- \frac{1}{x^2}\eta_{a\mu\nu}(f(1-f) - x^2f')\right], \\
&= -\frac{4}{g}\left[\eta_{a\mu\nu}f' - \frac{x_\mu\eta_{a\nu\alpha}x_\alpha - x_\nu\eta_{a\mu\alpha}x_\alpha}{x^2}(f(1-f) - x^2f')\right]. \tag{3.82}
\end{aligned}$$

Due to the self-dual equation, $f(x^2)$ should satisfy

$$f(1-f) - x^2f' = 0, \tag{3.83}$$

Solving this differential equation, we can obtain

$$f(x^2) = \frac{x^2}{x^2 + \rho^2}, \tag{3.84}$$

where ρ is called instanton size. Due to the translational invariance of the instanton, the shift $x_\mu \rightarrow x_\mu - z_\mu$ also provides other instanton solution which has the center at $x = z$.

In summary, the instanton solution at position z with size ρ is written as

$$A_\mu^a = 2\eta_{a\mu\nu}\frac{(x-x_0)_\nu}{(x-x_0)^2 + \rho^2}, \tag{3.85}$$

$$F_{\mu\nu}^a = -4\eta_{a\mu\nu}\frac{\rho^2}{((x-x_0)^2 + \rho^2)^2}, \tag{3.86}$$

This form of instanton solution is called as the BPST instanton. We can obtain the anti-instanton solution by changing $\eta \rightarrow \bar{\eta}$.

3.2.4 The singular solution and 't Hooft ansatz

In order to consider the multi-instanton, it is convenient to consider the so-called ‘singular gauge’, which has pole at the instanton position. The BPST instanton solution

and the singular solution is related by the following transformation,

$$\begin{aligned}\bar{A}_\mu &= U^\dagger A_\mu U + iU^\dagger \partial_\mu U, \\ \bar{F}_{\mu\nu} &= U^\dagger F_{\mu\nu} U,\end{aligned}\tag{3.87}$$

where U is the unitary unimodular matrix

$$U = \frac{i\tau_\mu^+(x-z)_\mu}{\sqrt{(x-z)^2}},\tag{3.88}$$

where τ_μ^\pm are defined in sec. A.1. This transformation is similar to the usual gauge transformation of BPST instanton A_μ and its field strength $F_{\mu\nu}$. However, this transformation modifies the gauge invariant variables such as $\text{Tr}F_{\mu\nu}F_{\mu\nu}$ due to the singularity of U .

We can explicitly calculate \bar{A}_μ and $\bar{F}_{\mu\nu}$ as follows. For simplicity, we use $X_\mu = (x-z)_\mu$ and $\epsilon_{a\mu\alpha}$ with $\mu, \alpha = 1, 2, 3$.

$$A_\mu^a T^a U = U^\dagger A_\mu^a T^a U + iU^\dagger \partial_\mu U,\tag{3.89}$$

The first term in eq. 3.89 is modified as follows.

$$U^\dagger A_\mu^a T^a U = \frac{X_\nu X_\alpha X_\beta}{X^2(X^2 + \rho^2)} \eta_{a\mu\nu} \tau_\alpha^- \tau^a \tau_\beta^+,\tag{3.90}$$

where we will use the following relation,

$$\begin{aligned}X_\alpha X_\beta \tau_\alpha^- \tau^a \tau_\beta^+ &= X_b X_c \tau^b \tau^a \tau^c + X_4 X_c (+i) \tau^a \tau^c + X_b X_4 \tau^b \tau^a (-i) + X_4^2 \tau^a, \\ &= X_b X_c \tau^b (\delta^{ac} + i\epsilon_{acd} \tau^d) + iX_4 X_c (\delta^{ac} + i\epsilon_{acd} \tau^d) - iX_b X_4 (\delta^{ab} + i\epsilon_{bad} \tau^d) + X_4^2 \tau^a, \\ &= (\vec{X} \cdot \vec{\tau}) X_a - \tau^a \vec{X}^2 + X_a (\vec{X} \cdot \vec{\tau}) - 2X_4 \epsilon_{acd} X_c \tau^d + X_4^2 \tau^a, \\ &= 2(\vec{X} \cdot \vec{\tau}) X_a - \tau^a \vec{X}^2 - 2X_4 \epsilon_{acd} X_c \tau^d + X_4^2 \tau^a.\end{aligned}\tag{3.91}$$

The second term in eq. 3.89 is modified as follows.

$$\begin{aligned}
iU^\dagger \partial_\mu U &= i \frac{\tau_\alpha^- X_\alpha}{\sqrt{X^2}} \partial_\mu \left(\frac{\tau_\beta^+ X_\beta}{\sqrt{X^2}} \right), \\
&= i \frac{\tau_\alpha^- X_\alpha}{\sqrt{X^2}} \left[-\frac{X_\mu \tau_\beta^+ X_\beta}{(X^2)^{3/2}} + \frac{\tau_\mu^+}{X^2} \right], \\
&= i \frac{1}{(X^2)^2} \left[-X_\alpha X_\mu X_\beta (\delta_{\alpha\beta} + i\bar{\eta}_{\alpha\beta} \tau^a) + X^2 X_\alpha (\delta_{\alpha\mu} + i\bar{\eta}_{\alpha\mu} \tau^a) \right], \\
&= -\frac{1}{X^2} \bar{\eta}_{\alpha\alpha\mu} X_\alpha \tau^a, \\
&= \frac{1}{X^2} \left(-\eta_{\alpha\mu\alpha} X_\alpha + 2\epsilon_{\alpha\mu\alpha} X_\alpha \right) \tau^a, \tag{3.92}
\end{aligned}$$

where, in the last line, we use relations $\eta_{\alpha\mu\nu} X_\nu = \epsilon_{abc} X_c + \delta_{a\mu} X_4$ and $\bar{\eta}_{\alpha\mu\nu} X_\nu = \epsilon_{abc} X_c - \delta_{a\mu} X_4$. Summarizing eq. 3.89, eq. 3.90, eq. 3.91 and eq. 3.92, we finally obtain

$$\begin{aligned}
U^\dagger A_\mu^a T^a U + iU^\dagger \partial_\mu U &= \frac{1}{X^2(X^2 + \rho^2)} \eta_{\alpha\mu\nu} X_\nu \left(2(\vec{X} \cdot \vec{\tau}) X_a - \tau^a \vec{X}^2 - 2X_4 \epsilon_{acd} X_c \tau^d + X_4^2 \tau^a \right) \\
&\quad - \frac{1}{X^2} \bar{\eta}_{\alpha\alpha\mu} X_\alpha \tau^a, \\
&= \frac{1}{X^2(X^2 + \rho^2)} \eta_{\alpha\mu\nu} X_\nu \left(2(\vec{X} \cdot \vec{\tau}) X_a - \tau^a \vec{X}^2 - 2X_4 \epsilon_{acd} X_c \tau^d + X_4^2 \tau^a \right) \\
&\quad + \frac{X^2}{X^2(X^2 + \rho^2)} \left(-\eta_{\alpha\mu\alpha} X_\alpha + 2\epsilon_{\alpha\mu\alpha} X_\alpha \right) \tau^a + \frac{\rho^2}{X^2(X^2 + \tau^2)} \bar{\eta}_{\alpha\mu\alpha} X_\alpha \tau^a, \\
&= \frac{1}{X^2(X^2 + \rho^2)} \left[2X_4 (\vec{X} \cdot \vec{\tau}) X_\mu - \vec{X}^2 \epsilon_{\alpha\mu\nu} \tau^a X_\nu - \vec{X}^2 X_4 \tau^\mu - 2X_4 \epsilon_{\alpha\mu\nu} X_\nu \epsilon_{acd} X_c \tau^d \right. \\
&\quad \left. - 2S_4 \delta_{\alpha\mu} X_4 \epsilon_{acd} X_c \tau^d + \epsilon_{\alpha\mu\nu} X_\nu \tau^a X_4^2 + \delta_{\alpha\mu} X_4^3 \tau^a - (\vec{X}^2 + X_4^2) \epsilon_{\alpha\mu\alpha} X_\alpha \tau^a \right. \\
&\quad \left. - (\vec{X}^2 + X_4^2) \delta_{\alpha\mu} X_4 \tau^a + 2\epsilon_{\alpha\mu\alpha} X_\alpha \tau^a (\vec{X}^2 + X_4^2) \right] + \frac{\rho^2}{X^2(X^2 + \tau^2)} \bar{\eta}_{\alpha\mu\alpha} X_\alpha \tau^a, \\
&= \frac{\rho^2}{X^2(X^2 + \tau^2)} \bar{\eta}_{\alpha\mu\alpha} X_\alpha \tau^a. \tag{3.93}
\end{aligned}$$

In terms of the field strength in singular gauge, we calculate as follows.

$$\begin{aligned}
& \partial_\mu \bar{A}_\mu^a - \partial_\nu \bar{A}_\mu^a + \epsilon^{abc} \bar{A}_\mu^b \bar{A}_\nu^c \\
= & 2\bar{\eta}_{av\rho} \left(\frac{\delta_{\mu\rho} \rho^2}{X^2(X^2 + \rho^2)} - \frac{2X_\mu X_\rho \rho^2}{(X^2)^2(X^2 + \rho^2)} - \frac{2X_\mu X_\rho \rho^2}{X^2(X^2 + \rho^2)^2} \right) \\
& - 2\bar{\eta}_{a\mu\rho} \left(\frac{\delta_{\nu\rho} \rho^2}{X^2(X^2 + \rho^2)} - \frac{2X_\nu X_\rho \rho^2}{(X^2)^2(X^2 + \rho^2)} - \frac{2X_\nu X_\rho \rho^2}{X^2(X^2 + \rho^2)^2} \right) \\
& + \epsilon_{abc} 2\bar{\eta}_{b\mu\rho} \frac{X_\rho \rho^2}{X^2(X^2 + \rho^2)} 2\bar{\eta}_{c\nu\kappa} \frac{X_\kappa \rho^2}{X^2(X^2 + \rho^2)},
\end{aligned} \tag{3.94}$$

$$\begin{aligned}
\text{(3rd term)} &= \frac{4}{g} \left(\delta_{\mu\nu} \bar{\eta}_{a\rho\kappa} - \delta_{\mu\kappa} \bar{\eta}_{a\rho\nu} - \delta_{\rho\nu} \bar{\eta}_{a\mu\kappa} + \delta_{\rho\kappa} \bar{\eta}_{a\mu\nu} \right) \frac{X_\rho X_\kappa \rho^4}{(X^2)^2(X^2 + \rho^2)^2}, \\
&= \frac{2}{g} \frac{\rho^4}{(X^2)^2(X^2 + \rho^2)^2} \left(2\bar{\eta}_{av\rho} X_\rho X_\mu - 2\bar{\eta}_{a\mu\kappa} X_\kappa X_\nu + 2X^2 \bar{\eta}_{a\mu\nu} \right)
\end{aligned} \tag{3.95}$$

In summary,

$$\begin{aligned}
\partial_\mu \bar{A}_\mu^a - \partial_\nu \bar{A}_\mu^a + \epsilon^{abc} \bar{A}_\mu^b \bar{A}_\nu^c &= 2 \frac{1}{(X^2)^2(X^2 + \rho^2)^2} \left[-\bar{\eta}_{a\mu\nu} (\rho^4 X^2 + \rho^2 X^4) \right. \\
&\quad \left. - 2\bar{\eta}_{av\rho} X_\rho X_\mu (2\rho^2 X^2 + \rho^4) + 2\bar{\eta}_{av\rho} X_\rho X_\mu \rho^4 + \rho^4 X^2 \bar{\eta}_{a\mu\nu} \right] \\
&\quad - (\mu \leftrightarrow \nu), \\
&= -8 \left[\frac{X_\mu X_\rho}{X^2} - \frac{1}{4} \delta_{\mu\rho} \right] \bar{\eta}_{av\rho} \frac{\rho^2}{(X^2 + \rho^2)^2} - (\mu \leftrightarrow \nu).
\end{aligned} \tag{3.96}$$

Thus, the singular instanton solution is written as

$$\bar{A}_\mu^a = 2\bar{\eta}_{a\mu\nu} (x-z)_\nu \frac{\rho^2}{(x-z)^2 [(x-z)^2 + \rho^2]}, \tag{3.97}$$

$$\bar{F}_{\mu\nu}^a = -8 \left[\frac{(x-z)_\mu (x-z)_\rho}{(x-z)^2} - \frac{1}{4} \delta_{\mu\rho} \right] \bar{\eta}_{av\rho} \frac{\rho^2}{[(x-z)^2 + \rho^2]^2} + (\mu \leftrightarrow \nu). \tag{3.98}$$

For the actual calculation it is better to use the following form introduced by 't hooft.

$$\bar{A}_\mu^a = -\bar{\eta}_{a\mu\nu} \partial_\nu \ln \left[1 + \frac{\rho^2}{(x-z)^2} \right]. \tag{3.99}$$

In general, Q -instanton solution is written as

$$A_\mu^a(x) = -\bar{\eta}_{a\mu\nu}\partial_\nu \ln \Pi(x), \quad (3.100)$$

$$\Pi(x) = 1 + \sum_{n=1}^Q \frac{\rho_n^2}{(x - x_n)^2}. \quad (3.101)$$

Using the singular instanton solution in eq. 3.100, $F_{\mu\nu}^a - \tilde{F}_{\mu\nu}^a$ is calculated as follows.

$$F_{\mu\nu}^a - \tilde{F}_{\mu\nu}^a = \bar{\eta}_{a\mu\nu} \frac{\partial_\alpha \partial_\alpha \Pi}{\Pi}. \quad (3.102)$$

Thus, the self-duality condition is $\square\Pi/\Pi = 0$.

3.2.5 Harrington-Sheperd caloron

We will introduce the instanton solution in the finite temperature Yang-Mills theory, following Harrington and Shepard [63]. Unlike the topology of the Euclidean space R^4 , the topology of the thermal field theory is $S^1 \times R^3$ because of the periodicity along the time component. The basics of the thermal field theory is discussed in sec. A.2.

In order to make the action finite, the gauge field should be the pure gauge form at the spatial infinity,

$$A_\mu \xrightarrow{r \rightarrow \infty} U^{-1}(\theta, \phi, \tau) \partial_\mu U(\theta, \phi, \tau), \quad (3.103)$$

where, due to the periodicity of $U(\vec{x}, \tau)$, τ is an independent variable from the other two angular variable in S^2 . Then, at spatial infinity $U(\theta, \phi, \tau)$ is a mapping from $S^2 \times S^1$ to the $SU(2)$ gauge group. It is known that this mapping $S^2 \times S^1 \xrightarrow{U} S^3$ can be divided into infinite set of homotopy classes. Thus we can define the topologically distinct gauge field with winding number in the Yang-Mills theory at finite temperature.

Harrington and Shepard [14] constructed the thermal instanton solution, called HS caloron¹, from the 't Hooft solution in eq. 3.100 discussed in sec. 3.2.4. The instanton solution in the 't Hooft ansatz is given as

$$A_\mu^a(\mathbf{x}, \tau) = -\bar{\eta}_{a\mu\nu}\partial_\nu \ln \Pi(\mathbf{x}, \tau). \quad (3.104)$$

¹caloron="calor"(heat)+"-on".

In order to confirm A_μ as the instanton solution, it should satisfy both the equation of motion and the self-duality condition. First, the equation of motion is satisfied if $\square\Pi = 0$ or $\square\Pi = c\Pi^3$.

$$D_\mu F_{\mu\nu}^a = \partial_\mu F_{\mu\nu}^a + f^{abc} A_\mu^b F_{\mu\nu}^c = 0, \quad (3.105)$$

Here, we define (anti)self-dual projection operator $p_{\mu\nu\lambda\kappa}^{(\pm)}$ as

$$\begin{aligned} p_{\mu\nu\lambda\kappa}^{(\pm)} &\equiv \frac{1}{4} (\delta_{\mu\lambda}\delta_{\nu\kappa} - \delta_{\mu\kappa}\delta_{\nu\lambda} \pm \epsilon_{\mu\nu\lambda\kappa}) = \frac{1}{4} \eta_{a\mu\nu}^{(\pm)} \eta_{a\lambda\kappa}^{(\pm)}, \\ d(p_{\mu\nu\lambda\kappa}^{(\pm)} f_{\lambda\kappa}) &= \pm f_{\mu\nu}, \end{aligned}$$

where $f_{\mu\nu}$ is anti-symmetric tensor and $d f_{\mu\nu} = \frac{1}{2} \epsilon_{\mu\nu\lambda\kappa} f_{\lambda\kappa}$ and $\eta_{a\mu\nu}^{(+)} = \eta_{a\mu\nu}$, $\eta_{a\mu\nu}^{(-)} = \bar{\eta}_{a\mu\nu}$. Using these relation, the self-dual condition is

$$\eta_{a\mu\nu}^{(-)} F_{\mu\nu}^a = 0, \quad (3.106)$$

which is satisfied if

$$\Pi^{-1} \square \Pi(\mathbf{x}, \tau) = 0, \quad (3.107)$$

where we used the relation $\eta_{a\mu\lambda}^{(\pm)} \eta_{b\nu\lambda}^{(\pm)} = \delta_{ab} \delta_{\mu\nu} + \epsilon_{abc} \eta_{c\mu\nu}^{(\pm)}$. This is the Laplace equation, which has solution

$$\Pi(\mathbf{x}) = 1 + \sum_{i=1}^n \frac{\rho_i^2}{(x - z)^2}. \quad (3.108)$$

Considering the periodicity of the gauge field, the thermal instanton becomes

$$\Pi(\mathbf{x}, \tau) = 1 + \sum_{k=-\infty}^{\infty} \frac{\rho^2}{(\mathbf{x} - \mathbf{x}_0)^2 + (\tau - \tau_k)^2}, \quad (3.109)$$

$$= 1 + \frac{\pi\rho^2}{\beta|\mathbf{x} - \mathbf{x}_0|} \frac{\sinh(2\pi\beta^{-1}|\mathbf{x} - \mathbf{x}_0|)}{\cosh(2\pi\beta^{-1}|\mathbf{x} - \mathbf{x}_0|) - \cos(2\pi\beta^{-1}(\tau - \tau_0))}, \quad (3.110)$$

where $\tau_k = \tau_0 + k\beta$. This solution denotes that 1-instanton solution settles in the physical strip $0 \leq \tau \leq \beta$. In eq. 3.110 the constant 1 is necessary to obtain the topologically non-trivial gauge field in the zero temperature limit $\beta \rightarrow \infty$. Otherwise, $F_{\mu\nu}^a(x) = 0$ in

this limit, which provides $Q = 0$.

The thermal multi-instanton solution is constructed as

$$\Pi(\mathbf{x}, \tau) = 1 + \sum_{k=1}^N \frac{\pi \rho_k^2}{\beta |\mathbf{x} - \mathbf{x}_{k,0}|} \frac{\sinh(2\pi\beta^{-1}|\mathbf{x} - \mathbf{x}_{k,0}|)}{\cosh(2\pi\beta^{-1}|\mathbf{x} - \mathbf{x}_{k,0}|) - \cos(2\pi\beta^{-1}(\tau - \tau_{k,0}))}. \quad (3.111)$$

3.3 Yang-Mills instanton density at zero and finite temperature

3.3.1 Background field method

Here we introduce the gauge fixed Lagrangian using the Faddeev and Popov's prescription. In this discussion, we follow the Peskin's textbook [60].

Considering the functional integral of the Yang-Mills action in the Euclidean space, the gauge field has infinite number of direction corresponding to the local color rotation. In order to compute the functional integral properly we need to factor out these directions, constraining the integral region much small. We constrain the path of the gauge configuration by inserting the unity,

$$\int [d\alpha] \delta(G(A_\mu^\alpha) - \omega) \det\left(\frac{\delta(G(A_\mu^\alpha))}{\delta\alpha}\right), \quad (3.112)$$

where $\omega(x)$ is arbitrary function of x . Then, we constrain $\omega(x)$ by the Gaussian distribution, so that the gauge direction is constrained by the condition $G(A) = 0$.

$$\begin{aligned} & \int [dA] e^{-S_g[A]} \\ &= \mathcal{N} \int [d\omega d\alpha dA] \delta(G(A_\mu^\alpha) - \omega) \det\left(\frac{\delta(G(A_\mu^\alpha))}{\delta\alpha}\right) \exp\left[-\int d^4x \frac{\omega^2}{2\xi}\right] e^{-S_g[A]}, \end{aligned}$$

where $S_g = \int d^4x \frac{1}{4g^2} (F_{\mu\nu}^a)^2$ and we introduce the normalization factor

$$\mathcal{N}^{-1} = \int [d\omega] \exp\left(-\int d^4x \frac{\omega^2}{2\xi}\right), \quad (3.113)$$

so as to keep the functional integral unchanged.

By choosing $G(A_\mu^\alpha) = \partial^\mu$ with $A_\mu^\alpha, A_\mu \rightarrow A_\mu^\alpha = A_\mu + D_\mu \alpha$, we obtain

$$\int [dA] e^{-S_g[A]} = \mathcal{N} \int [d\alpha dA] \det \left(\frac{\delta(G(A_\mu^\alpha))}{\delta\alpha} \right) \exp \left[- \int d^4x \left(\frac{1}{4g^2} (F_{\mu\nu}^a)^2 + \frac{(\partial_\mu A^\mu)^2}{2\xi} \right) \right].$$

Using the functional derivative, $\frac{\delta(G(A_\mu^\alpha))}{\delta\alpha} = \partial_\mu D_\mu$, we obtain

$$\det \left(\frac{\delta(G(A_\mu^\alpha))}{\delta\alpha} \right) = \int [dc d\bar{c}] \exp \left[- \int d^4x \bar{c} \partial_\mu D_\mu c \right]. \quad (3.114)$$

After the prescription the gauge fixed Lagrangian is written as

$$\mathcal{L}_{\text{FP}} = \frac{1}{4g^2} F_{\mu\nu}^a F_{\mu\nu}^a + \frac{1}{2\xi} (\partial_\mu A_\mu^a)^2 + \bar{c}^a \partial_\mu D_\mu c^a. \quad (3.115)$$

Hereafter, we introduce the background field method in the non-abelian gauge theory around the classical gauge field \bar{A}_μ . We start from the Lagrangian in the SU(N) gauge theory,

$$\mathcal{L} = \frac{1}{4g^2} (F_{\mu\nu}^a)^2 + \bar{\psi} (\not{D} + m) \psi, \quad (3.116)$$

$$F_{\mu\nu}^a = \partial_\mu A_\nu^a - \partial_\nu A_\mu^a + f^{abc} A_\mu^b A_\nu^c, \quad (3.117)$$

$$D_\mu \psi = (\partial_\mu + iA_\mu^a T^a) \psi. \quad (3.118)$$

We insert $A_\mu^a = \bar{A}_\mu^a + a_\mu^a$, where \bar{A}_μ^a denotes the classical solution and a_μ^a is the quantum fluctuation around the classical field. The functional integral $[dA]$ becomes $[da]$ in this notation. The field strength is modified as

$$\begin{aligned} F_{\mu\nu}^a &= \partial_\mu (\bar{A}_\nu^a + a_\nu^a) - \partial_\nu (\bar{A}_\mu^a + a_\mu^a) + f^{abc} (\bar{A}_\mu^b + a_\mu^b) (\bar{A}_\nu^c + a_\nu^c), \\ &= \left[\partial_\mu \bar{A}_\nu^a - \partial_\nu \bar{A}_\mu^a + f^{abc} \bar{A}_\mu^b \bar{A}_\nu^c \right] + \left[\partial_\mu a_\nu^a + f^{abc} \bar{A}_\mu^b a_\nu^c \right] \\ &\quad - \left[\partial_\nu a_\mu^a + f^{abc} \bar{A}_\nu^b a_\mu^c \right] + f^{abc} a_\mu^b a_\nu^c, \\ &\equiv \bar{F}_{\mu\nu}^a + D_\mu a_\nu^a - D_\nu a_\mu^a + f^{abc} a_\mu^b a_\nu^c. \end{aligned} \quad (3.119)$$

The fermion action is modified as

$$\begin{aligned}\bar{\psi} (\not{D} + m) \psi &= \bar{\psi} \gamma_\mu (\partial_\mu + i\bar{A}_\mu + m) \psi + i\bar{\psi} \gamma_\mu a_\mu \psi, \\ &\equiv \bar{\psi} (\not{D} + m) \psi + i\bar{\psi} \gamma_\mu a_\mu \psi.\end{aligned}\quad (3.120)$$

The gauge transformation for the classical gauge field and the background field is determined so as to be consistent with the usual gauge transformation for A_μ as follows.

$$A_\mu \rightarrow A^\alpha \equiv e^{+i\alpha} A_\mu e^{-i\alpha} - ie^{+i\alpha} \partial_\mu e^{-i\alpha}, \quad (3.121)$$

$$\bar{A}_\mu \rightarrow \bar{A}_\mu^\alpha \equiv e^{+i\alpha} \bar{A}_\mu e^{-i\alpha} - ie^{+i\alpha} \partial_\mu e^{-i\alpha}, \quad (3.122)$$

$$a_\mu \rightarrow a_\mu^\alpha \equiv e^{+i\alpha} a_\mu e^{-i\alpha}. \quad (3.123)$$

Considering the gauge fixing condition $G(a_\mu^\alpha) = D_\mu a_\mu^\alpha$ and the infinitesimal transformation of a_μ ,

$$a_\mu^a \rightarrow a_\mu^{\alpha a} = a_\mu^a + D_\mu \alpha^a + f^{abc} a_\mu^b \alpha^c, \quad (3.124)$$

the determinant becomes

$$\begin{aligned}\det \left(\frac{\delta G(a_\mu^{\alpha a})}{\delta \alpha^a} \right) &= \det D_\mu (D_\mu \delta^{ad} - f^{abc} a_\mu^b \delta^{cd}), \\ &= \int [d\phi d\bar{\phi}] \exp \left[- \int d^4x \left(\bar{\phi}^a (D^2)^{ac} \phi^c + \bar{\phi}^a D_\mu f^{abc} a_\mu^b \phi^c \right) \right].\end{aligned}$$

Thus the ghost term is

$$\mathcal{L}_{\text{gh}} = \bar{\phi}^a (D^2)^{ac} \phi^c + \bar{\phi}^a D_\mu f^{abc} a_\mu^b \phi^c \equiv \bar{\phi}^a (M_{\text{gh}})^{ac} \phi^c + \bar{\phi}^a D_\mu f^{abc} a_\mu^b \phi^c. \quad (3.125)$$

In summary, the gauge fixed Lagrangian in the background field gauge is written as

$$\begin{aligned}\mathcal{L}_{\text{FP}} &= \frac{1}{4g^2} \left(\bar{F}_{\mu\nu}^a + D_\mu a_\nu^a - D_\nu a_\mu^a + f^{abc} a_\mu^b a_\nu^c \right)^2 + \frac{1}{2\xi g^2} (D_\mu a_\mu)^2 \\ &\quad - \bar{\psi} (i\gamma_\mu D_\mu + im) \psi - a_\mu^a \bar{\psi} \gamma_\mu T^a \psi + \bar{\phi}^a (D^2)^{ac} \phi^c + \bar{\phi}^a D_\mu f^{abc} a_\mu^b \phi^c, \quad (3.126)\end{aligned}$$

where

$$D_\mu \psi = \partial_\mu \psi + i\bar{A}_\mu^a T^a \psi, \quad (3.127)$$

$$D_\mu a_\nu^a = \partial_\mu a_\nu^a + f^{abc} \bar{A}_\mu^b a_\nu^c \equiv (D_\mu)^{ab} a_\nu^b, \quad (3.128)$$

$$D_\mu \alpha^a = \partial_\mu \alpha^a + f^{abc} \bar{A}_\mu^b \alpha^c \equiv (D_\mu)^{ab} \alpha^b, \quad (3.129)$$

$$D_\mu \phi^a = \partial_\mu \phi^a + f^{abc} \bar{A}_\mu^b \phi^c \equiv (D_\mu)^{ab} \phi^b. \quad (3.130)$$

\mathcal{L}_{FP} has the local symmetries as

$$\begin{aligned} \bar{A}_\mu^a &\rightarrow \bar{A}_\mu^a + D_\mu \alpha^a, \\ a_\mu^a &\rightarrow a_\mu^a - f^{abc} \alpha^b a_\mu^c, \\ \psi &\rightarrow \psi + i\alpha^a T^a \psi, \\ \phi^a &\rightarrow \phi^a - f^{abc} \alpha^b \phi^c. \end{aligned} \quad (3.131)$$

More explicitly, \mathcal{L}_{FP} is

$$\begin{aligned} \mathcal{L}_{\text{FP}} &= \frac{1}{4g^2} \bar{F}_{\mu\nu}^a \bar{F}_{\mu\nu}^a + \mathcal{L}_a + \mathcal{L}'_a - \bar{\psi}(i\gamma_\mu D_\mu + im)\psi - a_\mu^a \bar{\psi} \gamma_\mu T^a \psi + \bar{\phi}^a (D^2)^{ac} \phi^c + \bar{\phi}^a D_\mu f^{abc} a_\mu^b \phi^c, \\ \mathcal{L}_a &= \frac{1}{2g^2} \left[\frac{1}{2} (D_\mu a_\nu^a - D_\nu a_\mu^a)^2 + \bar{F}_{\mu\nu}^a f^{abc} a_\mu^b a_\nu^c \right] + \frac{1}{2\xi} (D_\mu a_\mu^a)^2, \\ \mathcal{L}'_a &= \frac{1}{2g^2} \left[(D_\mu a_\nu^a - D_\nu a_\mu^a) f^{abc} a_\mu^b a_\nu^c + \frac{1}{2} f^{abc} a_\mu^b a_\nu^c f^{ade} a_\mu^d a_\nu^e \right]. \end{aligned} \quad (3.132)$$

By using the relations $-i\bar{F}_{\mu\nu} = [D_\mu, D_\nu]$ and $(T^b)^{ac} = if^{abc}$, \mathcal{L}_a is modified as below.

$$\begin{aligned} \mathcal{L}_a &= \frac{1}{2g^2} \left[a_\mu^a (-D^2)^{ab} a_\mu^b + a_\mu^a (D_\nu D_\mu)^{ab} a_\nu^b - \frac{1}{\xi} a_\mu^a (D_\mu D_\nu)^{ab} a_\nu^b - a_\mu^a f^{abc} \bar{F}_{\mu\nu}^b a_\nu^c \right], \\ &= \frac{1}{2g^2} \left[a_\mu^a (-D^2)^{ab} a_\mu^b + a_\mu^a (D_\mu D_\nu)^{ab} a_\nu^b + a_\mu^a ([D_\nu, D_\mu])^{ab} a_\nu^b - \frac{1}{\xi} a_\mu^a (D_\mu D_\nu)^{ab} a_\nu^b - a_\mu^a f^{abc} \bar{F}_{\mu\nu}^b a_\nu^c \right], \\ &= \frac{1}{2g^2} \left[a_\mu^a (-D^2)^{ab} a_\mu^b + a_\mu^a (D_\mu D_\nu)^{ab} a_\nu^b - 2ia_\mu^a (\bar{F}_{\mu\nu})^{ab} a_\nu^b - \frac{1}{\xi} a_\mu^a (D_\mu D_\nu)^{ab} a_\nu^b \right], \\ &\equiv \frac{1}{2g^2} a_\mu^a \left((M_A)_{\mu\nu}^{ab} - \frac{1}{\xi} (D_\mu D_\nu)^{ab} \right) a_\nu^b, \end{aligned} \quad (3.133)$$

where

$$(M_A)_{\mu\nu}^{ab} = (-D^2)^{ab} g_{\mu\nu} + (D_\mu D_\nu)^{ab} - 2i(\bar{F}_{\mu\nu})^{ab}. \quad (3.134)$$

In summary, we obtain

$$\mathcal{L}_{\text{FP}} = \frac{1}{4g^2} \bar{F}_{\mu\nu}^a \bar{F}_{\mu\nu}^a + \mathcal{L}_2 + \mathcal{L}_{\text{int}}, \quad (3.135)$$

$$\mathcal{L}_2 = \frac{1}{2g^2} a_\mu^a \left((M_A)_{\mu\nu}^{ab} - \frac{1}{\xi} (D_\mu D_\nu)^{ab} \right) a_\nu^b + \bar{\phi}^a (D^2)^{ab} \phi^b - \bar{\psi} (i\gamma_\mu D_\mu + m) \psi \quad (3.136)$$

$$\begin{aligned} \mathcal{L}_{\text{int}} = & \frac{1}{2g^2} \left[(D_\mu a_\nu^a - D_\nu a_\mu^a) f^{abc} a_\mu^b a_\nu^c + \frac{1}{2} f^{abc} a_\mu^b a_\nu^c f^{ade} a_\mu^d a_\nu^e \right] \\ & + \bar{\phi}^a D_\mu f^{abc} a_\mu^b \phi^c - a_\mu^a \bar{\psi} \gamma_\mu T^a \psi. \end{aligned} \quad (3.137)$$

3.3.2 Treatment for the collective coordinate

Here we will discuss how to deal with the collective coordinates in the path integral in the quantum field theory. We follow the discussion of C. Bernard [61]. As mentioned in sec. 3.1.2, the existence of the collective coordinates cause the zero mode. Then, the functional integral in terms of the zero mode comes into the divergence, where the change of the integration variable from the coefficient of the zero mode to the collective coordinate will factor out the divergence as the volume integral.

For simplicity we will consider the scalar field B which has the classical background $\bar{B}(\gamma)$ and the quantum fluctuation b as

$$\begin{aligned} B &= \bar{B}(\gamma) + b, \\ S[B] &= \bar{S} + \int d^4x \frac{1}{2} b M_B b + \dots, \end{aligned} \quad (3.138)$$

where the classical field has the single collective coordinate γ and \bar{S} denote the classical action $S[\bar{B}]$, and M_B denote the bilinear term of b . The operator M_B has a complete set of the orthogonal eigenfunction χ_i with the eigenvalue ϵ_i ,

$$M_B \chi_i = \epsilon_i \chi_i, \quad (3.139)$$

$$u_i \equiv \langle \chi_i | \chi_i \rangle = \int d^4x \chi_i \chi_i, \quad (3.140)$$

$$\langle \chi_i | \chi_j \rangle = 0 \quad (i \neq j). \quad (3.141)$$

Using the fact that the first derivative of the action in terms of B is zero, We can calculate

$$0 = \left. \frac{\delta S}{\delta B} \right|_{B=\bar{B}(\gamma+\Delta\gamma)} = \left. \frac{\delta S}{\delta B} \right|_{B=\bar{B}(\gamma)} + \left. \frac{\delta^2 S}{\delta B^2} \right|_{B=\bar{B}} \delta B + \dots \quad (3.142)$$

The relations $M_B = \delta^2 S / \delta B^2$ and $\delta B = (\partial \bar{B} / \partial \gamma) \Delta \gamma$ provide us

$$M_B \frac{\partial \bar{B}}{\partial \gamma} = 0. \quad (3.143)$$

Thus, as for the zero mode which has the zero eigenvalue $\epsilon_0 = 0$, we can express the eigenfunction as

$$\chi_0 = \frac{\partial \bar{B}}{\partial \gamma}. \quad (3.144)$$

The quantum field b can be expanded by the orthogonal set $\{\chi_i\}_{i \geq 0}$ as $b = \sum_{i \geq 0} \xi_i \chi_i$. Then the measure of the functional integral is changed as

$$[dB] = [db] = \prod_{i \geq 0} \sqrt{\frac{u_i}{2\pi}} d\xi_i. \quad (3.145)$$

After the Gaussian integral in terms of the non-zero mode, we obtain

$$\int [dB] e^{-S[B]} = \int \sqrt{\frac{u_0}{2\pi}} d\xi_0 e^{-\bar{S}} [\det' M_B]^{-1/2} + O(\alpha), \quad (3.146)$$

where \det' denotes the determinant without zero mode. Note that the first term of r.h.s. comes take into account only the bilinear term in the action. Then the interaction terms contributes $O(\alpha)$. Following the Faddeev-Popov's prescription, we insert unity

$$1 = \int d\gamma \delta(f(\gamma)) \frac{\partial f}{\partial \gamma}, \quad f(\gamma) = \langle \bar{B}(\gamma) - B | \chi_0(\gamma) \rangle. \quad (3.147)$$

Since B is independent of γ , we can calculate as

$$\begin{aligned} 1 &= \int d\gamma \left(\left\langle \frac{\partial \bar{B}}{\partial \gamma} \middle| \chi_0(\gamma) \right\rangle + \left\langle -b \middle| \frac{\partial \chi_0(\gamma)}{\partial \gamma} \right\rangle \right) \delta(\langle b | \chi_0(\gamma) \rangle), \\ &= \int d\gamma \left(u_0 - \left\langle b \middle| \frac{\partial \chi_0(\gamma)}{\partial \gamma} \right\rangle \right) \delta(\xi_0 u_0), \end{aligned} \quad (3.148)$$

where the second term in the r.h.s. can be ignored at 1-loop level. However, at 2-loop level we need this term. Thus, at 1-loop level we obtain simple form,

$$1 \simeq \int u_0 d\gamma \delta(\xi_0 u_0). \quad (3.149)$$

After inserting eq. 3.149 into eq. 3.146, we obtain

$$\begin{aligned} \int \sqrt{\frac{u_0}{2\pi}} d\xi_0 e^{-\bar{s}} [\det' M]^{-1/2} &= \int \sqrt{\frac{u_0}{2\pi}} d\xi_0 d\gamma u_0 \delta(\xi_0 u_0) e^{-\bar{s}} [\det' M]^{-1/2}, \\ &= \int d\gamma J(\gamma) e^{-\bar{s}} [\det' M]^{-1/2}, \end{aligned} \quad (3.150)$$

where $J(\gamma) = \sqrt{u_0/2\pi}$ is the Jacobian of changes of variables from the gauge zero modes to the collective coordinates.

3.3.3 The collective coordinates of the Yang-Mills instanton

In the pure Yang-Mills theory, there is no dimensionful parameter in the classical action or the Lagrangian. Then classically the conformal symmetry is preserved in this theory. Since the instanton configuration is the classical solution of the equation of motion, the collective coordinates which appear in the instanton are determined by the conformal symmetry. By choosing one instanton solution, some of the conformal symmetry is broken, but they are restored by considering the family of the instanton. The transformation which is no longer a symmetry after choosing the specific instanton solution changes one instanton solution into other instanton solution in the family of instanton. This means such transformation shifts the corrective coordinates of the instanton.

There are 15 transformations in the four dimensional conformal group, i.e. 4 spatial translations, 6 Lorentz rotations, 4 proper conformal transformations, 1 dilation. In

addition to the above transformation, we need to take into account the global rotations in the color space, which has 3 directions in the SU(2) gauge theory. In total, the SU(2) instanton depends on the 18 collective coordinates, including the instanton size ρ and its position z_μ . Hereafter, we consider the other direction than ρ and z_μ .

The proper conformal transformation is the combination of the translations and the inversion, where we have already see the translations provide the collective coordinates, the instanton position z_μ . The inversion is

$$x_\mu \rightarrow x'_\mu = \frac{x_\mu}{x^2}, \quad A_\mu(x) \rightarrow x'^2 A_\mu(x'), \quad (3.151)$$

which means

$$2\eta_{a\mu\nu} \frac{x_\nu}{x^2 + 1} \rightarrow x'^2 2\eta_{a\mu\nu} \frac{x'_\nu}{x'^2 + 1} = 2\eta_{a\mu\nu} \frac{x_\nu}{x^2(x^2 + 1)}, \quad (3.152)$$

where we fix $\rho = 1$. The inversion change one instanton into one anti-instanton in the singular gauge. Thus, no new collective coordinates appear from the proper conformal transformation.

In the following, we will consider that 3 collective coordinates appear from the linear combinations of the 6 generators of the Euclidean rotation and the 3 generators of the color rotation.

First, we introduce the generator which represent the $SO(4) = SU(2)_L \times SU(2)_R$ rotation. We define $V_{\alpha\dot{\alpha}}$ for any four-vector in the Euclidean space,

$$V_{\alpha\dot{\alpha}} = (\tau_\mu^+)_{\alpha\dot{\alpha}} V_\mu, \quad (\mu = 1, \dots, 4, \alpha, \dot{\alpha} = 1, 2), \quad (3.153)$$

where $\tau_\mu^+ = \{\tau^a, i1_{2 \times 2}\}$ ($a = 1, 2, 3$). The Greek indices α and $\dot{\alpha}$ are transformed by $SU(2)_L$ and $SU(2)_R$, respectively. The anti-symmetric tensor is introduced in order to lift up or let down the Greek indices,

$$\chi^\alpha = \epsilon^{\alpha\beta} \chi_\beta, \quad \chi_\alpha = \epsilon_{\alpha\beta} \chi^\beta, \quad (3.154)$$

where $\epsilon^{\alpha\beta} = -\epsilon^{\beta\alpha}$ and $\epsilon^{12} = -\epsilon_{12} = 1$.

The explicit computation of the coordinate vector is as follows:

$$\begin{aligned}
x_1^1 &= \epsilon^{12} x_{21} \\
&= (\tau_\mu^+)_{21} x_\mu \\
&= (\tau_1^+)_{21} x_1 + (\tau_2^+)_{21} x_2 \\
&= x_1 + ix_2.
\end{aligned} \tag{3.155}$$

By the straightforward computation,

$$x_2^1 = ix_4 - x_3, \tag{3.156}$$

$$x_1^2 = -ix_4 - x_3, \tag{3.157}$$

$$x_2^2 = -x_1 + ix_2. \tag{3.158}$$

Using this notation, the BPST instanton is expressed as

$$A_{\alpha\dot{\beta}}^{\eta\xi} = \frac{i}{x^2 + \rho^2} \left(x_{\dot{\beta}}^\eta \delta_\alpha^\xi + x_{\dot{\beta}}^\xi \delta_\alpha^\eta \right), \tag{3.159}$$

where the indices η, ξ couple with the global color rotation as

$$A_\mu^{\eta\xi} = \frac{1}{2} A_\mu^a (\tau^a)_\delta^\eta \epsilon^{\xi\delta}. \tag{3.160}$$

The field strength is represented as

$$F_{\alpha\beta}^{\gamma\delta} = 4i \frac{\rho^2}{(x^2 + \rho^2)^2} \left(\delta_\alpha^\gamma \delta_\beta^\delta + \delta_\beta^\gamma \delta_\alpha^\delta \right), \tag{3.161}$$

$$F_{\dot{\alpha}\dot{\beta}}^{\gamma\delta} = 0, \tag{3.162}$$

where

$$(\tau_\mu^+)_{\alpha\dot{\alpha}} (\tau_\nu^+)_{\beta\dot{\beta}} F_{\mu\nu} = \epsilon_{\dot{\alpha}\dot{\beta}} F_{\alpha\beta} + \epsilon_{\alpha\beta} F_{\dot{\alpha}\dot{\beta}}. \tag{3.163}$$

Here, the Lorentz rotation and the color rotation of the gauge field A_μ . Under the global color rotation, gauge field A is transformed as $A \rightarrow M^\dagger A M$, which is explicitly

written as

$$A^{\alpha\beta} \rightarrow (M^\dagger)_\gamma^\alpha (M^\dagger)_\delta^\beta A^{\gamma\delta}, \quad (3.164)$$

where $M = \exp(i\omega^a \tau^a / 2)$ and ω^a ($a = 1, 2, 3$) correspond to 3 parameters of the global color rotation.

As for the $SO(4) = SU(2)_L \times SU(2)_R$ rotation, the coordinate x is transformed as

$$x_\beta^\eta \rightarrow L_\alpha^\eta x_\beta^\alpha, \quad (3.165)$$

$$x_{\alpha\beta} \rightarrow (L^\dagger)_\alpha^\gamma x_{\gamma\beta}, \quad (3.166)$$

$$x_{\alpha\dot{\beta}} \rightarrow (R)_{\dot{\beta}}^{\dot{\alpha}} x_{\alpha\dot{\alpha}}, \quad (3.167)$$

$$x_\alpha^{\dot{\beta}} \rightarrow (R^\dagger)_{\dot{\alpha}}^{\dot{\beta}} x_\alpha^{\dot{\alpha}}, \quad (3.168)$$

where $L \in SU(2)_L$ and $R \in SU(2)_R$. The gauge field A is transformed as

$$A_{\alpha\dot{\beta}}^{\eta\xi} \rightarrow (R)_{\dot{\beta}}^{\dot{\alpha}} A_{\alpha\dot{\alpha}}^{\eta\xi}, \quad (3.169)$$

$$A_{\alpha\dot{\beta}}^{\eta\xi} = i \frac{x_\beta^\eta \delta_\alpha^\xi + x_\beta^\xi \delta_\alpha^\eta}{x^2 + \rho^2} \rightarrow (L^\dagger)_\alpha^\beta A_{\beta\dot{\beta}}^{\eta\xi} = i \frac{(L^\dagger)_\alpha^\xi x_\beta^\eta + (L^\dagger)_\alpha^\eta x_\beta^\xi}{x^2 + \rho^2}, \quad (3.170)$$

where $SU(2)_R$ does not change the instanton, while $SU(2)_L$ does.

When the gauge field A is transformed by the global color rotation and $SU(2)_L$ simultaneously,

$$A_{\alpha\dot{\beta}}^{\eta\xi} = \frac{i}{x^2 + \rho^2} (M^\dagger)_{\eta'}^\eta (M^\dagger)_{\xi'}^\xi (L_Y^{\eta'} L_\alpha^{\xi'} x_\beta^\gamma + L_Y^{\xi'} L_\alpha^{\eta'} x_\beta^\gamma). \quad (3.171)$$

If we choose $L = M$, the instanton field is unchanged. Then, only the 3 transformation is independent among the 6 global color rotation and 3 $SU(2)_L$ rotation. The corrective coordinates in terms of these 3 rotation are introduced as follows,

$$\eta_{a\mu\nu} \rightarrow O_{ab} \eta_{b\mu\nu}, \quad \bar{\eta}_{a\mu\nu} \rightarrow O_{ab} \bar{\eta}_{b\mu\nu}, \quad (3.172)$$

where O denotes 3×3 orthogonal matrix

$$O_{ab} = \frac{1}{2} \text{Tr}(M \tau^a M^\dagger \tau^b). \quad (3.173)$$

3.3.4 Calculation of the Yang-Mills instanton density

Consider the vacuum amplitude between two n -vacua e.g. from $|n\rangle$ to $|m\rangle$, the difference of the winding number $m - n = Q$ is the topological charge. If $Q = 0$, the perturbative contribution dominates the amplitude. However, if $Q \neq 0$, the transition occurs only by the contribution from the (anti-)instantons in the background. As we have seen in sec. 3.1.2, any combination of the n_I instantons and the $n_{\bar{I}}$ anti-instantons with $n_I - n_{\bar{I}} = Q$ can contribute. Assuming the (anti-)instantons are well separated so that the interaction between them is negligible, the dilute instanton contribution is valid. In this case, the amplitude with multiple (anti-)instantons can be constructed from the amplitude of the single instanton as a building block.

We will consider the ratio of two vacuum amplitude of $Q = 1$ and $Q = 0$. Here we assume the contribution of the single instanton dominates the amplitude with $Q = 1$.

$$Z_{Q=1} = \int_{\epsilon_{Q=1}} [da_\mu^a d\bar{c}dc d\psi d\bar{\psi}] \exp\left(-\int d^4x \mathcal{L}_{\text{FP}}\right) \quad (3.174)$$

We define the instanton density,

$$\begin{aligned} \frac{Z_{Q=1}}{Z_{Q=0}} &= \int [d\gamma] J(\gamma) e^{-\frac{8\pi^2}{g^2}} \exp(-\Gamma^A - \Gamma^{\text{gh}} - \Gamma^F) + O(\alpha_s), \\ &\equiv \int \frac{d^4z d\rho}{\rho^5} n(\rho) + O(\alpha_s), \end{aligned} \quad (3.175)$$

where γ represents the set of the collective coordinates of the Yang-Mills instanton solution which we clarify in sec. 3.3.3. The first term of the r.h.s. is result at 1-loop level which is so-called semi-classical approximation, where only the bilinear term of the fields in the \mathcal{L}_{FP} shown in eq. 3.136 is considered. The interaction term shown in eq. 3.137 is expanded from the exponential by order of the strong couplings α_s . Then, the $O(\alpha_s)$ contains the contribution at more than 2-loop level. $J(\gamma)$ denotes the Jacobian which appears in the change of variables from the gauge zero modes to the collective coordinates. Here the instanton position z_μ and the instanton size ρ is the collective coordinates. In order to make the density $n(\rho)$ dimensionless we choose the measure $d^4z d\rho/\rho^5$. The density is independent of the scale,

$$\frac{d}{d \ln \mu} n(\rho) = 0. \quad (3.176)$$

Γ^A , Γ^{gh} , and Γ^F are the effective action in the single instanton background of the gauge field, the ghost field, and the fermion, respectively. The ultraviolet part of these effective action is regularized divided by $Z_{Q=0}$.

In the semi-classical approximation, the effective action of the gauge field is

$$-\Gamma^A = \log \left[\frac{\det' \left((M_A)_{\mu\nu} - \frac{1}{\xi} D_\mu D_\nu \right) \Big|_{Q=1}}{\det' \left((M_A)_{\mu\nu} - \frac{1}{\xi} \partial_\mu \partial_\nu \right) \Big|_{Q=0}} \right]^{-\frac{1}{2}}, \quad (3.177)$$

where the operator $(M_A)_{\mu\nu}$ in $Q = 1$ sector is defined in eq. 3.134 and D_μ in $Q = 1$ sector is the covariant derivative for a_μ^a is defined in eq. 3.128. As for the $(M_A)_{\mu\nu}$ in $Q = 0$ sector is obtained by substituting $\bar{A}_\mu = 0$ to the $(M_A)_{\mu\nu}$ in $Q = 1$ sector.

The contribution from the ghost in the single instanton background is

$$-\Gamma^{\text{gh}} = \log \frac{\det(-D^2)|_{Q=1}}{\det(-\partial^2)|_{Q=0}}, \quad (3.178)$$

where the covariant derivative for the ghost in $Q = 1$ sector is defined in eq. 3.129.

The fermion contribution is written as

$$-\Gamma^F = \log \prod_{f=1}^{N_f} \frac{\det(-i\gamma_\mu D_\mu - im_f)|_{Q=1}}{\det(-i\gamma_\mu D_\mu - im_f)|_{Q=0}}, \quad (3.179)$$

where the covariant derivative for the fermion in $Q = 1$ sector is defined in eq. 3.130.

3.3.5 Calculation of $J(\gamma)$ in the semi-classical approximation

In the $SU(N)$ Yang-Mills theory the number of the zero mode is $4N$. The gauge zero mode is written as

$$z_\mu^{j,a}(x, \gamma^i) = \frac{\delta}{\delta \gamma^j} \bar{A}_\mu^a(x, \gamma^i) + D_\mu \Lambda^{i,a}(x, \gamma). \quad (3.180)$$

The gauge field a_μ^a in the single instanton background can be expanded by the orthogonal set $\{z_\mu^{i,a}(x, \gamma), q_\mu^{n,a}(x, \gamma)\}$ for $i = 1, \dots, 4N - 5$ and $n \in Z_{>0}$, where $z_\mu^{i,a}$ denotes the gauge zero mode and $q_\mu^{n,a}$ is the non-zero mode. For simplicity we omit the indices of the collective coordinates as γ . These zero modes and non-zero modes

have norm as follows,

$$\langle q_\mu^{n,a}(x, \gamma) | q_\mu^{m,a}(x, \gamma) \rangle \equiv \|q_\mu^{n,a}(\gamma, x)\|^2 \delta_{nm}, \quad (3.181)$$

$$\langle z_\mu^{i,a}(x, \gamma) | z_\mu^{j,a}(x, \gamma) \rangle \equiv \|z_\mu^{i,a}(\gamma, x)\|^2 \delta_{ij}, \quad (3.182)$$

$$\langle z_\mu^{i,a}(x, \gamma) | q_\mu^{n,a}(x, \gamma) \rangle = 0. \quad (3.183)$$

Then we can expand the gauge field A_μ as

$$A_\mu^a(x) = \bar{A}_\mu^a(x, \gamma) + a_\mu^a(x) = \bar{A}_\mu^a(x, \gamma) + \sum_{i=1}^{4N} \xi^i z_\mu^{i,a}(x, \gamma). \quad (3.184)$$

The measure of the functional integral is written as

$$[da_\mu^a] = \left[\prod_{i=1}^{4N} \frac{\|z_\mu^{i,a}\| d\xi^i}{\sqrt{2\pi}} \prod_{n=1}^{\infty} \frac{\|q_\mu^{n,a}\| d\xi^n}{\sqrt{2\pi}} \right] \equiv \left[\prod_{i=1}^{4N} \frac{\|z_\mu^{i,a}\| d\xi^i}{\sqrt{2\pi}} d' a_\mu^a \right], \quad (3.185)$$

where $[d'a]$ denotes the measure of the non-zero modes. Likewise the Faddeev-Popov's prescription, we introduce unity of the collective coordinates integration,

$$1 = \mathcal{N} \int \prod_{i,j=1}^{4N} [d\gamma^j] \delta(\langle a_\mu^a(x) | z_\mu^{i,a}(x, \gamma) \rangle) \det(J^{i,j}), \quad (3.186)$$

where $J^{i,j}$ can be calculated as follows.

$$\begin{aligned} J^{i,j} &= \frac{\partial \langle a_\mu^a(x) | z_\mu^{i,a}(x, \gamma) \rangle}{\partial \gamma^j}, \\ &= \left\langle \frac{\partial a_\mu^a(\gamma, x)}{\partial \gamma^j} \middle| z_\mu^a(\gamma, x) \right\rangle + \left\langle a_\mu^a(\gamma, x) \middle| \frac{\partial z_\mu^{i,a}(\gamma, x)}{\partial \gamma^j} \right\rangle, \\ &= - \int d^4x \left((z_\mu^{j,a} - D_\mu \Lambda^a) z_\mu^{i,a} \right) + \left\langle a_\mu^a(\gamma, x) \middle| \frac{\partial z_\mu^{i,a}(\gamma, x)}{\partial \gamma^j} \right\rangle, \\ &= - \langle z_\mu^{i,a} | z_\mu^{j,a} \rangle + \left\langle a_\mu^a(\gamma, x) \middle| \frac{\partial z_\mu^{i,a}(\gamma, x)}{\partial \gamma^j} \right\rangle. \end{aligned} \quad (3.187)$$

In the third equality, we use $a_\mu^a(x, \gamma) = A_\mu^a(x) - \bar{A}_\mu^a(x, \gamma)$ and $\partial A_\mu^a(x)/\partial \gamma^i = 0$ and the gauge fixing condition $D_\mu a_\mu^a \ni D_\mu z_\mu^{i,a} = 0$. At 1-loop level, the second term in the

last line does not contribute the amplitude. Then, we obtain $J^{i,j} = \|z_\mu^{i,a}(\gamma, x)\|^2 \delta_{ij}$ and $\det(J) = \prod_{i=1}^{4N} \|z_\mu^{i,a}\|^2$.

$$\begin{aligned}
\int [da_\mu^a] &= \mathcal{N} \int \left[\prod_{i,j=1}^{4N} d\gamma^j \frac{\|z_\mu^{i,a}\| d\xi^i}{\sqrt{2\pi}} d' a_\mu^a \right] \delta \left(\langle a_\mu^a(x) | z_\mu^{i,a}(\gamma, x) \rangle \right) \det(J) \\
&= \mathcal{N} \int \left[\prod_{i,j=1}^{4N} d\gamma^j \frac{\|z_\mu^{i,a}\| d\xi^i}{\sqrt{2\pi}} d' a_\mu^a \right] \frac{\delta(\xi^i)}{\det(J)^{1/2}} \det(J) \\
&= \mathcal{N} \int \left[\prod_{i=1}^{4N} \frac{d\gamma^j}{\sqrt{2\pi}} d' a_\mu^a \right] \det(J) \\
&\equiv \mathcal{N} \int [d\gamma d' a_\mu^a] \prod_{i=1}^{4N} \frac{\|z_\mu^{i,a}\|}{\sqrt{2\pi}}, \tag{3.188}
\end{aligned}$$

where we define $J(\gamma) = \prod_{i=1}^{4N} (\|z_\mu^{i,a}\|/\sqrt{2\pi})$. The Jacobian $J(\gamma)$ can be calculated in the $SU(N)$ gauge theory as

$$J(\gamma) = \frac{4}{\rho^5} \left(\frac{2\rho\sqrt{\pi}}{g} \right)^{4N}. \tag{3.189}$$

3.3.6 Calculation of $\Gamma^A + \Gamma^{\text{gh}}$

First, we show the result of the gluon and ghost contribution to the the effective action, following 't Hooft's seminal paper [19],

$$e^{-\Gamma^A - \Gamma^{\text{gh}}} = \mu^{4N} \exp \left[-\frac{N}{3} \ln(\mu\rho) - \alpha(1) - 2(N-2)\alpha(1/2) \right], \tag{3.190}$$

where

$$\alpha(t) \equiv C(t) \left[2R - \frac{1}{6} \ln 2 + \frac{1}{2} \sum_{s=1}^{2t+1} s(2t+1-s) \left(s - t - \frac{1}{2} \right) \ln s - \frac{1}{6} t(t+1) - \frac{1}{9} \right], \tag{3.191}$$

$$C(t) = \frac{2}{3} t(t+1)(2t+1), \tag{3.192}$$

$$R = \frac{1}{12} (\ln 2\pi + \gamma) + \frac{1}{2\pi^2} \sum_{s=2}^{\infty} \frac{\ln s}{s^2} \approx 0.248754. \tag{3.193}$$

The instanton size dependence ρ of the effective action is

$$e^{-\Gamma^A - \Gamma^{\text{gh}}} \propto (\mu\rho)^{4N} \exp\left(-\frac{N}{3} \ln(\mu\rho)\right) = (\mu\rho)^{\frac{11}{3}N}, \quad (3.194)$$

where the index $11N/3$ is the beta function coefficients.

The integration over the collective coordinates $[d\gamma]$ is calculated as follows. Since the integrand is independent of the collective coordinates other than z_μ and ρ , those direction can be integrated out and turns into the volume integral,

$$\int [d\gamma] = \int d^4z d\rho \text{Vol}\left(\frac{SU(N)}{T_N}\right), \quad (3.195)$$

where T_N is the direction of the gauge transformation which does not change the instanton solution. The explicit calculation of $\text{Vol}(SU(N)/T_N)$ is written in the paper of Bernard [61], which provides

$$\text{Vol}\left(\frac{SU(N)}{T_N}\right) = \frac{\pi^{2N-2}}{(N-1)!(N-2)!}. \quad (3.196)$$

In summary, the gluon and ghost contribution to the instanton density $n_G(\rho)$,

$$\begin{aligned} \frac{Z_{Q=1}}{Z_{Q=0}} &= \int \frac{d^4z d\rho}{\rho^5} n_G(\rho) n_F(\rho), \\ n_G(\rho) &= \rho^5 \text{Vol}\left(\frac{SU(N)}{T_N}\right) J(\gamma) \exp(-\Gamma^A - \Gamma^{\text{gh}}) e^{-\tilde{S}}, \\ &= \frac{4\pi^{2N-2}}{(N-1)!(N-2)!} \left(\frac{2\sqrt{\pi}}{g}\right)^{4N} (\mu\rho)^{\frac{11}{3}N} \exp\left(-\alpha(1) - 2(N-2)\alpha\left(\frac{1}{2}\right)\right) e^{-\frac{8\pi^2}{g^2}}, \\ &= C_I (\mu\rho)^{\frac{11}{3}N} \left(\frac{8\pi^2}{g^2(\mu)}\right)^{2N} e^{-8\pi^2/g^2(\mu)}, \end{aligned} \quad (3.197)$$

$$C_I = \frac{1}{4^N} \frac{2 e^{5/6}}{\pi^2 (N-1)!(N-2)!} e^{-2N\alpha + \frac{N}{6}} \quad (3.198)$$

where in the last equality we use $4\alpha(1/2) = \alpha(1) - \log 2 + 5/6$.

3.3.7 Calculation of Γ^F

The fermion part of the effective action is originally calculated by 't Hooft [19] using the massless fermion. In the large fermion mass limit, Γ^F is also calculated in the literature [64, 65]. In the region of the arbitrary fermion mass, actually they use the dimensionless variable ($m\rho$), the interpolating result is obtained by Dunne *et al.* [62]. Hereafter, we will show the Γ^F following Dunne *et al.* [62].

The fermion contribution to the renormalized effective action at 1-loop level Γ^F is written as follows,

$$\Gamma^F(m\rho) = -2 \left(\tilde{\Gamma}^S(m\rho) + \frac{1}{6} \log(\mu\rho) \right) - \log \left(\frac{m}{\mu} \right), \quad (3.199)$$

where μ is the renormalization scale and $\tilde{\Gamma}^S$ is the scalar effective action.

Using the above notation, the fermion contribution to the instanton density is obtained as

$$n_F(\rho) = e^{-\Gamma^F} = (\mu\rho)^{-\frac{2}{3}N_f} \prod_{f=1}^{N_f} (m_f\rho) e^{2\tilde{\Gamma}^S(m_f\rho)}. \quad (3.200)$$

Combining this ρ dependence with the gluon and the ghost contribution to the instanton density in eq. 3.194,

$$\begin{aligned} n(\rho) &\propto \exp(-\Gamma^A - \Gamma^{\text{gh}}) \exp(-\Gamma^F) \\ &\propto (\mu\rho)^{\frac{11}{3}N - \frac{2}{3}N_f} \\ &= (\mu\rho)^{\beta_0}. \end{aligned} \quad (3.201)$$

The scalar fermion function $\tilde{\Gamma}^S(m\rho)$ is known as follows. In the $m\rho \rightarrow 0$ limit [19, 66, 64],

$$\tilde{\Gamma}^S(m\rho) = \alpha \left(\frac{1}{2} \right) + \frac{1}{2} (\log(m\rho) + \gamma - \log 2) (m\rho)^2 + \dots, \quad (3.202)$$

$$e^{-\Gamma^F} = (\rho\mu)^{-\frac{2}{3}N_f} e^{2N_f\alpha(\frac{1}{2})} \prod_{f=1}^{N_f} (m_f\rho) e^{O((m_f\rho)^2)}. \quad (3.203)$$

In the $m\rho \rightarrow \infty$ limit [64, 65],

$$\tilde{\Gamma}^S(m\rho) = -\frac{1}{6} \log(m\rho) - \frac{1}{75(m\rho)^2} - \frac{17}{735(m\rho)^4} + \frac{232}{2835(m\rho)^6} - \frac{7916}{148225(m\rho)^8} \quad (3.204)$$

$$e^{-\Gamma^F}(\mu\rho) = (\mu\rho)^{-\frac{2}{3}N_f} \prod_{f=1}^{N_f} (m_f\rho)^{\frac{2}{3}} e^{-\frac{2}{75(m_f\rho)^2} + \mathcal{O}\left(\frac{1}{(m_f\rho)^4}\right)} \quad (3.205)$$

In the region of the arbitrary $m\rho$, the fitting of the interpolating function using Pade approximation which is consistent with the above two limit is obtained by Kown *et al.* [64]. The analytic calculation of the fermion determinant is performed by Dunne *et al.* [62]. Using the analytic formula they obtained, they numerically obtain the curve of $\tilde{\Gamma}^S(m\rho)$, which is fit using the following fitting function,

$$\tilde{\Gamma}^S(m\rho) = -\frac{1}{6} \log(m\rho) + \frac{\frac{1}{6} \log(m\rho) + \alpha - (3\alpha + c)(m\rho)^2 + A_1(m\rho)^4 - A_2(m\rho)^6}{1 - 3(m\rho)^2 + B_1(m\rho)^4 + B_2(m\rho)^6 + B_3(m\rho)^8} \quad (3.206)$$

Finally, the fermion contribution to the effective action in the single instanton background is obtained as

$$n_F(\rho) = e^{-\Gamma^F} = (\mu\rho)^{-\frac{2}{3}N_f} \prod_{f=1}^{N_f} (m_f\rho)^{\frac{2}{3}} \times \exp\left(2 \frac{\frac{1}{6} \log(m_f\rho) + \alpha - (3\alpha + c)(m_f\rho)^2 + A_1(m_f\rho)^4 - A_2(m_f\rho)^6}{1 - 3(m_f\rho)^2 + B_1(m_f\rho)^4 + B_2(m_f\rho)^6 + B_3(m_f\rho)^8}\right) \quad (3.207)$$

where

$$\begin{aligned} \alpha &\equiv \alpha\left(\frac{1}{2}\right) \simeq 0.145873, & c &\equiv \frac{1}{2}(\ln 2 - \gamma) \simeq 0.05797, \\ a_1 &= -13.4138, & a_2 &= 2.64587, \\ b_1 &= 25 \left(\frac{592955}{21609} a_2 + \frac{255}{49} a_1 + 9\alpha + 3\beta' \right), & b_2 &= -75 \left(\frac{85}{49} a_2 + a_1 \right), \\ b_3 &= 75a_2, \end{aligned}$$

$$\begin{aligned}
\beta' &= \beta_0 + \left(\beta_1 - 4\beta_0 N + \gamma_0 N_f\right) \frac{g^2(\mu)}{16\pi^2}, \\
\beta_0 &= \frac{11}{3}N - \frac{2}{3}N_f, \quad \beta_1 = \frac{34}{3}N^2 - \left(\frac{13}{3}N - \frac{1}{N}\right)N_f, \\
\gamma_0 &= 3\frac{N^2 - 1}{N}
\end{aligned} \tag{3.208}$$

3.3.8 The Yang-Mills instanton density at zero temperature

Combining the conclusion of sec. 3.3.5, sec. 3.3.6 and sec. 3.3.7, the instanton density in the SU(N) Yang-Mills theory with fermion is summarized as follows,

$$\begin{aligned}
\frac{Z_{Q=1}}{Z_{Q=0}} &= \int \frac{d^4z d\rho}{\rho^5} n(\rho), \\
n(\rho) &= n_G(\rho)n_F(\rho), \\
&= (\mu\rho)^\beta \frac{2e^{5/6}}{\pi^2(N-1)!(N-2)!} e^{-2\alpha(\frac{1}{2})N + \frac{N}{6}} \left(\frac{2\pi}{g(\mu)}\right)^{4N} e^{-\frac{8\pi^2}{g^2(\mu)}} \\
&\times \begin{cases} e^{2N_f\alpha(\frac{1}{2})} \prod_{f=1}^{N_f} (m_f\rho) e^{O((m_f\rho)^2)} & m_f\rho \rightarrow 0 \\ \prod_{f=1}^{N_f} (m_f\rho)^{\frac{2}{3}} e^{-\frac{2}{75(m_f\rho)^2} + O\left(\frac{1}{(m_f\rho)^4}\right)} & m_f\rho \rightarrow \infty \end{cases} \tag{3.209} \\
&\quad \left[\prod_{f=1}^{N_f} (m_f\rho)^{\frac{2}{3}} \exp\left(2\frac{\frac{1}{6}\log(m_f\rho) + \alpha - (3\alpha + c)(m_f\rho)^2 + A_1(m_f\rho)^4 - A_2(m_f\rho)^6}{1 - 3(m_f\rho)^2 + B_1(m_f\rho)^4 + B_2(m_f\rho)^6 + B_3(m_f\rho)^8}\right) \right] \forall m_f\rho
\end{aligned}$$

At the 1-loop level,

$$\beta = \beta_0 = \frac{11}{3}N - \frac{2}{3}N_f, \tag{3.210}$$

The exponent $N/6$ in eq. 3.209 is depend on the renormalization scheme. In the Pauli-Villas regularization, $e^{N/6}$ does not appear, while in the $\overline{\text{MS}}$ scheme it does appear [67]. Morris *et al.* [68] partially calculate the 2-loop correction to the effective action in the massless fermion limit and obtain the μ -independent instanton density by modify β as

$$\beta = \beta_0 + \left(\beta_1 - 4\beta_0 N + \gamma_0 N_f\right) \frac{g^2(\mu)}{16\pi^2}, \tag{3.211}$$

where $\beta_0 = \frac{11}{3}N - \frac{2}{3}N_f$, $\beta_1 = \frac{34}{3}N^2 - \left(\frac{13}{3}N - \frac{1}{N}\right)N_f$, $\gamma_0 = 3\frac{N^2-1}{N}$, by which the scale

independence of the instanton density is manifest,

$$\frac{\partial}{\partial \ln \mu} n(\rho) = 0. \quad (3.212)$$

3.3.9 The finite temperature correction

In the finite temperature QCD, the instanton density $n(\rho, T)$ is defined as

$$\frac{Z_{Q=1}}{Z_{Q=0}} = \int_0^{1/T} dz_4 \int \frac{d^3 \vec{z} d\rho}{\rho^5} n(\rho, T), \quad (3.213)$$

$$n(\rho, T) = n_G(\rho) n_F(\rho) n_T(\pi\rho T), \quad (3.214)$$

where $n_G(\rho)$ and $n_F(\rho)$ are the gluon and fermion contribution to the instanton density at zero temperature. $n_G(\rho)$ is written in eq. 3.197, and $n_F(\rho)$ is written in eq. 3.207. At zero temperature, the integration in terms of ρ ,

$$\int_0^\infty \frac{d\rho}{\rho^5} n_G(\rho) n_F(\rho), \quad (3.215)$$

is IR divergent. However, by taking into account the thermal fluctuation this integral becomes finite at finite temperature [20] since the Debye screening exponentially suppresses the large size instanton. This effect is embedded in $n_T(\lambda)$, which is known to be

$$\begin{aligned} n_T(\lambda) &= \exp \left[-\frac{1}{3} (2N + N_f) \lambda^2 - 12A(\lambda) \left(1 + \frac{1}{6} (N - N_f) \right) \right], \\ A(\lambda) &= -\frac{1}{12} \log \left(1 + \frac{\lambda^2}{3} \right) + c_1 \left(\frac{1}{1 + c_2 \lambda^{-\frac{3}{2}}} \right)^8, \end{aligned} \quad (3.216)$$

where $\lambda = \pi\rho T$, $c_1 = 0.01289764$, and $c_2 = 0.15858$. In eq. 3.216, apparently the distribution of the instanton size ρ is cutoff by the Gaussian suppression, $n_T(\pi\rho T) \propto \exp \left(-(2N_c + N_f)(\pi\rho T)^2/3 \right)$, which suppress the large size instanton larger than the scale $\rho_{\text{cut}} \sim 1/\pi T$.

The instanton density denote the quantum weight of the the size and the position of the instanton. Since the instanton density is independent of the position z_μ , the instanton settle at anywhere in R^4 and R^3 at zero temperature and finite temperature, respectively. However, the density is a function of the instanton size. At zero tem-

3.4 The calculation of the topological susceptibility at finite temperature 61

perature, the function $n_G(\rho)/\rho^5$ is an increasing function of ρ , namely the large size instanton dominates the functional integral without IR cutoff in the infinite volume. Thus, the dilute gas picture of the instanton does not make sense at zero temperature. On the other hand, at finite temperature the function $n_G(\rho)n_T(\tau\rho T)/\rho^5$ is effectively cutoff at size $\rho_{\text{cut}} \sim 1/\pi T$. Then, as the temperature of the Yang-Mills gas increases, the typical instanton size in the system decreases. This is consistent with the fact that the instanton calculus of the topological susceptibility in the $SU(N)$ gauge theory at high temperature is consistent with the numerical results using lattice simulation.

3.4 The calculation of the topological susceptibility at finite temperature

Collecting the above expressions, the DIGA predicts the topological susceptibility $\chi_t(T)$ at finite temperature to be

$$\chi_t(T)V_4 \approx \frac{Z_{Q=1} + Z_{Q=-1}}{Z_{Q=0}} = 2 \int d^4z \int_0^\infty \frac{d\rho}{\rho^5} n(\rho, T). \quad (3.217)$$

Later, $d \ln \chi_t(T)V_4/d \ln T$ in the DIGA is numerically estimated to compare with the lattice result, where the running coupling is calculated with the four loop β function. Focusing on the temperature dependence in the high temperature limit where the DIGA is reliable, it follows from eq. 3.217 that

$$\begin{aligned} \lim_{T \rightarrow \infty} \chi_t(T) &\propto \int_0^{\rho_{\text{cut}}} d\rho \rho^{\beta'_0 - 5} (\pi\rho T)^{2 + \frac{1}{3}(N - N_f)} \\ &= \frac{1}{\beta'_0 + \frac{1}{3}(N - N_f) - 2} \rho_{\text{cut}}^{\beta'_0 + \frac{1}{3}(N - N_f) - 2} (\pi T)^{2 + \frac{1}{3}(N - N_f)}, \\ &\propto T^{4 - \beta'_0}, \end{aligned} \quad (3.218)$$

where $\rho_{\text{cut}} = \sqrt{3}/(\sqrt{2N + N_f} \pi T)$.

3.5 The calculation of the gluon correlator at zero temperature

We will review the calculation of the two point function of the gluon in the one instanton background in both SU(2) and SU(3) pure Yang-Mills theory. We follow the past literature [33, 34].

3.5.1 The result in SU(2) Yang-Mills theory

In the single instanton background, due to the self-duality of the instanton namely $F_{\mu\nu}^a = \tilde{F}_{\mu\nu}^a$, the topological charge density $q(x)$ is related with the action density $s(x)$ as

$$q(x) = \frac{1}{2^5 \pi^2} F_{\mu\nu}^a \tilde{F}_{\mu\nu}^a = \frac{g^2}{8\pi^2} \left(\frac{1}{4g^2} F_{\mu\nu}^a F_{\mu\nu}^a \right) = \frac{g^2}{2^3 \pi^2} s(x). \quad (3.219)$$

Thus the x dependence of the leading instanton contribution to the three correlator, $\langle s(x)s(0) \rangle$, $\langle q(x)q(0) \rangle$, and $\langle s(x)q(0) \rangle$ is same. Hereafter, for simplicity we will calculate the two point function of the gluon

$$\left\langle F_{\mu\nu}^a(x) F_{\mu\nu}^a(x) F_{\mu\nu}^b(0) F_{\mu\nu}^b(0) \right\rangle_{Q=1}. \quad (3.220)$$

Considering the background field gauge in terms of the BPST instanton and the semi-classical approximation, the operator $F_{\mu\nu}^a(x) F_{\mu\nu}^a(x) F_{\mu\nu}^a(0) F_{\mu\nu}^a(0)$ is replaced by the BPST instanton in eq. 3.86,

$$\bar{F}_{\mu\nu}^a = -4\eta_{a\mu\nu} \frac{\rho^2}{((x-x_0)^2 + \rho^2)^2}, \quad (3.221)$$

where we puts bar ($\bar{\quad}$) to express the classical configuration. Then the expectation

value of the operator is calculated as

$$\begin{aligned}
& \left\langle F_{\mu\nu}^a(x)F_{\mu\nu}^a(x)F_{\mu\nu}^b(0)F_{\mu\nu}^b(0) \right\rangle_{Q=1} \\
&= \int \frac{d\rho d^4z}{\rho^5} n_G(\rho) \bar{F}_{\mu\nu}^a(x) \bar{F}_{\mu\nu}^a(x) \bar{F}_{\mu\nu}^b(0) \bar{F}_{\mu\nu}^b(0), \\
&= 2^{12} 3^2 \int \frac{d\rho d^4z}{\rho^5} n_G(\rho) \frac{\rho^8}{((x-z)^2 + \rho^2)^4 (z^2 + \rho^2)^4}, \\
&= \frac{2^{11} 3\pi^2}{7} \int \frac{d\rho}{\rho^9} n_G(\rho) {}_2F_1\left(4, 6, \frac{9}{2}, -\frac{x^2}{4\rho^2}\right), \tag{3.222}
\end{aligned}$$

where we use the instanton density in the Yang-Mills theory,

$$n_G^{\text{trunc}}(\rho) = C_I(\Lambda\rho)^{\beta_0} \left(\beta_0 \ln\left(\frac{\mu}{\Lambda}\right)\right)^{2N}, \tag{3.223}$$

$$n_G^{2\text{-loop}}(\rho) = C_I(\mu\rho)^\beta \left(\frac{8\pi^2}{g^2(\mu)}\right)^{2N} e^{-8\pi^2/g^2(\mu)}, \tag{3.224}$$

$$C_I = \frac{1}{4^N} \frac{2e^{5/6}}{\pi^2(N-1)!(N-2)!} e^{-2\alpha(\frac{1}{2})N + \frac{N}{6}},$$

where Λ is the dynamical scale in the $SU(N)$ Yang-Mills theory. In eq. 3.223, we use truncated gauge coupling

$$\frac{g^2(\mu)}{8\pi^2} = \frac{1}{\beta_0 \ln(\mu/\Lambda)} \tag{3.225}$$

and the instanton density at 1-loop level where the power of ρ is $\beta_0 = 11N/3$. In eq. 3.224, the ρ dependence is the power of $\beta = \beta_0 + (\beta_1 - 4\beta_0N)g^2(\mu)/16\pi^2$, where $\beta_1 = 34N^2/3$ in the $SU(N)$ Yang-Mills theory.

Substituting $n_G^{\text{trunc}}(\rho)$ for $n_G(\rho)$ in eq. 3.222, we analytically obtain

$$\begin{aligned}
& \left\langle F_{\mu\nu}^a(x)F_{\mu\nu}^a(x)F_{\mu\nu}^b(0)F_{\mu\nu}^b(0) \right\rangle_{Q=1} \\
&= \frac{2^{11} 3\pi^2}{7} C_I \Lambda^{\beta_0} \left(\beta_0 \log\left(\frac{\mu}{\Lambda}\right)\right)^{2N} x^{\beta_0-8} \int_0^\infty d\lambda \lambda^{\beta_0-9} {}_2F_1\left(4, 6, \frac{9}{2}, -\frac{1}{4\lambda^2}\right). \\
&= 724360 \log^4\left(\frac{\mu}{\Lambda}\right) \Lambda^{\frac{22}{3}} x^{-\frac{2}{3}}, \tag{3.226}
\end{aligned}$$

where $\beta_0 = 11N/3$ in the $SU(N)$ Yang-Mills theory. This integral is convergent if $N = 2$

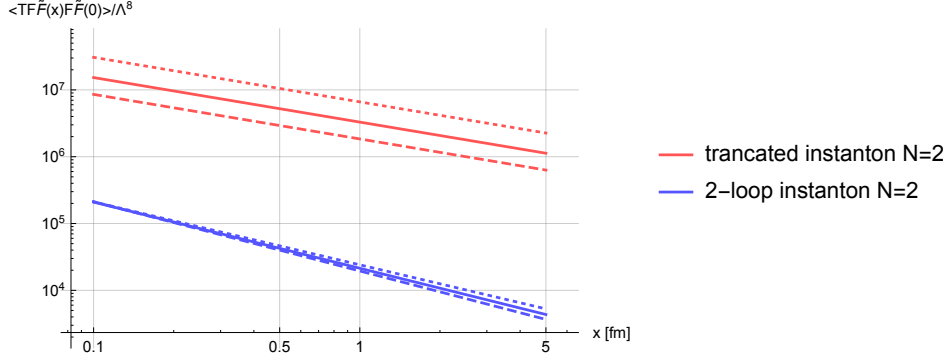


Figure 3.1: The dimension-less correlator $\langle F_{\mu\nu}^a(x)F_{\mu\nu}^a(x)F_{\mu\nu}^b(0)F_{\mu\nu}^b(0) \rangle_{Q=1} / \Lambda^8$ in the SU(2) Yang-Mills theory is shown in the red and blue line, which correspond to the instanton density n_G^{trunc} and $n_G^{2\text{-loop}}$, respectively. In both plot, the dashed, solid and dotted line denote the different scale $\mu/\Lambda = 5, 20/3, 10$, respectively.

but diverges if $N = 3$.

Here, we note the asymptotic behavior,

$${}_2F_1\left(4, 6, \frac{9}{2}, -\frac{x^2}{4\rho^2}\right) \rightarrow \begin{cases} 1 - \frac{4}{3}\frac{x^2}{\rho^2} + O\left(\left(\frac{x^2}{\rho^2}\right)^2\right), & x^2 \ll \rho^2, \\ 14\left(\frac{\rho^2}{x^2}\right)^4 + O\left(\left(\frac{\rho^2}{x^2}\right)^5\right), & \rho^2 \ll x^2. \end{cases} \quad (3.227)$$

The power behavior of the correlator in both type of the instanton density is, when using $\mu/\Lambda = 5$,

$$\langle F_{\mu\nu}^a(x)F_{\mu\nu}^a(x)F_{\mu\nu}^b(0)F_{\mu\nu}^b(0) \rangle_{Q=1} \propto \begin{cases} x^{-2/3} & (\text{truncated}), \\ x^{-1.1} & (2\text{-loop}), \end{cases} \quad (3.228)$$

where we use the strong coupling at the 4-loop level [69].

3.5.2 The result of SU(3) YM theory

As for the SU(3) YM theory, the integral in terms of instanton size ρ badly diverges. In order to somehow provide predictions about the power behavior, we use following model about the instanton distribution $n(\rho)$, where in the dilute instanton gas approx-

imation (DIGA) the instanton density $n(\rho)$ satisfies $n_{\text{DIGA}}(\rho) = n_G(\rho)/\rho^5$.

$$n_{\text{sp}}(\rho) = \bar{n}\delta(\rho - \bar{\rho}), \quad (3.229)$$

$$n_{\text{exp}}(\rho) = \frac{(n+1)^{n+1} \bar{n}}{n!} \frac{\left(\frac{\rho}{\bar{\rho}}\right)^n}{\bar{\rho}} \exp\left(-\frac{\rho}{\bar{\rho}}\right), \quad (3.230)$$

$$n_{\text{gauss}}(\rho) = 2 \frac{\bar{n}}{\bar{\rho}} \left(\frac{\rho}{\bar{\rho}}\right)^n \frac{\Gamma\left(\frac{n+2}{2}\right)^{n+1}}{\Gamma\left(\frac{n+1}{2}\right)^{n+2}} \exp\left[-\left(\frac{\Gamma\left(\frac{n+2}{2}\right)}{\Gamma\left(\frac{n+1}{2}\right)}\right)^2 \left(\frac{\rho}{\bar{\rho}}\right)^2\right], \quad (3.231)$$

$$\begin{aligned} n_{\text{ILM}}(\rho) &= \frac{(\beta_0 - 4)^{\frac{\beta_0 - 4}{2}}}{\Gamma\left(\frac{\beta_0}{2} - 2\right) 2^{\frac{\beta_0 - 6}{2}}} \frac{\bar{n}}{\bar{\rho}^{\beta_0 - 4}} \rho^{\beta_0 - 5} \exp\left(-\frac{\beta_0 - 4}{2} \left(\frac{\rho}{\bar{\rho}}\right)^2\right), \\ &= \frac{343}{15} \sqrt{\frac{14}{\pi}} \frac{\bar{n}}{\bar{\rho}^7} \rho^6 \exp\left[-\frac{7}{2} \left(\frac{\rho}{\bar{\rho}}\right)^2\right], \end{aligned} \quad (3.232)$$

where $\bar{\rho}$ is the average size of the instanton and \bar{n} is the average density of the instanton defined as

$$\begin{aligned} \bar{\rho} &= \frac{1}{\bar{n}} \int_0^\infty d\rho \rho n(\rho), \\ \bar{n} &= \frac{1}{\bar{n}} \int_0^\infty d\rho n(\rho). \end{aligned}$$

Using the instanton distribution $n(\rho)$, the leading instanton contribution to the correlator of $F_{\mu\nu}^a F_{\mu\nu}^a$ is calculated as below.

$$\begin{aligned} &\left\langle F_{\mu\nu}^a(x) F_{\mu\nu}^a(x) F_{\mu\nu}^b(0) F_{\mu\nu}^b(0) \right\rangle_{Q=1} \\ &= \frac{2^{11} 3 \pi^2}{7} \int \frac{d\rho}{\rho^4} n(\rho) {}_2F_1\left(4, 6, \frac{9}{2}, -\frac{x^2}{4\rho^2}\right) \end{aligned} \quad (3.233)$$

In the case of the spike distribution,

$$\begin{aligned} &\left\langle F_{\mu\nu}^a(x) F_{\mu\nu}^a(x) F_{\mu\nu}^b(0) F_{\mu\nu}^b(0) \right\rangle_{Q=1}^{(\text{sp})} \\ &= \left(\frac{\bar{n}}{\bar{\rho}^4}\right) \frac{2^{11} 3 \pi^2}{7} {}_2F_1\left(4, 6, \frac{9}{2}, -\frac{x^2}{4\bar{\rho}^2}\right) \end{aligned} \quad (3.234)$$

In the case of the exponential-like distribution with $n = 6$, which provide the small

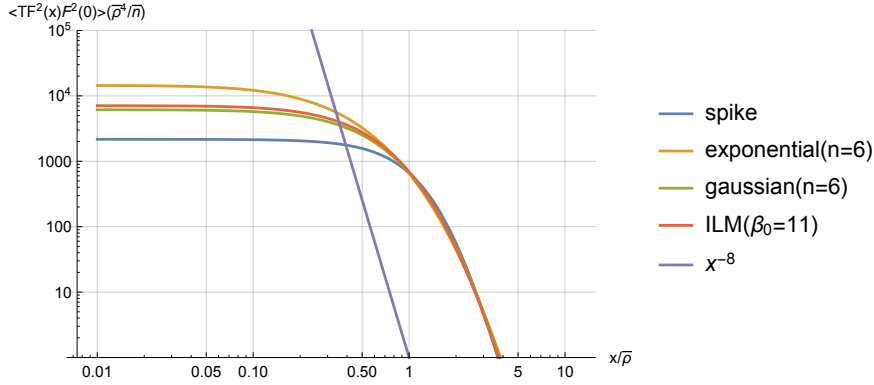


Figure 3.2: The dimension-less correlator $\langle F_{\mu\nu}^a(x)F_{\mu\nu}^a(x)F_{\mu\nu}^b(0)F_{\mu\nu}^b(0) \rangle_{Q=1} (\bar{\rho}^4/\bar{n})$ is shown for four hypothesis of instanton distribution $n(\rho)$. In every cases correlators behave as x^{-8} in $|x| \gg \bar{\rho}$, where $\bar{\rho}$ is the average size of instantons.

ρ behavior same as the DIGA, the correlator is calculated as follows.

$$\begin{aligned}
& \langle F_{\mu\nu}^a(x)F_{\mu\nu}^a(x)F_{\mu\nu}^b(0)F_{\mu\nu}^b(0) \rangle_{Q=1}^{(\text{exp})} \\
&= \frac{15059072\pi^2}{15} \int_0^\infty d\rho \frac{\rho^2}{\bar{\rho}^3} \exp\left(\frac{7\rho}{\bar{\rho}}\right) {}_2F_1\left(4, 6, \frac{9}{2}, -\frac{x^2}{4\rho^2}\right) \\
&= \left(\frac{\bar{n}}{\bar{\rho}^4}\right) \frac{2401\pi^2}{90} G_{2,4}^{3,2}\left(\frac{49x^2}{16\bar{\rho}^2} \middle| \begin{matrix} -5, -3 \\ 0, \frac{3}{2}, 2, -\frac{7}{2} \end{matrix}\right) \quad (3.235)
\end{aligned}$$

In the case of the gaussian-like distribution with $n = 6$, the correlator is calculated as follows.

$$\begin{aligned}
& \langle F_{\mu\nu}^a(x)F_{\mu\nu}^a(x)F_{\mu\nu}^b(0)F_{\mu\nu}^b(0) \rangle_{Q=1}^{(\text{gauss})} \\
&= \left(\frac{\bar{n}}{\bar{\rho}^4}\right) \frac{8796093022208}{2734375\pi^2} \int_0^\infty d\rho \frac{\rho^2}{\bar{\rho}^3} \exp\left[-\frac{256}{25\pi^2} \frac{\rho^2}{\bar{\rho}^2}\right] {}_2F_1\left(4, 6, \frac{9}{2}, -\frac{x^2}{4\rho^2}\right) \quad (3.236)
\end{aligned}$$

In the case of the ILM distribution with $\beta_0 = 11$, the correlator is calculated as follows.

$$\begin{aligned}
& \langle F_{\mu\nu}^a(x)F_{\mu\nu}^a(x)F_{\mu\nu}^b(0)F_{\mu\nu}^b(0) \rangle_{Q=1}^{(\text{ILM})} \\
&= \left(\frac{\bar{n}}{\bar{\rho}^4}\right) \frac{100352\sqrt{14}\pi^{3/2}}{5} \int_0^\infty d\rho \frac{\rho^2}{\bar{\rho}^3} \exp\left[-\frac{7}{2} \left(\frac{\rho}{\bar{\rho}}\right)^2\right] {}_2F_1\left(4, 6, \frac{9}{2}, -\frac{x^2}{4\rho^2}\right) \quad (3.237)
\end{aligned}$$

As a result, the x dependence of the correlator in the SU(2) Yang-Mills theory (fig. 3.5.1) is quite different from that in the SU(3) Yang-Mills theory (fig. 3.5.2). The crucial difference comes from the existence of the (ad-hoc) cutoff in the integration of the instanton size ρ in SU(3). If there is IR cutoff scale ρ_{cut} , the correlator should be constant in the small distance, i.e. $x \ll \rho_{\text{cut}}$. This can be understood as follows. If we introduce ad-hoc IR cutoff ρ_{cut} in the ρ integration,

$$\begin{aligned} & \int \frac{d\rho d^4z}{\rho^5} n_G(\rho) \bar{F}_{\mu\nu}^a(x) \bar{F}_{\mu\nu}^a(x) \bar{F}_{\mu\nu}^b(0) \bar{F}_{\mu\nu}^b(0), \\ & \propto \int d^4z \int_0^{\rho_{\text{cut}}} d\rho \rho^{b-5} \frac{\rho^8}{((x-z)^2 + \rho^2)^4 (z^2 + \rho^2)^4}, \end{aligned}$$

When $x \ll \rho$, the integrand can be expanded around $x/\rho = 0$.

$$\frac{1}{\left(\left(\frac{x}{\rho} - \frac{z}{\rho}\right)^2 + 1\right)^4 \left(\left(\frac{z}{\rho}\right)^2 + 1\right)^4} = \frac{1}{\left(\left(\frac{z}{\rho}\right)^2 + 1\right)^8} + O\left(\frac{x}{\rho}\right). \quad (3.238)$$

Thus, the x dependent part becomes sub-leading in this limit. On the other hand, at long distance, i.e. $x \gg \rho_{\text{cut}}$, the x dependence is determined only by the dimensionality. The integrand should have x dependence of $1/x^{-8}$ at large distance where $x/z \gg 1$ and $x/\rho \gg 1$.

The correlator in the SU(2) Yang-Mills theory is interesting. Since the instanton-size integration naturally conserves without any ad-hoc cutoff, the correlator has no special scale and behaves like

$$\Lambda^{22/3} x^{-2/3}, \quad (3.239)$$

which applies with the dimensional analysis.

4

Lattice field theory

In this chapter, we review the basic of the lattice gauge theory. We refer ref. [36] and [70] for more detailed discussion. We use the convention of ref. [71].

The lattice gauge theory proposed by Wilson [72] is one of the non-perturbative regularizations of the quantum field theory (QFT). The continuous infinite degrees of freedom in the QFT is approximated as the discrete finite degrees of freedom on the lattice with a lattice spacing a and a volume V . Due to the limited degrees of freedom, the physical observables calculated on the lattice is finite. In the continuum limit $a \rightarrow 0$ and thermodynamic limit $V \rightarrow \infty$, the lattice gauge theory becomes the QFT.

QCD is the asymptotic free theory and its perturbative calculation is only valid at high energy region. The growth of the strong coupling at the infrared region requires the use of non-perturbative method. In the lattice regularization of QCD, called the lattice QCD, the quark field is defined on the site of the discretized hypertorus with a lattice spacing a . The gluons are defined on the link between the adjacent sites.

To construct the action on the lattice, there are two guiding principles. First, the lattice action must become the action in the continuum theory in the zero lattice spacing limit, $a \rightarrow 0$. Second, the lattice action should have the same symmetry as the

continuum action as much as possible. Note that there is no shift symmetry and rotational symmetry on the lattice, while the discretized shift symmetry by a shift of a and the rotational symmetry by an angle $\pi/2$ still remain.

4.1 gauge actions on lattice

We introduce the link variable $U_\mu(x)$ to construct the gauge invariant gluon action on the lattice. The link variable is defined as

$$U_\mu(x) = \exp\left(igaA_\mu(x + a\hat{\mu}/2)\right) \in \text{SU}(N), \quad (4.1)$$

where $x = a\hat{n}$ is defined by the coordinate on the lattice $\hat{n} = (n_x, n_y, n_z, n_t)$. $\hat{\mu}$ denotes the unit vector along the μ direction. The link variable with the opposite direction is its inverse operator as

$$U_{-\mu}(x + \hat{\mu}) = U_\mu^\dagger(x). \quad (4.2)$$

The gauge transformation to the link variable is

$$U_\mu(x) \rightarrow g(x)U_\mu(x)g^\dagger(x + a\hat{\mu}), \quad (4.3)$$

where $g(x) \in \text{SU}(N)$ is the local operator of the gauge transformation. Then, the path ordered product of the link variables is transformed as

$$\Pi_{x \rightarrow y} U = U_{\mu_1}(x)U_{\mu_2}(x + a\hat{\mu}_1) \cdots U_{\mu_k}(y - a\hat{\mu}_k) \rightarrow g(x) \left[\Pi_{x \rightarrow y} U \right] g^\dagger(y), \quad (4.4)$$

where the subscript $x \rightarrow y$ denotes the path from x to $y = x + a \sum_{i=1}^k \hat{\mu}_i$. Then, we can construct the gauge invariant operator by considering the path ordered product along the closed loop C_x starting from x ,

$$\text{tr} \Pi_{C_x} U \rightarrow \text{tr} g(x) \left[\Pi_{C_x} U \right] g^\dagger(x) = \text{tr} \Pi_{C_x} U. \quad (4.5)$$

Thus, the simplest gauge invariant variable is the square such as

$$P_{\mu\nu}(x) = U_\mu(x)U_\nu(x + a\hat{\mu})U^\dagger(x + a\hat{\nu})U^\dagger(x) = \begin{array}{ccc} & x + a\hat{\nu} & \\ & \begin{array}{c} \leftarrow \quad \rightarrow \\ \leftarrow \quad \rightarrow \\ \leftarrow \quad \rightarrow \end{array} & \\ x & & x + a\hat{\mu} \end{array} \quad (4.6)$$

which is called a plaquette.¹ Suppose the lattice action have the gauge invariance as the continuum theory, the gauge action is, in general, written as

$$S = \sum_x \sum_{C_x} \beta_C \text{tr} \Pi_{C_x} U, \quad (4.7)$$

where C_x denotes the element of the set of the closed loops crossing the point x . We will determine the parameter β_C so that the lattice action becomes the continuum action in the limit of $a \rightarrow 0$.

The simplest lattice gauge action, called the Wilson gauge action, is constructed from the plaquette in eq. 4.6 as

$$S_g^W = \beta \sum_x \sum_{\mu > \nu} \left(1 - \frac{1}{N_c} \text{ReTr} P_{\mu\nu}(x) \right), \quad (4.8)$$

where $\beta = 2N_c/g^2(\beta)$ is the lattice gauge coupling.

In the continuum limit, Wilson gauge action becomes the action in $SU(N)$ gauge theory

$$\lim_{a \rightarrow 0} S_G^W = \int d^4x \frac{1}{4} F_{\mu\nu}^a F_{\mu\nu}^a + O(a^2). \quad (4.9)$$

In practice, the lattice calculation has non-zero lattice spacing a , which causes the systematic error to the observables. Concerning the Wilson gauge action, the extent of the error is of $O(a^2)$. The appropriate choice of the additional term in the other closed loop and the parameters β_C would cancel the $O(a^2)$ contribution to construct the improved action [74, 75]. The Symanzik-improved gauge action, called the Lüscher-Weisz action [76], is constructed from the linear combination of the plaquette and the 1×2 rectangular plaquette,

$$R_{\mu\nu} = U_\mu(x) U_\mu(x + a\hat{\mu}) U_\nu(x + 2a\hat{\mu}) U_\mu^\dagger(x + a\hat{\mu} + a\hat{\nu}) U_\mu^\dagger(x + a\hat{\nu}) U_\nu^\dagger(x), \quad (4.10)$$

$$= \begin{array}{c} \begin{array}{ccc} \bullet & \xrightarrow{\quad} & \bullet \\ \uparrow & & \uparrow \\ \bullet & \xrightarrow{\quad} & \bullet \\ \downarrow & & \downarrow \\ \bullet & \xrightarrow{\quad} & \bullet \end{array} \\ x \qquad \qquad \qquad x + 2a\hat{\mu} \end{array} \quad (4.11)$$

¹To write the diagram of the plaquette, we use the new command in \TeX defined in the manuscript of ref. [73].

The Lüscher-Weisz action is written as

$$S_g = 2N_c \beta N_{\text{site}} \left\{ (c_0 + 2c_1) - \left(c_0 \langle P_{\mu\nu}(x) \rangle + 2c_1 \langle R_{\mu\nu}(x) \rangle \right) \right\}, \quad (4.12)$$

where $\langle P_{\mu\nu}(x) \rangle$ and $\langle R_{\mu\nu}(x) \rangle$ denote the 1×1 plaquette and 1×2 rectangle averaged over the four-dimensional lattice sites, respectively. c_0 and c_1 satisfying $c_0 = 1 - 8c_1$ so as to be consistent with the continuum action. To cancel the $O(a^2)$ error, the parameters are determined as $c_0 = 5/3$ and $c_1 = -1/12$.

de Forcrand *et al.* [73] provide the $O(a^4)$ improved gauge action as

$$S_{m,n} = \frac{1}{m^2 n^2} \sum_{x,\mu,\nu} \text{Tr} \left(1 - \begin{array}{c} x+n\nu \\ \begin{array}{ccc} \bullet & \xrightarrow{\quad} & \bullet \\ \downarrow & & \downarrow \\ x & \xrightarrow{\quad} & x+m\mu \end{array} \end{array} \right)$$

$$S = \sum_{i=1}^5 c_i S_{m_i, n_i}, \quad (4.13)$$

where $(m_i, n_i) = (1, 1), (2, 2), (1, 2), (1, 3), (3, 3)$ for $i = 1, \dots, 5$ and:

$$\begin{aligned} c_1 &= (19 - 55 c_5)/9, & c_2 &= (1 - 64 c_5)/9 \\ c_3 &= (-64 + 640 c_5)/45, & c_4 &= 1/5 - 2 c_5. \end{aligned} \quad (4.14)$$

Here, they choose $c_5 = 1/20$.

The total number of lattice sites is $N_{\text{site}} = N_S^3 \times N_T = V_4/a^4(\beta)$, where N_S and N_T represent the number of lattice sites in the spatial and time directions, respectively. For fixed N_S and N_T , the physical, the four dimensional volume $V_4(\beta)$ and the lattice spacing $a(\beta)$ depend only on β . The temperature of the system in the physical unit is given by

$$T(\beta, N_T) = \frac{1}{a(\beta)N_T}, \quad (4.15)$$

and hence it can be changed by adjusting either the temporal size N_T or the lattice bare coupling $g^2(\beta) = (2N_c)/\beta$ ².

In chap. 6, we adopt the improved topological charge operator [73] to calculate the

²Thus, we take the mass independent scale setting prescription, where the lattice spacing a does not depend on the quark mass.

topological charge of the configurations. The topological charge Q is obtained as

$$Q = \sum_{i=1}^5 c_i Q_{m_i, n_i}, \quad (4.16)$$

where the parameters c_i is the same as eq. 4.14.

$$Q_{m,n} = \frac{1}{32\pi^2} \frac{1}{m^2 n^2} \sum_x \sum_{\mu, \nu, \rho, \sigma} \epsilon_{\mu\nu\rho\sigma} \text{Tr} \left(\hat{F}_{\mu\nu}(x; m, n) \hat{F}_{\rho\sigma}(x; m, n) \right), \quad (4.17)$$

with $\hat{F}_{\mu\nu}(x; m, n)$ given in terms of oriented clover averages of $m \times n$ plaquettes

$$\hat{F}_{\mu\nu}(x; m, n) = \frac{1}{8} \text{Im} \left\{ \left(\begin{array}{c} \text{---} \rightarrow \text{---} \rightarrow \text{---} \rightarrow \\ \uparrow \quad \uparrow \quad \uparrow \quad \uparrow \\ \leftarrow \text{---} \leftarrow \text{---} \leftarrow \text{---} \leftarrow \\ \downarrow \quad \downarrow \quad \downarrow \quad \downarrow \end{array} \right) + \left(\begin{array}{c} \rightarrow \text{---} \rightarrow \text{---} \rightarrow \\ \leftarrow \text{---} \leftarrow \text{---} \leftarrow \\ \rightarrow \text{---} \rightarrow \text{---} \rightarrow \\ \leftarrow \text{---} \leftarrow \text{---} \leftarrow \end{array} \right) \right\}. \quad (4.18)$$

4.2 The fermion action and the topology fixing term

The Wilson and overlap actions mentioned in chap. 5 are described below. The Wilson quark action is given by

$$S_f^W(\bar{m}_f) = \sum_{f=1}^{N_f} \sum_{x,y} \bar{\psi}_f(x) D_W(\bar{m}_f)_{x,y} \psi_f(y), \quad (4.19)$$

where

$$D_W(\bar{m}_f)_{x,y} = (\bar{m}_f + 4) \delta_{x,y} - \frac{1}{2} \sum_{\mu} \left\{ (1 - \gamma_{\mu}) U_{\mu}(x) \delta_{x+a\hat{\mu},y} + (1 + \gamma_{\mu}) U^{\dagger}(x - a\hat{\mu}) \delta_{x-a\hat{\mu},y} \right\} \quad (4.20)$$

where $\bar{m}_f = am_f$ is the dimension-less fermion mass. The Hermitian Wilson Dirac operator appearing in eq. (5.26) is then given by

$$H_W(\bar{m}_f) = \gamma_5 D_W(\bar{m}_f). \quad (4.21)$$

Note that, when using the Hermitian Wilson Dirac operator in the topology fixing term and the kernel of the overlap Dirac operator (see below), the mass has to be negative.

The overlap quark action and the Dirac operator is given by

$$S_q^{\text{ov}}(\bar{m}_f) = \sum_{f=1}^{N_f} \sum_{x,y} \bar{\psi}_f(x) D^{\text{ov}}(\bar{m}_f)_{x,y} \psi_f(y), \quad (4.22)$$

$$D^{\text{ov}}(\bar{m}_f)_{x,y} = D^{\text{ov}}(0)_{x,y} + \bar{m}_f \left(\delta_{x,y} - \frac{1}{2M_0} D^{\text{ov}}(0)_{x,y} \right), \quad (4.23)$$

$$D^{\text{ov}}(0)_{x,y} = M_0 \left[1 + \gamma_5 \text{sign}(H_W(-M_0)) \right]_{x,y}. \quad (4.24)$$

In chap. 5, we adopt the fermionic definition based on the index theorem to estimate the topological charge Q for given configurations, which requires the number of zero modes of the overlap Dirac operator [77].

To suppress the near-zero modes of H_W , the ghost term is introduced as

$$\det \left(\frac{H_W^2}{H_W^2 + \mu^2} \right) = \int [d\phi_W^\dagger d\phi_W] \exp(-S_{\text{TF}}), \quad (4.25)$$

$$S_{\text{TF}} = \phi_W^\dagger \left[(D_W + i\gamma_5\mu)(D_W^\dagger D_W)^{-1}(D_W + i\gamma_5\mu)^\dagger \right] \phi_W, \quad (4.26)$$

where μ is the mass of the twisted mass ghost. Introducing this term to the action used in the HMC update as $S_g + S_q^{\text{ov}} + S_{\text{TF}}$, the topological charges of the configurations are fixed during the HMC update. Introducing S_{TF} modifies the original lattice action into the one which does not go to the continuum action in the continuum limit. To reproduce the continuum action, we need to take $\mu \rightarrow 0$ limit, as well.

4.3 The partition functions on lattice

The QCD partition function on the lattice in θ -vacuum and in the fixed topological charge sector is written as

$$Z_\theta(\beta, \bar{m}_f) = \sum_{Q=-\infty}^{+\infty} Z_Q(\beta, \bar{m}_f) e^{-i\theta Q} = e^{-V_4 E(\theta)}, \quad (4.27)$$

$$\begin{aligned} Z_Q(\beta, \bar{m}_f) &= \int_{\epsilon_Q} [dU] \left[\prod_{f=1}^{N_f} d\psi_f d\bar{\psi}_f \right] e^{-S_g(\beta) - S_f(\bar{m}_f)} \\ &= \frac{1}{2\pi} \int_{-\pi}^{\pi} d\theta Z_\theta(\beta, \bar{m}_f) e^{i\theta Q}, \end{aligned} \quad (4.28)$$

respectively, where $\langle \cdot \rangle_Q$ denotes that the ensemble average of the gauge configurations is restricted to ones with topological charge Q and $E(\theta)$ ($-\pi < \theta \leq \pi$) is the energy density.

In the vacuum with $\theta = 0$, the expectation value of an operator O is written as

$$\langle O \rangle_{\theta=0}(\beta, \bar{m}_f) = \frac{1}{Z_{\theta=0}(\beta, \bar{m}_f)} \sum_{Q=-\infty}^{+\infty} Z_Q(\beta, \bar{m}_f) \langle O \rangle_Q(\beta, \bar{m}_f) \quad (4.29)$$

where we have defined the expectation value in the fixed topological charge Q sector as

$$\langle O \rangle_Q(\beta, \bar{m}_f) = \frac{1}{Z_Q(\beta, \bar{m}_f)} \int_{\epsilon_Q} [dU] \left[\prod_{f=1}^{N_f} d\psi_f d\bar{\psi}_f \right] e^{-S_g(\beta) - S_f(\bar{m}_f)} O. \quad (4.30)$$

Thus, the topological susceptibility times four dimensional volume is written as

$$\begin{aligned} & \chi_t(\beta, \bar{m}_f) V_4(\beta), \\ &= \langle Q^2 \rangle_{\theta=0}(\beta, \bar{m}_f), \\ &= \frac{1}{Z_{\theta=0}(\beta, \bar{m}_f)} \sum_{Q=-\infty}^{+\infty} Z_Q(\beta, \bar{m}_f) Q^2 \\ &= \frac{Z_1(\beta, \bar{m}_f) + Z_{-1}(\beta, \bar{m}_f) + 4 Z_2(\beta, \bar{m}_f) + 4 Z_{-2}(\beta, \bar{m}_f) + \dots}{\sum_{Q=-\infty}^{+\infty} Z_Q(\beta, \bar{m}_f)}. \end{aligned} \quad (4.31)$$

The simplest method to calculate χ_t is to generate an ensemble on the lattice and look at the distribution of Q . As is seen, for example, in fig. 1 of ref. [27], an update algorithm employed there only generate configurations with $Q = 0$ or ± 1 at some high temperature³. Since those with $Q = 0$ dominates the other, $Z_0 \gg Z_{\pm 1}$ should hold, and it follows from eq. (4.31)

$$\frac{Z_{\pm 1}(\beta, \bar{m}_f)}{Z_0(\beta, \bar{m}_f)} \approx \frac{w(\beta, \bar{m}_f)}{2}, \quad (4.32)$$

where we have defined $w(\beta, \bar{m}_f) = \chi_t V_4$.

So far, the partition function, Z_Q , has been written as a function of β and \bar{m}_f , but

³Note that, even in such a case, the resulting value of χ_t turns out to be consistent with more extensive lattice simulations such as refs. [28, 29].

an arbitrary pair of arguments can be chosen as long as they fix the QCD coupling and the quark masses. In the following, we consider (T, m_f) and $(w = \chi_t V_4, m_f)$ as a pair of arguments, and fix m_f to the physical quark mass as function of T or w . In this case, Z_Q can be viewed as the function of T or w . Furthermore, the numbers of lattice sites in the spatial and the temporal directions, i.e., N_T and N_S , are also fixed.

The observables calculated by the lattice QCD, in general, have both statistical and systematic errors compared to the ones calculated in QCD. The former one comes from the Monte-Carlo method used in the configuration generation

5

Topological susceptibility at high temperature on the lattice

5.1 Method

In this section, we will show how the temperature dependence of the topological susceptibility $d \ln \chi_t(T)/d \ln T$ can be obtained through the difference of the gauge actions and the quark condensates in two distinct topological charge sectors. In the following, for simplicity, we denote $\chi_t(T)V_4$ as $w(T)$.

The partition function at topological charge Q sector, $Z_Q(T, m_q, N_{\text{site}})$, is a function of temperature T and the quark mass m_q and the lattice size N_{site} . The derivative of the ratio Z_Q in terms of temperature with m_q and N_{site} fixed is related to the $d \ln w(T)/d \ln T$ via the chain rule as

$$\left. \frac{d \ln \frac{Z_{Q_2}(T)}{Z_{Q_1}(T)}}{d \ln T} \right|_{N_{\text{site}}} = \left. \frac{d \ln w(T)}{d \ln T} \right|_{N_{\text{site}}} \left. \frac{d \ln \frac{Z_{Q_2}(w)}{Z_{Q_1}(w)}}{d \ln w} \right|_{N_{\text{site}}}, \quad (5.1)$$

where the symbol $\Big|_{N_{\text{site}}}$ denotes the N_{site} is fixed. Then, the T dependence of w is expressed as

$$\frac{d \ln w(T)}{d \ln T} \Big|_{N_{\text{site}}} = \frac{d \ln \frac{Z_{Q_2}(T)}{Z_{Q_1}(T)}}{d \ln T} \Big|_{N_{\text{site}}} \times \left(\frac{d \ln \frac{Z_{Q_2}(w)}{Z_{Q_1}(w)}}{d \ln w} \Big|_{N_{\text{site}}} \right)^{-1}. \quad (5.2)$$

In the following, the symbol $\Big|_{N_{\text{site}}}$ is omitted for simplification. Below, we will estimate the both factors in the r.h.s.

The first factor, $d \ln(Z_{Q_2}/Z_{Q_1})/d \ln T$, is calculated on the lattice with temperature $T(\beta)$ as follows. As the lattice action is depend on the lattice gauge coupling β and the quark mass \bar{m}_q , the derivative of $Z_Q(T)$ in terms of $T = 1/N_t a(\beta)$ is written as

$$\frac{d \ln Z_Q(T)}{d \ln T} = \left(\frac{d\beta}{d \ln T} \frac{\partial}{\partial \beta} + \frac{d \ln \bar{m}_q}{d \ln T} \frac{\partial}{\partial \ln \bar{m}_q} \right) \ln Z_Q(\beta, \bar{m}_q). \quad (5.3)$$

The β derivative term in eq. (5.3) becomes

$$\frac{d\beta}{d \ln T} \frac{\partial \ln Z_Q(\beta, \bar{m}_q)}{\partial \beta} = -\frac{\beta \beta_g}{2N_c} \langle S_g \rangle_{\beta, \bar{m}_q}^{(Q)}, \quad (5.4)$$

where we have used eq. (4.12), eq. (4.15) and the β function for the QCD coupling

$$\beta_g = \frac{dg^2}{d \ln a} = 2g \frac{dg}{d \ln a}, \quad (5.5)$$

In perturbation theory, the first two coefficients of β_g are given by

$$\beta_g = 2b_0 g^4 + 2b_1 g^6 + O(g^8), \quad (5.6)$$

$$b_0 = \frac{11 - \frac{2}{3}N_f}{(4\pi)^2}, \quad b_1 = \frac{102 - \frac{38}{3}N_f}{(4\pi)^4}. \quad (5.7)$$

For our purpose, β_g has to be numerically determined as the temperature considered here is of $O(T_c)$.

The term including the mass derivative in eq. (5.3) are estimated as follows. The first factor is found to be

$$\frac{d \ln \bar{m}_q}{d \ln T} = \frac{d \ln a}{d \ln T} \frac{d \ln \bar{m}_q}{d \ln a} = -\left(1 + \frac{d \ln m_q}{d \ln a} \right), \quad (5.8)$$

which is related to the anomalous dimension of the quark mass. The second factor is calculated to be

$$\frac{\partial \ln Z_Q(\beta, \bar{m}_q)}{\partial \ln \bar{m}_q} = -N_f \bar{m}_q \langle s_{\bar{q}q} \rangle_{\beta, \bar{m}_q}^{(Q)}, \quad (5.9)$$

where the explicit form of the scalar density operator, $s_{\bar{q}q}$, requires specifying the quark action, S_q . For example, it is given by

$$s_{\bar{q}q} = \sum_x \bar{q}_x q_x, \quad (5.10)$$

for the Wilson fermion, and

$$s_{\bar{q}q} = \sum_{x,y} \bar{q}_x \left(\delta_{x,y} - \frac{1}{2M_0} D_{x,y}^{\text{ov}}(0) \right) q_y, \quad (5.11)$$

for the overlap fermion. For details, see Sec. 4.2.

Gathering eqs. (5.4), (5.8) and (5.9), eq. (5.3) becomes

$$\frac{d \ln Z_Q(T)}{d \ln T} = -\frac{\beta \beta_g}{6} \langle S_g \rangle_{\beta, \bar{m}_q}^{(Q)} + N_f \left(1 + \frac{d \ln m_q}{d \ln a} \right) \bar{m}_q \langle s_{\bar{q}q} \rangle_{\beta, \bar{m}_q}^{(Q)}. \quad (5.12)$$

Taking the difference of eq. (5.12) for Q_2 and Q_1 , we obtain

$$\frac{d \ln \frac{Z_{Q_2}}{Z_{Q_1}}}{d \ln T} = \frac{\beta^2 \beta_g}{6} \Delta S_g^{(Q_2, Q_1)}(\beta, \bar{m}_q) + N_f \left(1 + \frac{d \ln m_q}{d \ln a} \right) \bar{m}_q \left(\langle s_{\bar{q}q} \rangle_{\beta, \bar{m}_q}^{(1)} - \langle s_{\bar{q}q} \rangle_{\beta, \bar{m}_q}^{(0)} \right), \quad (5.13)$$

where we have defined

$$\Delta S_g^{(Q_2, Q_1)}(\beta, \bar{m}_q) = -\frac{1}{\beta} \left(\langle S_g \rangle_{\beta, \bar{m}_q}^{(Q_2)} - \langle S_g \rangle_{\beta, \bar{m}_q}^{(Q_1)} \right), \quad (5.14)$$

for later use. From eq. (5.13), it turns out that the differences of the gauge action and the chiral condensate between two topological sectors are required to determine the temperature dependence of Z_{Q_2}/Z_{Q_1} .

Next, we turn to the second factor in eq. (5.2), $d \ln(Z_{Q_2}/Z_{Q_1})/d \ln w$. In the following, the arguments of the partition functions are omitted for the sake of simplicity. When $w \gg 1$, existing lattice methods should work well, and our method is not more

efficient than those. Hereafter, we focus on the $w \ll 1$ case. Note that, although $w \ll 1$, we assume that the spatial volume is still larger than the typical length scale of the system ($\sim 1/T$).

Due to the analyticity, Z_Q can be expanded in terms of w as

$$Z_Q = a_Q w^{n_Q} + O(w^{n_Q+1}), \quad (5.15)$$

with an unknown coefficient a_Q . While n_Q for arbitrary Q is not known, previous numerical simulations tell that there is a temperature region where $Z_{\pm 1}/Z_0 \approx w/2$ holds [eq. (4.32)], indicating $n_{\pm 1} - n_0 = 1$. With the assumption eq. (5.15), it follows that

$$\left(\frac{d \ln \frac{Z_{Q_2}}{Z_{Q_1}}}{d \ln w} \right) = n_{Q_2} - n_{Q_1} + O(w) \quad (5.16)$$

Using eqs. (5.13) and (5.16) and recalling $d \ln V_4/d \ln T = -4$, eq. (5.2) is rewritten as

$$\begin{aligned} \frac{d \ln \chi_t(T)}{d \ln T} &= \left[\frac{\beta^2 \beta_g}{6} \Delta S_g^{(Q_2, Q_1)}(\beta, \bar{m}_q) + N_f \left(1 + \frac{d \ln m_q}{d \ln a} \right) \bar{m}_q \left(\langle s_{\bar{q}q} \rangle_{\beta, \bar{m}_q}^{(1)} - \langle s_{\bar{q}q} \rangle_{\beta, \bar{m}_q}^{(0)} \right) \right] \\ &\times \frac{1}{n_{Q_2} - n_{Q_1}} + 4 + O(w). \end{aligned} \quad (5.17)$$

If the boundary condition for this differential equation is provided, we can determine the absolute value of $\chi_t(T)$.

It should be noted that the l.h.s. of eq. (5.17) is independent of the choice of Q_1 and Q_2 up to $O(w)$. By equating the r.h.s. of eq. (5.2) for different pairs of Q , we can numerically determine the ratio $(d \ln(Z_{Q_1}/Z_{Q_2})/d \ln w)/(d \ln(Z_{Q_3}/Z_{Q_4})/d \ln w)$ by

$$R^{(Q_1, Q_2, Q_3, Q_4)}(\beta) = \frac{d \ln \frac{Z_{Q_1}}{Z_{Q_2}}}{d \ln T} \times \left(\frac{d \ln \frac{Z_{Q_3}}{Z_{Q_4}}}{d \ln T} \right)^{-1} = \frac{d \ln \frac{Z_{Q_1}}{Z_{Q_2}}}{d \ln w} \times \left(\frac{d \ln \frac{Z_{Q_3}}{Z_{Q_4}}}{d \ln w} \right)^{-1}, \quad (5.18)$$

independently of the size of w . Then, the assumption eq. (5.15) gives

$$R^{(Q_1, Q_2, Q_3, Q_4)}(\beta) = \frac{n_{Q_1} - n_{Q_2}}{n_{Q_3} - n_{Q_4}} + O(w). \quad (5.19)$$

Especially, when $Q_2 = Q_4 = 0$ and $Q_3 = 1$, $R^{(Q_1,0,1,0)}(\beta) = n_{Q_1} - n_0$. Thus, measuring $R^{(Q,0,1,0)}(\beta)$ with various Q enables us to investigate the leading power of Z_Q/Z_0 , *i.e.* $n_Q - n_0$. On the other hand, when $w \gg 1$, the behavior of $R^{(Q_1, Q_2, Q_3, Q_4)}(\beta)$ becomes

$$R^{(Q_1, Q_2, Q_3, Q_4)}(\beta) \propto \frac{Q_1^2 - Q_2^2}{Q_3^2 - Q_4^2} + O(1/w). \quad (5.20)$$

In this case, calculating $R^{(Q_1, Q_2, Q_3, Q_4)}(\beta)$ may serve to check whether $w \gg 1$ indeed holds.

Here let us comment on our method. If one could calculate the right hand side of eq. (5.13) over a wide range of T , Z_{Q_2}/Z_{Q_1} can be obtained by the numerical integration with an suitable input. By repeating this procedure for arbitrary pairs of (Q_1, Q_2) and substituting Z_{Q_2}/Z_{Q_1} thus obtained into eq. (4.31), one can determine $\chi_t(T)$ over a wide range of T without any assumptions, in principle. If that is possible, the most of above arguments are unnecessary. However, as we will show soon, it turns out that the numerical accuracy is rather limited and the above naive procedure does not work well.

In this work, we instead focus on $d \ln \chi_t(T)/d \ln T$ in the temperature region, where $\chi_t(T)V_4 \approx 2Z_{\pm 1}/Z_0$ is valid, because this quantity still provides useful information. For example, the leading powers of w in Z_{Q_2}/Z_0 , *i.e.* $n_{Q_2} - n_0$, extracted through eq. (5.19) for various Q_2 (Q_1 is fixed to zero for simplicity) can be used to identify the θ dependence of the energy density¹. Furthermore, once an integer value of $n_{Q_2} - n_0$ was determined, $d \ln(Z_{Q_2}/Z_0)/d \ln T$ provides an independent determination of $d \ln(Z_{\pm 1}/Z_0)/d \ln T$ through eq. (5.17) with $n_{Q_1} = n_0$ as we will explicitly show in the next section.

5.1.1 high temperature limit

It is instructive to see the high temperature limit of eq. (5.17). In this limit, the gauge action in each topological sector is expected to realize the BPST instanton solution, at least in the continuum theory, *i.e.* $\langle S_g \rangle_{\beta, \tilde{m}_q}^{(Q)} \rightarrow \frac{8\pi^2}{g^2}|Q|$. Thus, $\langle S_g \rangle_{\beta, \tilde{m}_q}^{(Q)}/\beta$ has a finite value in the high T limit,

$$\lim_{T \rightarrow \infty} \frac{1}{\beta} \langle S_g \rangle_{\beta, \tilde{m}_q}^{(Q)} = \frac{4\pi^2}{3}|Q|. \quad (5.21)$$

¹The general form of it is given in eq. (5.33).

Using the perturbative expression for β_g and keeping only the leading order contribution, $\beta^2\beta_g$ takes

$$\lim_{T \rightarrow \infty} \beta^2\beta_g = \frac{11 - \frac{2}{3}N_f}{(4\pi)^2} \times 72. \quad (5.22)$$

Collecting the above yields

$$\begin{aligned} \lim_{T \rightarrow \infty} \frac{d \ln \chi_t(T)}{d \ln T} = & \frac{1}{n_{Q_2} - n_{Q_1}} \left[(|Q_2| - |Q_1|) \left(\frac{2}{3}N_f - 11 \right) \right. \\ & \left. + N_f \lim_{T \rightarrow \infty} \bar{m}_q \left(\langle s_{\bar{q}q} \rangle_{\beta, \bar{m}_q}^{(Q_2)} - \langle s_{\bar{q}q} \rangle_{\beta, \bar{m}_q}^{(Q_1)} \right) \right] + 4, \quad (5.23) \end{aligned}$$

where the $O(w)$ contribution is omitted.

With $N_f = 0$, the r.h.s. of eq. (5.23) gives $-11 \times (|Q_2| - |Q_1|)/(n_{Q_2} - n_{Q_1}) + 4$. In this case, instanton calculus predicts $\chi_t \sim T^{-7}$, which is reproduced when $n_Q = |Q|$. The instanton calculus for $N_f = 0$ should also be reproduced in the heavy quark limit, in which the heavy quarks will be decoupled from the theory and hence the β -function is reduced to the one for $N_f = 0$. By imposing that the heavy quark limit of eq. (5.23) yields $\chi_t \sim T^{-7}$,

$$\lim_{\bar{m}_q \rightarrow \infty} \lim_{T \rightarrow \infty} \bar{m}_q \left(\langle s_{\bar{q}q} \rangle_{\beta, \bar{m}_q}^{(Q_2)} - \langle s_{\bar{q}q} \rangle_{\beta, \bar{m}_q}^{(Q_1)} \right) = O(1/\bar{m}_q), \quad (5.24)$$

is obtained.

When $N_f = 3$, the instanton calculus predicts $\chi_t \sim T^{-8}$, which indicates

$$\lim_{T \rightarrow \infty} \bar{m}_q \left(\langle s_{\bar{q}q} \rangle_{\beta, \bar{m}_q}^{(Q_2)} - \langle s_{\bar{q}q} \rangle_{\beta, \bar{m}_q}^{(Q_1)} \right) = -(n_{Q_2} - n_{Q_1}) + O(\bar{m}_q). \quad (5.25)$$

This coincides with the contributions from the fermion zero modes, $-(|Q_2| - |Q_1|)$, when $n_Q = |Q|$.

5.2 test in the quenched approximation

5.2.1 lattice setup

In order to see how well the method described in the previous section works, we perform a test in the quenched approximation. The configurations are generated using the renormalization group improved Iwasaki gauge action, *i.e.* $c_1 = -0.331$. The lattice volume is fixed to $16^3 \times 4$ in this feasibility test except one simulation, in which the calculation is repeated on $24^3 \times 4$ lattice to see the volume dependence. However, the number of configurations required for a fixed statistical error grows as N_{site} , and our limited computational resources did not allow us to investigate the size dependence in detail.

We use the index theorem in defining the topological charge, $Q = \text{Index}[D_{\text{ov}}]$, where D_{ov} is the overlap Dirac operator shown in (4.23). Since the configurations in a fixed topological sector is needed, we insert the topology fixing (TF) term,

$$\frac{\det [H_W(-M_0)^2]}{\det [H_W(-M_0)^2 + \mu^2]}, \quad (5.26)$$

into the path integral [78] to fix Q during the update process. The explicit form of the Hermitian Wilson Dirac operator, H_W , is found in eq. (4.21). Due to this term, the appearance of the eigenvalues of H_W smaller than μ , $|\lambda_{H_W}| \lesssim \mu$, is suppressed, and so is the topology change. In this work, $\mu = 0.2$ and $M_0 = 1.6$ are used. The standard hybrid Monte Carlo (HMC) method is applied in the configuration generation. The step size in the molecular dynamics procedure is tuned to realize the acceptance ratio of 75% to 90 %.

In the preparation step, we first generate configurations at around T_c without the TF term to sample the configurations with various Q values. Then, the TF term is turned on, and β is changed to a desired value. The topological charge of configurations thus generated is monitored by calculating the index of the overlap Dirac operator [see eq. (4.23)] with the same value of M_0 as that in the TF term, and we checked that no transition to a different Q sector occurs within the configurations used in the analysis except in the $Q = -2$ sector on $24^3 \times 4$ lattice, where $Q = -2$ is changed to -1 after 1,310 trajectories.

In the following plots, we present the statistical error only, which is estimated by

the standard single elimination jackknife method with the bin size of 50 trajectories. Increasing the bin size by a factor two only changes the size of uncertainty by a few %.

The theory with the TF term (5.26) is not rigorously equivalent to the quenched QCD, because the TF term (5.26) would break Z_3 symmetry. Thus, strictly speaking, the action with the TF term may not allow us to study the phase transition of the quenched QCD. Thus, our study focuses on the temperature region like $T \geq 2 T_c$.

It is also important to note that the presence of the TF term, in general, changes the correspondence between the simulation parameter β and temperature T . By using the fact that the spectrum of the Dirac operator is sensitive to the temperature, we see how much the correspondence between the simulation parameter β and temperature T is shifted in the presence of the TF term. The distribution of the smallest eigenvalues of the Hermitian Wilson (H_W) and overlap (H_{ov}) Dirac operators are shown in Fig. 5.1 as examples, where $\beta = 2.450, 2.802$ and 10 correspond to $T \sim 1.3 T_c, 2.25 T_c$ and $8 \times 10^3 T_c$, respectively.

In Fig. 5.1 (left), the suppression of the appearance of small eigenvalues is clear at $T \sim 1.3 T_c$ (left) while no significant difference is observed at $T > 2 T_c$. As for the Hermitian overlap Dirac operator [Fig. 5.1 (right)], while the effect of the TF term is again clear at low temperature (top) especially in the near-zero mode region, the distributions reasonably agree at high temperatures (middle and bottom). The temperature region we are interested in is $T \gtrsim 2 T_c$ and in such a region the Dirac spectra with and without the TF term turn out to agree at the same β values. This observation allows us to employ the relationship between the simulation parameter β and temperature T obtained in simulations with the same gauge action but without the TF term. Although it would be possible to numerically take the $\mu=0$ limit, we do not pursue the limit in this exploratory study.

The configurations are generated at 12 values of β ranging from T_c to $10^4 T_c$ and in four different topological sectors, $Q = 0, 1, -1, -2$. The configurations are stored every 10 and 5 trajectories for $16^3 \times 4$ and $24^3 \times 4$ lattices, respectively. The simulation parameters and statistics are tabulated in Tab. 5.1. The values of T/T_c in the table are obtained by using the formula provided in Ref. [79], where the lattice spacings are determined in a wide range of β using the same gauge action as ours but without the TF term.

N_{site}	β	T/T_c	$Q = 0$	+1	-1	-2	$Q = +1$	-1	-2
$16^3 \times 4$	2.300	1.02	1453	1737	1240	1207	-1.3(9)	-1.0(10)	-2.5(10)
	2.400	1.23	1255	1352	1053	1772	-3.4(9)	-3.2(10)	-5.3(8)
	2.500	1.45	1490	1228	1101	1109	-1.9(8)	-0.8(9)	-3.1(8)
	2.600	1.69	1217	1105	1074	1229	-2.1(9)	-1.3(9)	-3.6(8)
	2.700	1.96	1137	1388	1344	1876	-1.5(8)	-1.4(8)	-3.2(8)
	2.802	2.25	1397	1338	1430	1351	-1.7(7)	-1.8(7)	-4.0(7)
	3.000	2.90	1876	1359	1754	1297	-1.5(6)	-1.6(6)	-3.5(6)
	3.200	3.70	1750	1732	2719	1204	-1.3(5)	-0.9(5)	-2.9(6)
	3.500	5.23	1328	1114	1100	1255	-1.4(6)	-1.4(6)	-3.1(5)
	4.000	9.16	1445	1197	1239	1346	-1.3(5)	-1.3(5)	-2.9(5)
	5.000	27.82	1097	1256	1237	1043	-1.3(4)	-1.3(4)	-3.0(4)
10.00	8.2×10^3	1051	1054	1001	1001	-1.4(2)	-1.6(2)	-2.7(2)	
$24^3 \times 4$	3.200	3.70	4152	3104	6990	262	-0.4(2)	-0.5(2)	-1.6(7)

Table 5.1: Simulation parameters and the number of configurations used in the analysis. The rightmost three columns are $\Delta S_g^{(Q,0)}/(6N_{\text{site}})$ in unit of 10^{-4} .

5.2.2 numerical results

In quenched QCD, the T dependence of χ_t is determined by

$$\frac{d \ln \chi_t(T)}{d \ln T} = \frac{1}{n_{Q_2} - n_{Q_1}} \frac{\beta^2 \beta_g}{6} \Delta S_g^{(Q_2, Q_1)}(\beta) + 4 + O(w). \quad (5.27)$$

The results of $\Delta S_g^{(Q,0)}(\beta)$ with $Q = \pm 1$ and -2 are shown in Fig. 5.2, where it is seen that the data for $Q = 1$ and -1 agree well within the statistical error as expected. Thus, the averaged value over $Q = 1$ and -1 is used in the following analysis.

The horizontal dotted lines represent the action difference in the BPST instanton solutions, or in the high temperature limit, for $|Q| = 1$ and 2 from top to bottom. The lattice data for $Q = \pm 1$ are on top of the corresponding BPST line down to $\beta \sim 2.5$ (or $T \sim 1.45 T_c$) and suddenly decrease at $\beta \sim 2.4$. The similar behavior is observed for $Q = -2$ but the deviation from the corresponding BPST line starts at slightly larger β , $\beta \sim 3$. The jump observed at $\beta \sim 2.4$ may be associated with the phase transition. Studying the phase transition itself within this framework is interesting, but we focus on the high temperature region in this paper.

The large volume results are also shown in Fig. 5.2 (filled symbols). It is confirmed that the $Q = \pm 1$ result are consistent with that from the smaller lattice. We omit the

$Q = -2$ result on the larger lattice from the figure because of a large uncertainty.

In order to estimate $d \ln \chi_t / d \ln T$ using $\Delta^{(Q,0)} S_g(\beta)$ with $Q = \pm 1$ or -2 , we need to know $n_Q - n_0$. $n_{\pm 1} - n_0 = 1$ is empirically known². We can estimate $n_2 - n_0$ by looking at $R^{(2,0,1,0)}(\beta)$ [see eq. (5.19)]. Fig. 5.3 shows that $R^{(2,0,1,0)}(\beta)$ is consistent with two over the whole range of β we have studied, but the large statistical errors do not allow the precise determination except for the region of $\beta \geq 10$. It is seen that, when the mean value is relatively large, the error is also large. Thus, we assume $n_{-2} - n_0 = 2$ in the following analysis.

The QCD beta function, β_g , down to a low energy scale ($\sim T_c$) is necessary in estimating eq. (5.27). We use the result of ref. [79], in which the lattice spacing is expressed as a function of the lattice gauge coupling, β , as

$$(a\sqrt{\sigma})(\beta) = \frac{f(\beta)}{c_0} \left[1 + c_2 \hat{a}(\beta)^2 + c_4 \hat{a}(\beta)^4 \right], \quad (5.28)$$

where σ denotes the string tension and

$$\hat{a}(\beta) = \frac{f(\beta)}{f(\beta_1)}, \quad f(\beta) = e^{-\frac{\beta}{12b_0}} \left(\frac{6b_0}{\beta} \right)^{-\frac{b_1}{2b_0^2}}, \quad (5.29)$$

$$c_0 = 0.524(15), \quad c_2 = 0.274(76), \quad c_4 = 0.105(36), \quad \beta_1 = 2.40. \quad (5.30)$$

Using this expression, β_g is numerically determined through

$$\beta_g = -\frac{6}{\beta^2} \frac{1}{\frac{d \ln(a\sqrt{\sigma})}{d\beta}}. \quad (5.31)$$

At the same time, the relationship between T/T_c and β is found to be

$$\frac{T(\beta)}{T_c} = \frac{(a\sqrt{\sigma})(\beta_c)}{(a\sqrt{\sigma})(\beta)}, \quad (5.32)$$

where $T_c = T(\beta_c)$ and $\beta_c = 2.288$ [79]. β_g and $T(\beta)/T_c$ are shown as a function of the lattice gauge coupling β in fig. 5.4. In the plot, we also show $\beta^2 \beta_g$, which approaches

²See the discussion around eq. (4.32).

to $\beta^2 \beta_g \rightarrow 792/(4\pi)^2 \sim 5$ in the large β limit.

Substituting the above results into eq. (5.27), $d \ln \chi_t / d \ln T$ is calculated as shown in fig. 5.5, where the two solid curves represent the prediction of the DIGA (3.217) with $\mu = \pi T/2$ and $2\pi T$, respectively although they can not be distinguished at this axis scale.

The results with $|Q| = 1$ and 2 are consistent with each other, which is expected from the observation in fig. 5.3. These results are also consistent with the high temperature limit and the DIGA down to $T/T_c \sim 1.5$. Note that the results using the $Q = -2$ sector has the uncertainty smaller than those using $Q = \pm 1$ by a factor $n_{-2} - n_0 = 2$, which indicates that once the $n_Q - n_0$ has been fixed one can obtain very accurate result by performing a simulation at large Q .

One of the concerns in this approach is the finite volume effect since the physical volume becomes extremely small at large β . Fig. 5.5 shows that the lattice results well reproduce the high temperature limit at high temperature. From this observation, it is unlikely that the finite size effect significantly affects the lattice results, and it is natural to think that $N_T \ll N_S$ is the necessary condition for the finite volume effects to be under control. Indeed, the aspect ratio of our lattices is $N_S/N_T = 4$, and hence the above condition seems to be satisfied. Nevertheless, calculations with different lattice sizes are clearly useful to explicitly check the finite size effect and whether $w \ll 1$ holds or not. However, since the uncertainty of the action value grows as $\sqrt{N_{\text{site}}}$, we need the statistics proportional to N_{site} to keep the size of the uncertainty constant.

From the phenomenological point of view, $\chi_t(T)$ for $T_c \lesssim T \lesssim 10 T_c$ is important. In this range of T , the statistical uncertainty is relatively large (typically ± 4 for $O(10,000)$ trajectories), which makes the axion abundance ambiguous. It is thus important to accumulate a large number of statistics. On the other hand, if $\chi_t(T)$ behaves like a step function, our method should be able to detect such a behavior.

5.3 summary and future prospects

The QCD topological susceptibility, χ_t , at high temperature provides an important input for the estimate of the axion abundance in the present universe. Existing methods to calculate χ_t on the lattice in the literature fail when $\chi_t(T)V_4 \ll 1$. We proposed a novel lattice method to calculate the temperature dependence of the susceptibility, which is expected to work well especially in high temperature region where $\chi_t(T)V_4 \ll$

1. To see how it works, we performed quenched simulations on the $16^3 \times 4$ lattice, and found that the results of $d \ln \chi_t / d \ln T$ well agree with the DIGA prediction above $1.5 T_c$. The simulation on a slightly larger lattice confirms that there is no unexpected large finite volume effect, although keeping the statistical error constant requires statistics proportional to N_{site} . Thus, that error may be the main source of uncertainty in future serious works.

To predict the axion abundance, we still have to include dynamical quarks with the physical masses. In order for the method to work, the difference of the chiral condensate between two topological sectors has to be precisely determined, for which the dynamical overlap fermion seems to be preferred. Then, accumulating a large number of configurations requires large amount of resources. But, if $\chi_t(T)$ behaves like a step function, a large number of statistics may not be necessary to detect such a behavior.

A possible way out is to generate configurations in large Q sectors, with which one can achieve an uncertainty smaller than that with $|Q| = 1$ by a factor of $n_Q - n_0$. Note that this requires the signal on $R^{(Q,0,1,0)}$ [eq. (5.20)] at $w \ll 1$ to be sufficiently precise to unambiguously identify the integer $n_Q - n_0$. Knowing $n_Q - n_0$ for various Q is also useful to put the constraints on the θ dependence of $E(\theta)$ in eq. (4.27), whose general form would be given by

$$E(\theta) = \sum_n c_n (1 - \cos(n\theta)) , \quad (5.33)$$

with $\chi_t = \sum_n c_n / n^2$.

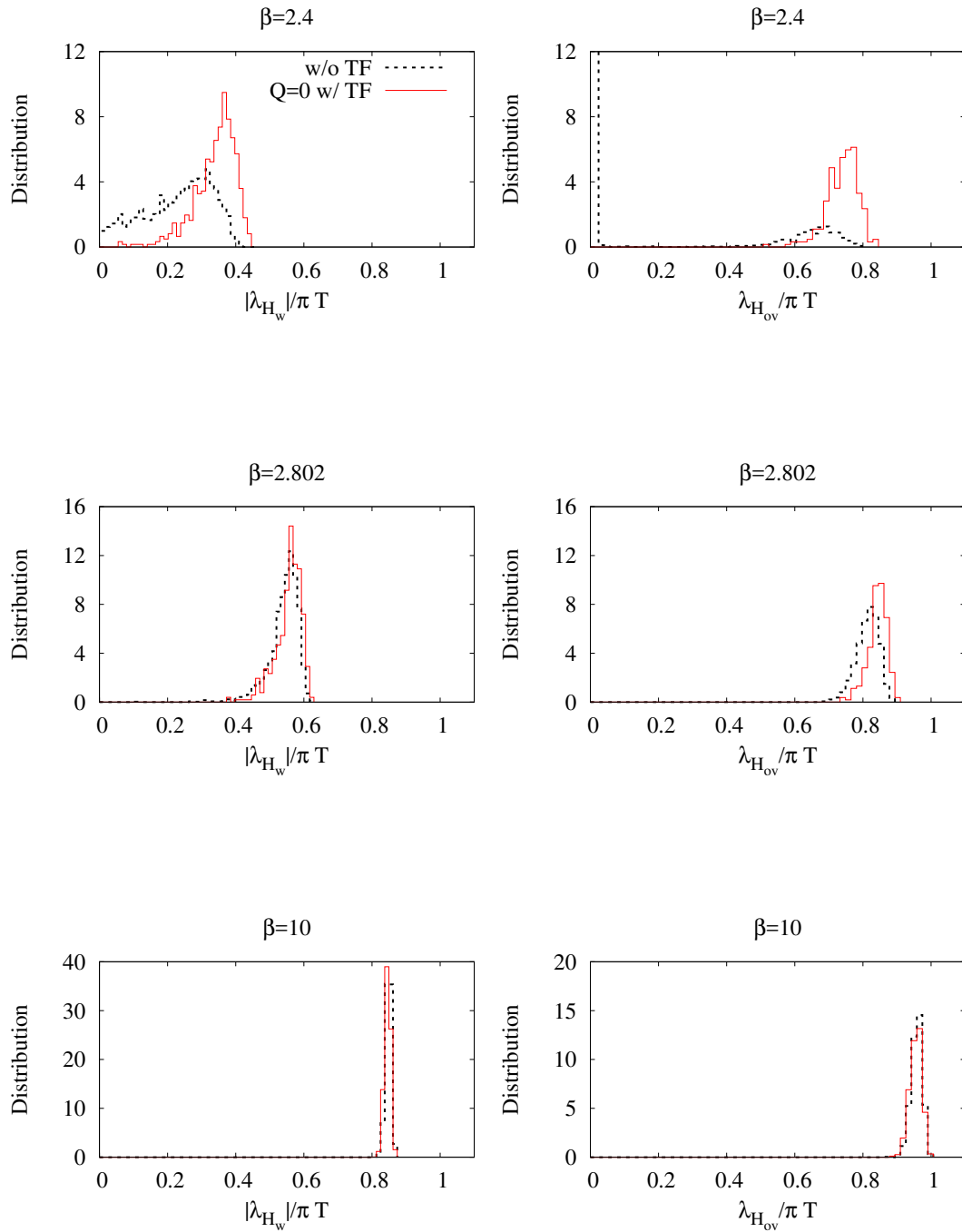


Figure 5.1: Comparison of the distribution of the smallest eigenvalue on the configurations generated at the same β with and without the TF term. Those of H_W (left) and H_{Ov} (right) are shown for three β values.

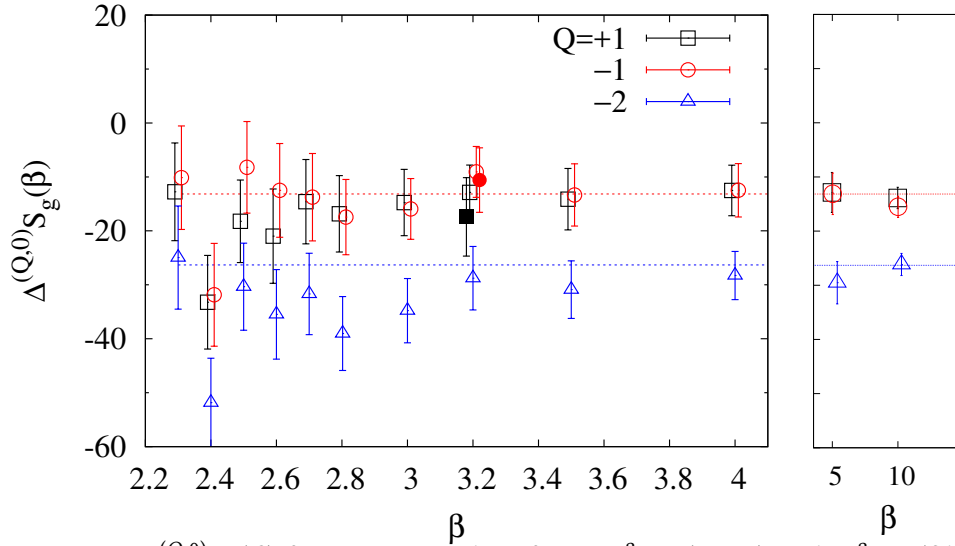


Figure 5.2: $\Delta^{(Q,0)}S_g(\beta)$ for $Q = \pm 1$ and -2 from $16^3 \times 4$ (open) and $24^3 \times 4$ (filled) lattices. The horizontal dotted lines are the high temperature limit with $|Q| = 1$ and 2 from top to bottom.

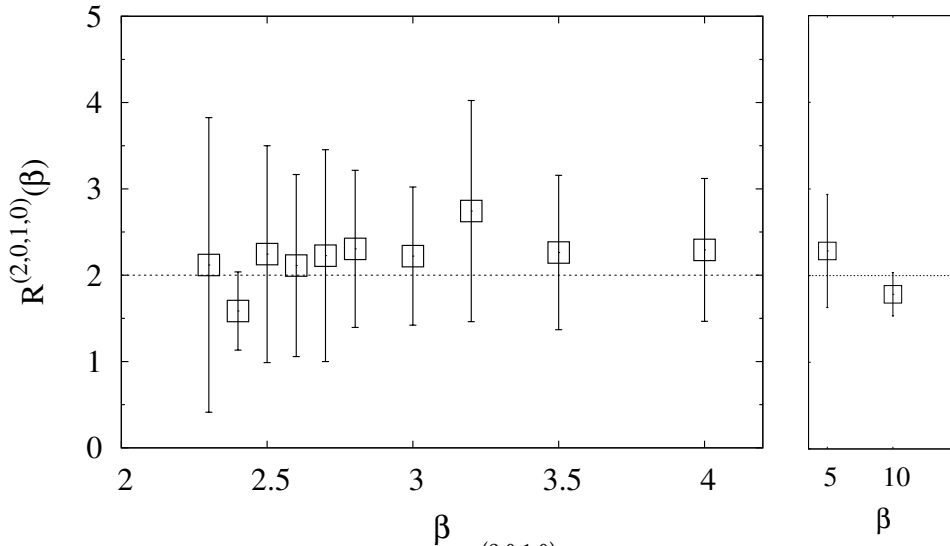
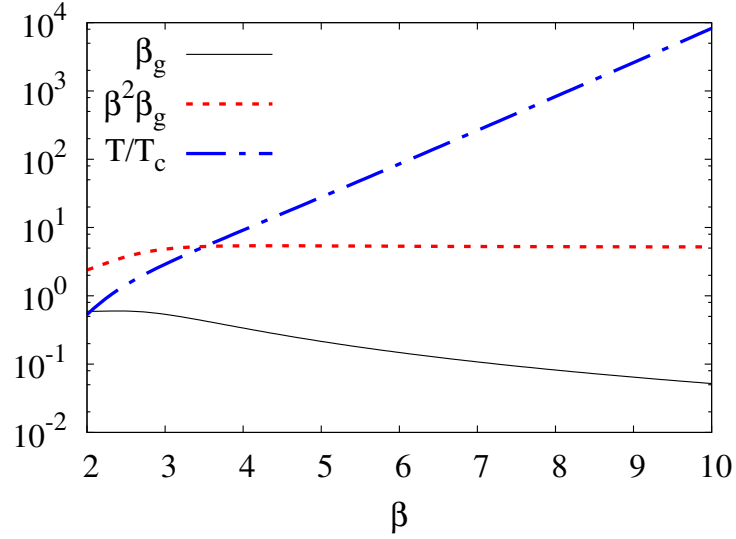
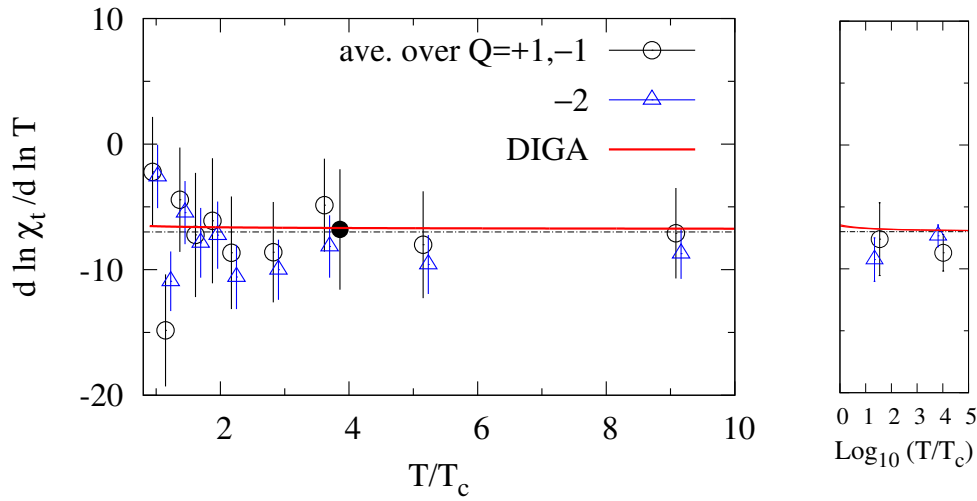


Figure 5.3: $R^{(2,0,1,0)}(\beta)$ in eq. (5.18).

Figure 5.4: β dependence of β_g , $\beta^2 \beta_g$ and T/T_c .Figure 5.5: T dependence of χ_t , eq. (5.27) obtained on $16^3 \times 4$ (open) and $24^3 \times 4$ (filled). The estimate based on the DIGA (3.217) with $\mu = \pi T/2$ and $2\pi T$ (solid curves) and the high temperature limit (dashed line) are also shown.

6

Instanton effects on CP-violating gluonic correlators

6.1 Instanton calculus

In this section, we show the semi-classical calculation of the CP-violating (CPV) gluonic correlation function in the single instanton background in SU(2) Yang-Mills theory at finite temperature. As mentioned in sec. 3.3.4 the instanton calculus we will perform in the following is based on the semi-classical approximation, where we ignore the contribution to the partition function from the cubic terms and quartic terms of the fields in the Lagrangian. Thus, this approximation is only valid in the weak coupling regime. Hereafter we assume the temperature of the system of the Yang-Mills gas is enough high to ignore the $O(\alpha_s)$ correction in eq. 3.175. Since the following calculation does not make sense in the low temperature limit, taking low temperature limit of the results obtained at high temperature may not be consistent with the result calculated at zero temperature.

As shown in eq. 3.197 and eq. 3.216, the instanton density in SU(N) Yang-Mills

theory at finite temperature is given by the semi-classical calculation in the single instanton background as,

$$\frac{Z_{Q=1}}{Z_{Q=0}} = \int_0^{1/T} dz_4 \int d^3\vec{z} \frac{d\rho}{\rho^5} n_G(\rho) n_T(\pi\rho T), \quad (6.1)$$

$$n_G(\rho) = C_I(\mu\rho)^b \left(\frac{8\pi^2}{g^2(\mu)} \right)^{2N} e^{-8\pi^2/g^2(\mu)},$$

$$n_T(\lambda) = \exp \left[-\frac{2N}{3}\lambda^2 - 12A(\lambda) \left(1 + \frac{N}{6} \right) \right],$$

$$A(\lambda) = -\frac{1}{12} \log \left(1 + \frac{\lambda^2}{3} \right) + c_1 \left(\frac{1}{1 + c_2\lambda^{-\frac{3}{2}}} \right)^8, \quad (6.2)$$

where N is the number of colors, μ denotes the renormalization scale and $b = 11N/3$ the leading coefficients of the β function. In the following calculation, we use the instanton density at 1-loop level because of the high temperature. We also assume that the scale μ is replaced by the temperature T . Then, in eq. 6.1 the ρ independent factor can be factored out as

$$\begin{aligned} & \int_0^{1/T} dz_4 \int d^3\vec{z} \frac{d\rho}{\rho^5} n_G(\rho) n_T(\pi\rho T) \\ &= C_I T^b \left(\frac{8\pi^2}{g^2(T)} \right)^{2N} e^{-8\pi^2/g^2(T)} \int_0^{1/T} dz_4 \int d^3\vec{z} d\rho \rho^{b-5} n_T(\pi\rho T). \end{aligned} \quad (6.3)$$

Note that the exponential factor in $n_T(\pi\rho T)$ effectively provides the upper limit for the ρ integral, $\rho_{\text{cut}} \sim 1/\pi T$.

In the following, we consider the CPV correlation function of the action density $s(x) = (1/4g^2)F_{\mu\nu}^a F_{\mu\nu}^a(x)$ and the topological charge density $q(x) = (1/32\pi^2)F_{\mu\nu}^a \tilde{F}_{\mu\nu}^a(x)$ in the $Q = 1$ sector,

$$\begin{aligned} & \langle s(x) q(0) \rangle_{Q=1} \\ &= C_I T^b \left(\frac{8\pi^2}{g^2(T)} \right)^{2N} e^{-8\pi^2/g^2(T)} \int_0^\beta d\tau_0 \int d^3z d\rho \rho^{b-5} n_T(\pi\rho T) s(x) q(0), \end{aligned} \quad (6.4)$$

where we assume the contribution of the $Q = 1$ sector is dominated by the contribution of the single instanton background. For general N , the correlation function (6.4) is not well defined at zero temperatures due to the IR divergence. But, in the SU(2) Yang-Mills

theory, it is finite and found to be [34]

$$\langle s(x) q(0) \rangle_{Q=1} = C x^{-8} (x \Lambda)^b, \quad (6.5)$$

where Λ is the dynamical scale. Once temperature is switched on, (6.5) is modified as

$$\langle s(x) q(0) \rangle_{Q=1} = C T^8 \left(\frac{\Lambda}{T} \right)^b (x T)^{-\gamma(xT)}, \quad (6.6)$$

where the precise form of $\gamma(xT)$ is determined by an explicit calculation.

In the single instanton background the field strength $F_{\mu\nu}^a$ in the action density and the topological charge density is substituted by the instanton solution $\bar{F}_{\mu\nu}^a$ at finite temperature. This procedure is the same as what we reviewed in sec. 3.5 for the $N = 2, 3$ case in $SU(N)$ Yang-Mills theory. As shown in sec. 3.2.5 the instanton configuration at finite temperature is constructed as a sum of the countably infinite number of instantons at zero temperature periodically aligned along the Euclidean time z_4 direction. In order to deal with the multi-instanton configuration, the singular instanton in eq. 3.100 is considered here, and thus the HS caloron in eq. 3.111 is also in the singular gauge, which has singularity at the position of the instanton. In order to calculate the leading instanton contribution to the two point function of the gluon such as eq. 6.4, strictly speaking the integration in terms of the position $d^3 z dz_4$ may diverge by the pole of the caloron.

There is a counterpart solution at zero temperature, called the 't Hooft solution in eq. 3.100, which is singular at the position of the instanton. When calculating physical quantities at zero temperature using the 't Hooft solution, one usually applies a singular transformation in eq. 3.88 and obtain the BPST instanton in eq. 3.85, which is regular anywhere [20, 80]. Here, we follow the similar prescription. In order to remove the singularity of HS caloron, we take the periodicity in the time direction into account, and modify the singular transformation employed at zero temperature to the one for finite temperature [20].

We define the dimension-less coordinates as

$$\begin{aligned}
R &= 2\pi T |\vec{x} - \vec{z}_0|, \\
R_i &= 2\pi T (x_i - z_{0,i}), \\
R_4 &= 2\pi T (x_4 - z_{0,4}), \\
\lambda &= \pi \rho T.
\end{aligned} \tag{6.7}$$

Using the above notation, the potential of the HS caloron is written as

$$\Pi = 1 + \frac{\pi T \rho^2}{|\vec{x} - \vec{z}_0|} \frac{\text{sh}(2\pi T |\vec{x} - \vec{z}_0|)}{\text{ch}(2\pi T |\vec{x} - \vec{z}_0|) - \cos(2\pi T (\tau - \tau_0))}, \tag{6.8}$$

$$\begin{aligned}
&= 1 + \frac{2\lambda^2}{R} \frac{\text{sh}R}{\text{ch}R - \cos R_4}, \\
&\approx 1 + \frac{4\lambda^2}{R^2 + R_4^2},
\end{aligned} \tag{6.9}$$

where \vec{z} and τ_0 denotes the instanton position in the 3-dimensional space and the imaginary time, respectively.

As eq. 6.9 shows, Π has the singularity at the position of the instanton. Since this singularity propagate to the A_μ and $F_{\mu\nu}^a F_{\mu\nu}^a$ and avoid us to calculate the correlator, we need to move this singularity to the infinity by singular transformation, which must be unitary and periodic in the imaginary time direction. Such gauge transformation is realized by

$$g = \frac{i\tau_\mu^+ \bar{R}_\mu}{\sqrt{\bar{R}^2}}, \tag{6.10}$$

$$\bar{R}_\mu = (R_i, \sin R_4). \tag{6.11}$$

Using the above gauge transformation, we obtain the regular instanton configuration in the finite temperature as follows. In the end, we obtain the following solution,

$$A_\mu = -4\pi T \left(\tilde{a}_\alpha \bar{R}_\alpha + \bar{I}_\mu \right) \frac{i\tau_{\mu\nu}^+ \bar{R}_\nu}{\bar{R}^2}, \tag{6.12}$$

where

$$\begin{aligned}\tilde{a}_\mu &= \frac{\partial}{\partial x_\mu} \frac{1}{4\pi T} \ln \Pi(x), & \bar{R}_\mu &= \{R_i, \sin R_4\} \quad (i = 1, 2, 3), \\ \bar{I}_\mu &= \begin{cases} 1 & \text{for } \mu = 1, 2, 3 \\ \cos R_4 & \text{for } \mu = 4 \end{cases}, \\ \tau_{\mu\nu}^\pm &= \frac{1}{4} (\tau_\mu^\pm \tau_\nu^\mp - \tau_\nu^\pm \tau_\mu^\mp), & \tau_\mu^\pm &= \{\tau^a, \pm i\},\end{aligned}$$

with τ^a Pauli matrices.

Since in the limit of $R \rightarrow 0$ and $R_4 \rightarrow 0$

$$\begin{aligned}\tilde{a} \cdot \bar{R} &= \lambda^2 \frac{\text{sh}R (\cos R_4 - \sin^2 R_4) - \text{ch}R (R \cos R_4 + \text{sh}R) + R}{(\text{ch}R - \cos R_4) (R \text{ch}R - R \cos R_4 + 2\lambda^2 \text{sh}R)}, \\ &\approx \frac{\lambda^2 (R^2 - 4)}{4\lambda^2 + R^2 + R_4^2},\end{aligned}\tag{6.13}$$

the gauge field A'_μ and its derivative, $F_{\mu\nu}$, is regular at this point.

The field strength tensor in the instanton background A'_μ is straightforwardly calculated as

$$\begin{aligned}F'_{\mu\nu} &= \partial_\mu A'_\nu - \partial_\nu A'_\mu + i[A'_\mu, A'_\nu], \\ &= 8\pi^2 T^2 \frac{i\tau_{\nu\rho}^{(+)}}{\bar{R}^2} \left[\tilde{a} \cdot \bar{R} \left(\delta_{\rho\mu} - \frac{2\bar{R}_\rho \bar{R}_\mu}{\bar{R}^2} \right) - \bar{R}_\rho \partial_\mu \right] (\tilde{a} \cdot \bar{R} + \bar{I}_\nu) - (\mu \leftrightarrow \nu),\end{aligned}\tag{6.14}$$

$$\equiv i\tau_{\nu\rho}^{(+)} f_{\rho\mu}^{(\nu)} - i\tau_{\mu\rho}^{(+)} f_{\rho\nu}^{(\mu)},\tag{6.15}$$

where

$$f_{\rho\mu}^{(\nu)} = \frac{8\pi^2 T^2}{\bar{R}^2} \left[\tilde{a} \cdot \bar{R} \left(\delta_{\rho\mu} - \frac{2\bar{R}_\rho \bar{R}_\mu}{\bar{R}^2} \right) - \bar{R}_\rho \partial_\mu \right] K^{(\nu)},\tag{6.16}$$

$$K^{(\nu)} = \tilde{a} \cdot \bar{R} + \bar{I}_\nu.\tag{6.17}$$

Then using the relation,

$$\text{Tr} (\tau_{\mu\nu}^{(+)} \tau_{\rho\sigma}^{(+)}) = \frac{1}{2} (\delta_{\mu\sigma} \delta_{\nu\rho} - \delta_{\mu\rho} \delta_{\nu\sigma} + \hat{\epsilon}_{\mu\nu\rho\sigma}),\tag{6.18}$$

we obtain

$$\text{Tr}F'_{\mu\nu}F'_{\mu\nu} = -f_{\mu\rho}^{(\mu)}f_{\mu\rho}^{(\mu)} - f_{\rho\mu}^{(\mu)}f_{\rho\mu}^{(\mu)} + \delta_{\nu\nu}f_{\rho\mu}^{(\nu)}f_{\rho\mu}^{(\nu)} + f_{\mu\mu}^{(\nu)}f_{\nu\nu}^{(\mu)}, \quad (6.19)$$

where these tensor products are calculated as

$$\begin{aligned} & f_{\mu\rho}^{(\mu)}f_{\mu\rho}^{(\mu)} \\ = & \left(\frac{8\pi^2T^2}{\bar{R}^2}\right)^2 \left[(\tilde{a} \cdot \bar{R})^2 (3K_1^2 + K_4^2) \right. \\ & + \frac{4(\tilde{a} \cdot \bar{R})}{\bar{R}^2} \left\{ K_1 (\bar{R} \cdot \partial(\tilde{a} \cdot \bar{R})) \bar{R}^2 + (K_4 - K_1) \bar{R}_4^2 (\bar{R} \cdot \partial(\tilde{a} \cdot \bar{R})) - K_4 (\bar{R}_4)^4 \right\} \\ & \left. + \left\{ \bar{R}^2 \partial_\alpha(\tilde{a} \cdot \bar{R}) \partial_\alpha(\tilde{a} \cdot \bar{R}) + \bar{R}_4^4 - 2\partial_4(\tilde{a} \cdot \bar{R}) \bar{R}_4^3 \right\} \right], \quad (6.20) \end{aligned}$$

$$\begin{aligned} f_{\rho\mu}^{(\mu)}f_{\rho\mu}^{(\mu)} &= \left(\frac{8\pi^2T^2}{\bar{R}^2}\right)^2 \left[(\tilde{a} \cdot \bar{R})^2 (3K_1^2 + K_4^2) \right. \\ & \left. + \bar{R}^2 \partial_\alpha(\tilde{a} \cdot \bar{R}) \partial_\alpha(\tilde{a} \cdot \bar{R}) - 2\bar{R}^2 \bar{R}_4 \partial_4(\tilde{a} \cdot \bar{R}) + \bar{R}^2 \bar{R}_4^2 \right], \quad (6.21) \end{aligned}$$

$$\begin{aligned} & \delta_{\nu\nu}f_{\rho\mu}^{(\nu)}f_{\rho\mu}^{(\nu)} \\ = & \left(\frac{8\pi^2T^2}{\bar{R}^2}\right)^2 \left[4(\tilde{a} \cdot \bar{R})^2 (3K_1^2 + K_4^2) + 2(\tilde{a} \cdot \bar{R}) \left\{ (3K_1 + K_4) (\bar{R} \cdot \partial(\tilde{a} \cdot \bar{R})) - K_4 \bar{R}_4^2 \right\} \right. \\ & \left. + \bar{R}^2 \left\{ 4\partial_\alpha(\tilde{a} \cdot \bar{R}) \partial_\alpha(\tilde{a} \cdot \bar{R}) - 2\bar{R}_4 \partial_4(\tilde{a} \cdot \bar{R}) + \bar{R}_4^2 \right\} \right], \quad (6.22) \end{aligned}$$

$$\begin{aligned}
& f_{\mu\mu}^{(\nu)} f_{\nu\nu}^{(\mu)} \\
= & \left(\frac{8\pi^2 T^2}{\bar{R}^2} \right)^2 \left[(\tilde{a} \cdot \bar{R})^2 (3K_1 + K_4)^2 - 4(\tilde{a} \cdot \bar{R})^2 (3K_1 + K_4) \left(K_1 + \frac{\bar{R}_4^2}{\bar{R}^2} (K_4 - K_1) \right) \right. \\
& + 4(\tilde{a} \cdot \bar{R})^2 \left(K_1 + \frac{\bar{R}_4^2}{\bar{R}^2} (K_4 - K_1) \right)^2 \\
& - 2(\tilde{a} \cdot \bar{R}) \left\{ 4K_1 (\bar{R} \cdot \partial(\tilde{a} \cdot \bar{R})) + 4(K_4 - K_1) \bar{R}_4 \partial_4(\tilde{a} \cdot \bar{R}) - \bar{R}_4^2 K_4 \right\} \\
& + 4(\tilde{a} \cdot \bar{R}) \left\{ K_1 (\bar{R} \cdot \partial(\tilde{a} \cdot \bar{R})) + (K_4 - K_1) \bar{R}_4 \partial_4(\tilde{a} \cdot \bar{R}) - K_4 \frac{\bar{R}_4^4}{\bar{R}^2} \right\} \\
& \left. + (\bar{R} \cdot \partial(\tilde{a} \cdot \bar{R}))^2 - 2\bar{R}_4^3 \partial_4(\tilde{a} \cdot \bar{R}) + \bar{R}_4^4 \right]. \tag{6.23}
\end{aligned}$$

The building blocks of the above formulae are $K_1 = (\tilde{a} \cdot \bar{R}) - 1$, $K_4 = (\tilde{a} \cdot \bar{R}) - \cos R_4$, and the following formulae.

$$(\tilde{a} \cdot \bar{R}) = \frac{\lambda^2 \left(-\text{ch}(R)(R \cos(R_4) + \text{sh}(R)) + \text{sh}(R) \left(\cos(R_4) - \sin^2(R_4) \right) + R \right)}{(\text{ch}(R) - \cos(R_4)) (R \text{ch}(R) - R \cos(R_4) + 2\lambda^2 \text{sh}(R))}, \tag{6.24}$$

$$\begin{aligned}
\partial_4(\tilde{a} \cdot \bar{R}) = & \frac{1}{2(\text{ch}(R) - \cos(R_4))^2 (R \text{ch}(R) - R \cos(R_4) + 2\lambda^2 \text{sh}(R))^2} \\
& \lambda^2 \sin(R_4) \left[-\text{ch}(R) \left(R^2 (\cos(2R_4) + 5) + 8\lambda^2 \text{sh}(R)^2 \cos(R_4) - 2R \text{sh}(R) (-2 \cos(R_4) + \cos(2R_4) + 3) \right) \right. \\
& + 2R^2 \text{ch}(R)^3 + 2R \text{ch}(R)^2 \text{sh}(R) \left(2\lambda^2 - 2 \cos(R_4) + 1 \right) + 4R^2 \cos(R_4) + 2\lambda^2 \text{sh}(R)^2 (\cos(2R_4) + 3) \\
& \left. + R \text{sh}(R) \left(-4\lambda^2 - 4 \cos(R_4) + \cos(2R_4) + 1 \right) \right], \tag{6.25}
\end{aligned}$$

$$\begin{aligned}
& \partial_\alpha(\tilde{a} \cdot \bar{R}) \partial_\alpha(\tilde{a} \cdot \bar{R}) \\
= & \frac{1}{4(\text{ch}(R) - \cos(R_4))^4 (R\text{ch}(R) - R\cos(R_4) + 2\lambda^2\text{sh}(R))^4} \\
& \lambda^4 \left[\sin^2(R_4) \left(-\text{ch}(R) \left(R^2(\cos(2R_4) + 5) + 8\lambda^2\text{sh}(R)^2 \cos(R_4) \right. \right. \right. \\
& \left. \left. - 2R\text{sh}(R)(-2\cos(R_4) + \cos(2R_4) + 3) \right) + 2R^2\text{ch}(R)^3 + 2R\text{ch}(R)^2\text{sh}(R) (2\lambda^2 - 2\cos(R_4) + 1) \right. \\
& \left. + 4R^2\cos(R_4) + 2\lambda^2\text{sh}(R)^2(\cos(2R_4) + 3) + R\text{sh}(R) (-4\lambda^2 - 4\cos(R_4) + \cos(2R_4) + 1) \right)^2 \\
& + 4 \left((\text{ch}(R) - \cos(R_4)) (R\text{ch}(R) - R\cos(R_4) + 2\lambda^2\text{sh}(R)) \right. \\
& \left. (\text{ch}(R) \sin^2(R_4) + \text{ch}(R)^2 + R\text{sh}(R) \cos(R_4) + \text{sh}(R)^2 - 1) \right. \\
& \left. + (\text{ch}(R) - \cos(R_4)) (2\lambda^2\text{ch}(R) + \text{ch}(R) + R\text{sh}(R) - \cos(R_4)) \right. \\
& \left. (-\text{ch}(R)(R\cos(R_4) + \text{sh}(R)) + \text{sh}(R) (\cos(R_4) - \sin^2(R_4)) + R) \right. \\
& \left. + \text{sh}(R) (R\text{ch}(R) - R\cos(R_4) + 2\lambda^2\text{sh}(R)) \right. \\
& \left. (-\text{ch}(R)(R\cos(R_4) + \text{sh}(R)) + \text{sh}(R) (\cos(R_4) - \sin^2(R_4)) + R) \right)^2 \Big], \tag{6.26}
\end{aligned}$$

$$\begin{aligned}
& R \cdot \partial(\tilde{a} \cdot \bar{R}) \\
= & \frac{1}{(\text{ch}(R) - \cos(R_4))^2 (R\text{ch}(R) - R\cos(R_4) + 2\lambda^2 \text{sh}(R))^2} \\
& \lambda^2 \left[R\text{ch}(R)^2 \left\{ \text{sh}(R) \left(\cos(R_4) \left(-2\lambda^2 + R^2 + \cos(2R_4) - 4 \right) + 2 \left(\lambda^2 + 1 \right) \sin^2(R_4) \right) \right. \right. \\
& \left. \left. + R \left(-2\lambda^2 - \left(2\lambda^2 + 3 \right) \cos^2(R_4) + \sin(R_4) \sin(2R_4) \right) + R\text{sh}(R)^2 \right\} \right. \\
& \left. - \frac{1}{4} \text{ch}(R) \left\{ R^2 \left(- \left(\left(8\lambda^2 + 3 \right) \cos(R_4) + 4 \cos(2R_4) + \cos(3R_4) + \cos(4R_4) - 5 \right) \right) \right. \right. \\
& \left. \left. + R\text{sh}(R) \left(-12\lambda^2 + 8R^2 - 2 \left(2\lambda^2 + 1 \right) \cos(2R_4) + 4 \cos(R_4) - 4 \cos(3R_4) + \cos(4R_4) - 11 \right) \right. \right. \\
& \left. \left. + 8\text{sh}(R)^2 \left(\sin^2(R_4) \left(2\lambda^2 \cos(R_4) - R^2 \right) + R^2 \cos(R_4) \right) \right\} \right. \\
& \left. - R^2 \text{ch}(R)^4 + R\text{ch}(R)^3 \left(\left(2\lambda^2 + 3 \right) R \cos(R_4) + \text{sh}(R) \right) \right. \\
& \left. - \frac{1}{4} R\text{sh}(R) \left(4\lambda^2 + \left(8\lambda^2 - 5R^2 + 5 \right) \cos(R_4) + R^2 \cos(3R_4) \right. \right. \\
& \left. \left. - 4\lambda^2 \cos(2R_4) - \cos(3R_4) + \cos(4R_4) - 1 \right) + \text{sh}(R)^2 \left(\lambda^2 \left(-2R^2 + 2 \sin^4(R_4) + \sin^2(2R_4) \right) \right. \right. \\
& \left. \left. + \left(2\lambda^2 + 1 \right) R^2 \cos^2(R_4) - 2R^2 \sin^2(R_4) \cos(R_4) \right) \right. \\
& \left. \left. + R^2 \sin(R_4) \sin(2R_4) + 2\lambda^2 R\text{sh}(R)^3 \sin^2(R_4) \right] \right]. \tag{6.27}
\end{aligned}$$

Substituting this solution into the integrand of eq. (6.4), the correlation function is numerically evaluated as shown in fig. 6.1, where the normalized correlation function is plotted as a function of $\log(2\pi T|\vec{x}|)$. The correlation function behaves like $|\vec{x}|^{-6}$ for $2\pi T|\vec{x}| \gg 1$ as indicated in the figure, while it stays constant for $2\pi T|\vec{x}| \ll 1$, *i.e.* it turns out that $\lim_{x \rightarrow \infty} \gamma(xT) = 6$ and $\lim_{x \rightarrow 0} \gamma(xT) = 0$. Later we will compare this behavior to the one calculated on the lattice. Since the comparison is made at a given temperature and the overall factor is adjusted by hand, the factor $(\Lambda/T)^b$ is treated as a part of the overall factor.

6.2 Simulation setup

The gauge configurations are generated using the Wilson plaquette gauge action with $N = 2$ at several β values. Two lattice sizes are chosen to be $24^3 \times 6$ and $32^3 \times 8$. The simulation code is developed from the Bridge++ code set [81] to perform SU(2) simulations. The physical temperatures, T/T_c , listed in Tab. 6.1, are borrowed from

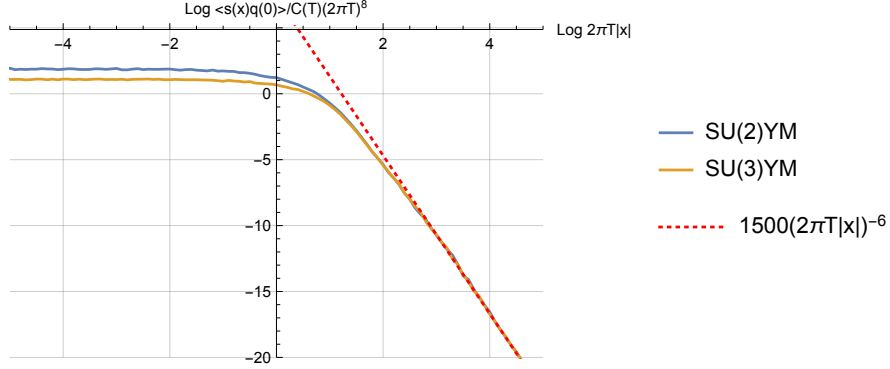


Figure 6.1: The x -dependence of the correlation function eq. (6.4) in one instanton background, eq. (6.12). The $\langle s(x)q(0) \rangle_{Q=1} / C(T)(2\pi T)^8$ is a function of xT , where all the T dependent factor of $\langle s(x)q(0) \rangle_{Q=1}$ is factored out as $C(T)T^8$.

Table 6.1: Lattice parameters, physical temperatures, statistics.

Lattice	β	T/T_c	$N_{\text{conf}}(Q = 1)$	N_{tot}
$24^3 \times 6$	2.322	0.7215	122	824
$24^3 \times 6$	2.468	1.163	87	372
$32^3 \times 8$	2.582	1.246	154	540
$32^3 \times 8$	2.714	1.857	90	786

Ref. [82]. The measurements described below are carried out every ten trajectories. The total number of configurations and the number of configurations in the $Q = \pm 1$ sector in each ensemble are listed shown in Tab. 6.1.

6.3 Gradient flow with large flow time

The gradient flow in Yang-Mills theory [83, 84] is an evolution of gauge field in terms of the diffusion equation along the fictitious time t , so called flow time. In the continuum theory the flow equation is given by

$$\frac{\partial B_\mu(x, t)}{\partial t} = -\frac{\delta S_{\text{YM}}}{\delta B_\mu(x, t)}, \quad B_\mu(x, t = 0) = A_\mu(x), \quad (6.28)$$

where $A_\mu(x)$ is the gauge field in 4d Euclidean Yang-Mills theory, and S_{YM} is the Yang-Mills action. This procedure makes the field configurations be smoothed with the smearing radius $\sim \sqrt{8t}$. Importantly, the flow equation (6.28) leaves classical solutions

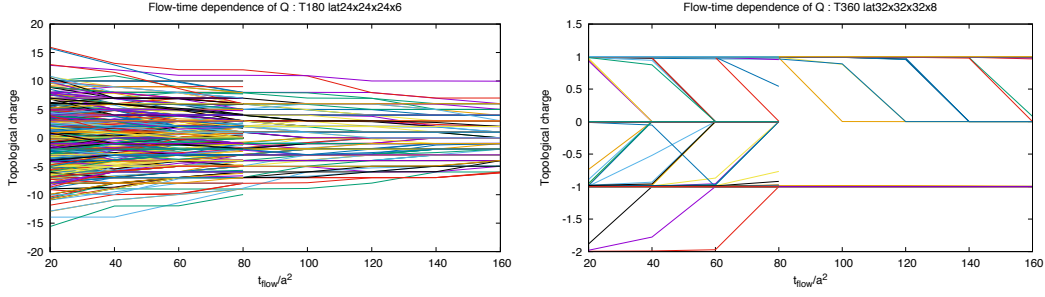


Figure 6.2: The flow time history of the topological charge for $24^3 \times 6$ with $T/T_c \approx 0.72$ (left) and $32^3 \times 8$ with $T/T_c \approx 1.9$ (right).

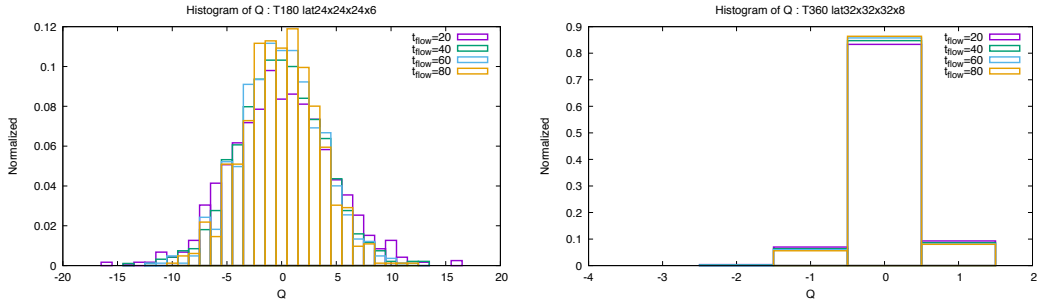


Figure 6.3: Histogram of Q at various t/a^2 for $24^3 \times 6$ with $T/T_c \approx 0.72$ (left) and $32^3 \times 8$ with $T/T_c \approx 1.9$ (right).

untouched because the force becomes zero for stationary solutions. This property is suitable for our purpose since the size of instantons is kept during the flow and hence the distribution of instanton size of the original gauge configurations $n(\rho, T)$ is also preserved even after the flow.

To identify the $|Q| = 1$ configurations, we first measure the topological charge using the Wilson flow. The examples of the flow time history of the topological charge in $t/a^2 \in [20, 160]$ are shown in fig. 6.2. Since the calculation is still on-going, some of lines end at $t/a^2 = 80$. Unfortunately, Q of some configurations is changing even after the long flow. This can happen on relatively coarse lattices. We hope that the situation is settled at finer lattice spacings.

Fig. 6.3 shows the resulting histogram of Q obtained at $t/a^2 = 20, 40, 60, 80$. Since Q is more stable at a larger t/a^2 and the full statistics are available at $t/a^2 = 80$, we take the configurations at $t/a^2 = 80$ in the following analysis.

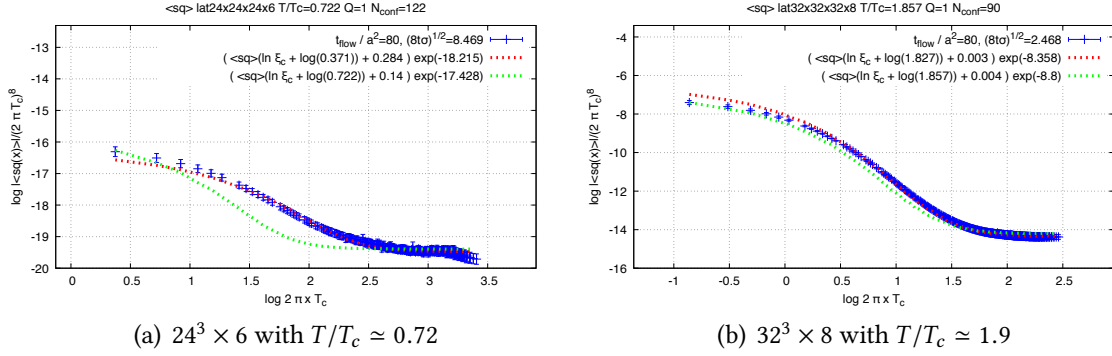


Figure 6.4: The CP violating gluonic correlator in the fixed topological charge sector with $|Q| = 1$. The data points with error bar are the lattice results. The dotted lines are the predictions of the instanton calculus. For details, see the text.

6.4 CP violating correlation function in the $Q = 1$ sector

From the configurations evolved by the Wilson flow with a large flow time, we choose those with $|Q| = 1$ to calculate the CPV gluonic correlation function in the $Q = 1$ sector, $\langle s(x) q(0) \rangle_{Q=1}$. Note that the ensemble average of CPV correlation function should vanish when using all configurations or those with $Q = 0$. To enhance the statistics, the configurations with $Q = -1$ are also used, where the sign of the correlation functions is flipped in taking the average.

Fig. 6.4 shows the lattice results of the correlation function (blue) below (left) and above (right) T_c . Note that the both axes are different from those in fig. 6.1. The change of the vertical axis is just the change of the overall normalization, which we do not care in the following analysis. We choose as the horizontal axis $\xi_c \equiv \ln(2\pi T_c x)$, where the physical distance between operators is denoted as $x = a\sqrt{n_x^2 + n_y^2 + n_z^2}$.

Recalling the HS caloron prediction (6.6), it can be rewritten as

$$\left. \frac{\langle s(x) q(0) \rangle_{Q=1}}{C (2\pi T_c)^8} \right|_{T/T_c = \text{fixed}} = A (xT)^{-\gamma(xT)} = A \left(x T_c \frac{T}{T_c} \right)^{-\gamma(xT_c \frac{T}{T_c})} = A \Pi(\xi_c, T/T_c). \quad (6.29)$$

Since we know the values of (xT) and (T/T_c) , the curve in fig. 6.1 in a give temperature can be expressed in fig. 6.4 with the horizontal shift of $\ln(T/T_c)$ up to the overall normalization, A .

Another caution in comparing the HS caloron prediction to the lattice result is the behavior at large x . Since the lattice calculations are carried out under the periodic boundary condition in all directions, the correlation function at large x receives a contribution from the mirror images. This finite size effect is indeed seen in the plot. The correlation function is supposed to monotonically decrease whereas it looks constant at large x . To take care this effect, we add a proper constant to the caloron prediction. In summary, in the comparison, we plot the caloron prediction as

$$\ln [A\Pi(\xi_c, T/T_c) + B] , \quad (6.30)$$

as a function of ξ_c . To be specific, the overall factor A is tuned so that the caloron prediction and the lattice result agree at the left most data point, and B is obtained by the fit to the lattice data. The curve thus obtained is shown in fig. 6.4 (green). While both the results nicely agree at $T/T_c \sim 1.9$ over the whole region plotted, significant deviation is observed in the middle range of the plot for $T/T_c \sim 0.72$. Note that this disagreement never disappear whatever A is.

From the observation above, we found that, at high temperature, the instanton picture is reasonable in the sense that the instanton indeed exists in the $Q = 1$ sector with the expected size distribution. We can not draw a definite conclusion for the lower temperature case, but one possible interpretation would be that the instanton size is bigger than expected. It is somewhat interesting. One naive picture is that as temperature decreases, the instanton size gets larger and stops changing the size near $T = T_c$, so that the size of instanton below T_c is smaller than the prediction from the semi-classical analyses. The data says somewhat different. The instanton size gets larger as temperature decreases, but below T_c we find larger instantons than expected.

In order to explore a reasonable interpretation for the lower temperature case, we attempted to fit the lattice result to

$$\ln [A\Pi(\xi_c, r) + B] , \quad (6.31)$$

where the temperature T/T_c is replaced with the fit parameter $r = T_{\text{eff}}/T_c$. The fit results are shown in fig. 6.4 (red dotted curves). This time, all of A , B and r are determined by the fit. At the low temperature, the significant deviation observed in the case of eq. 6.30 disappears, and the best fit is obtained at $T_{\text{eff}} \sim 0.37 T_c$, which is far below

the actual temperature $0.72 T_c$. On the other hand, at high temperature, the resulting effective temperature is $T_{\text{eff}} \sim 1.8 T_c$, which is almost the same as $1.9 T_c$.

6.5 Summary and outlook

Instanton is believed to play crucial roles not only in the dynamics of QCD but also in the particle physics phenomenology. The topological susceptibility at high temperature in the pure $SU(N)$ Yang-Mills theory is one of the examples, where the instanton calculus works well. However, as the temperature decreases, the instanton calculus becomes questionable and would eventually fail to estimate most of quantities at zero temperature. In this work, we are trying to clarify the temperature at which the instanton picture breaks down. Since the direct reason for the failure in the instanton calculus is the divergence of the integration over ρ , we start to look at the distribution of the instanton size ρ .

To this end, we calculate a gluonic two point function in the instanton calculus and on the lattice since the calculation of the one point functions or their integration over the volume does not tell any information on the size. In the instanton calculus, the ρ distribution $n(\rho, T)$ at a given temperature is known. In the lattice calculation, $n(\rho, T)$ is an output. Since we are only interested in the instanton, the configurations generated on the lattice are processed by a long gradient flow so that only the instantons survive, where we use the property that the gradient flow leaves the instanton solutions untouched and hence $n(\rho, T)$ in the original configurations unchanged and only the fluctuations are diffused. At high temperature, the lattice result of the two point function remarkably agrees with the instanton prediction as expected.

It can be inferred from the expression of $n(\rho, T)$ used in the instanton calculus in eq. 6.2 that a large-size instanton contributes more at lower T . To see this, we simply repeated the same procedure at low temperature. It turned out that the size distribution obtained on the lattice is significantly different from the instanton prediction but interestingly it agrees with that at the temperature much lower than the actual one. It would be a future work to find dynamical reason for the mismatch of the temperatures and to see the temperature at which this mismatch starts to appear.

7

Conclusion

The instanton is believed to play crucial roles not only in the dynamics of QCD but also in the phenomenology of the elementary particle physics. Because the instanton solution has non-zero value of $F_{\mu\nu}^a \tilde{F}_{\mu\nu}^a$, it could be a source of the CP violating interaction in QCD. In other words, there could be the CP-violating term $\theta F_{\mu\nu}^a \tilde{F}_{\mu\nu}^a$ which is renormalizable and gauge invariant operator. Although we have no reason to ignore this term in the Standard Model, the experimental limits on the electric dipole moment of the neutron put an extremely tight bound on the parameter θ . This is what is called the Strong CP problem. The Peccei-Quinn mechanism provides a solution to this problem. In this mechanism, the axion is introduced as a pseudo NG boson of the $U(1)_{\text{PQ}}$ symmetry which is broken at high energy, and dynamically falls into the CP-conserving vacuum. The possibility of the axion is interesting because it becomes a candidate of the cold dark matter in the universe.

The QCD topological susceptibility $\chi_t(T)$ at high temperature provides an important input for the estimate of the axion abundance in the present universe. The estimate requires the topological susceptibility in the temperature region $T \geq O(1)$ GeV. There are the analytic and numerical methods to approach this non-perturbative observable.

However, the analytic calculation, the DIGA, is not justified in the strong-coupling regime, $T \sim O(1)$ GeV. Also, the existing method to measure the susceptibility on the lattice does not work at high temperature, because the production rate of the configuration with the non-trivial topological charge rapidly decreases under the Monte-Carlo simulation.

The determination of $\chi_t(T)$ at high temperature is important not only for the phenomenology but also for solving the inconsistencies among the lattice results. In the $N_f = 3$ QCD, several groups report that $\chi_t(T)$ decreases with T^{-8} [56] as expected by the DIGA, while one group reports T^{-3} [57, 30]. In the $N_f = 2$ QCD, Fukaya *et al.* [25] report that $\chi_t(T)$ becomes vanish at $T > T_c$. As pointed out by Kitano and Yamada [27], the rapid decrease of $\chi_t(T)$ at the deconfine phase makes the energy density of the axion significantly larger and thus the axion cannot naturally explain the dark matter.

In the first work described in chap. 5, we propose a novel framework to measure $\chi_t(T)$, which, in contrast to the existing method, is expected to work mainly at high temperature, where $\chi_t(T)V_4 \ll 1$. In order to check the validity of this method, we performed the quenched simulations on the $16^3 \times 4$ lattice, and found that $d \ln \chi_t / d \ln T$ agree with the DIGA prediction about $1.5T_c$ within the error.

Our method does not determine the absolute value of $\chi_t(T)$, while we can determine the power behavior at high temperature. In the current technology, we cannot determine $\chi_t(T)$ above the maximum temperature, say T_{\max} . Our method can calculate $d \ln \chi_t / d \ln T$ above some temperature, say T_{\min} . Increasing the statistics, T_{\max} gets higher and T_{\min} gets lower. If $T_{\min} < T_{\max}$, we can extrapolate the plot of $\chi_t(T)$ above T_{\max} using the power behavior of $d \ln \chi_t / d \ln T$ and the absolute value $\chi_t(T_{\max})$. This framework would provide us the reasonable $\chi_t(T)$ at any temperature region, and thus, if done with $N_f = 3$ QCD, we would obtain the axion abundance using the input which depends only on the first principle calculation. Also, the determination of $d \ln \chi_t / d \ln T$ at high temperature could solve the inconsistencies of $\chi_t(T)$ at the deconfine phase.

The above extrapolation confronts us a new question about the validity of the DIGA. The lattice determination of $d \ln \chi_t / d \ln T$ in the Yang-Mills theory is consistent with the instanton calculus, while the absolute value of $\chi_t(T)$ at $T > T_c$ determined by the lattice calculation is ten times larger than the DIGA calculation [29]. If we apply the extrapolation described above, the absolute value of $\chi_t(T)$ much differs from the DIGA prediction in the high temperature limit. This contradicts the expectation that

in the high temperature limit the full partition function can be approximated by the partition function with the DIGA.

In the first work, as shown in fig. 5.2, we checked that in the Yang-Mills theory the action difference $(1/\beta)(\langle S \rangle_{Q=1} - \langle S \rangle_{Q=0})$ becomes the classical value $(4\pi^2/3)$. This checks the general property of the gluon configuration with the non-trivial topological charge, i.e., the Bogomol'nyi completion (eq. 3.68). Although this indicates that some classical configuration dominates at high temperature, it does not directly prove the instanton picture. To better understand the actual instanton picture at high temperature, we need more information which is characteristic of the instanton configuration. In the latter work, we investigate the local structure of the instanton via the CP-violating two-point function.

In the second work described in chap. 6, we investigate the region of the validity of the instanton picture from the two perspectives. First, we ask whether the instanton picture is consistent with the lattice calculation not only in the global observable, e.g., χ_t but also in the local observable, e.g., the two-point gluonic correlation function. The local observable should have information of the instanton size, which controls that the instanton approximation works or not. Second, we ask from which temperature the instanton picture applies and how it disappears at low temperature. The instanton calculus is justified only at high temperature, while, as temperature decreases, the instanton calculus becomes questionable and would eventually break down. We try to clarify the temperature at which the instanton picture fails.

To this end, we calculate a gluonic two point function in the instanton calculus and on the lattice, since the calculation of the one point functions or their integration over the volume does not tell any information on the size. In the instanton calculus, the ρ distribution $n(\rho, T)$ at a given temperature is known. In the lattice calculation, $n(\rho, T)$ is an output. Since we are only interested in the instanton, the configurations generated on the lattice are processed by a long gradient flow so that only the instantons survives, where we use the property that the gradient flow leaves instanton solutions untouched and hence $n(\rho, T)$ in the original configurations unchanged and only the quantum fluctuations are smeared. At high temperature, the lattice result of the two point function remarkably agrees with the instanton prediction as expected.

It can be inferred from the expression of $n(\rho, T)$ used in the instanton calculus in eq. 6.2 that a large-size instanton contributes more at lower T . To see this, we simply repeated the same procedure at low temperature. It turned out that the size distribu-

tion obtained on the lattice is significantly different from the instanton prediction but interestingly it agrees with that at the temperature much lower than the actual one. It would be a future work to find dynamical reason for the mismatch of temperatures and to see the temperature at which this mismatch starts to appear.

A

Appendix

A.1 Notations in Minkowski space and Euclidean space

In four dimensional Minkowski space, the covariant vector x^μ ($\mu = 0, \dots, 3$) is related with the contravariant vector x_μ as $x_\mu = g_{\mu\nu}x^\nu$, where the metric is $g_{\mu\nu} = \text{diag}(1, -1, -1, -1)$. We use the four vector in Euclidean space, \hat{x}_μ ($\mu = 1, \dots, 4$), where only in this appendix we adopt hat (^) to the Euclidean vector and we omit hat in the main text. The four vectors x^μ and \hat{x}_μ have relations as

$$x^0 = -i\hat{x}_4, \quad x^i = \hat{x}_i \quad (i = 1, 2, 3). \quad (\text{A.1})$$

Then, the four vector of derivative ∂_μ and $\hat{\partial}_\mu$ in Minkowski and Euclidean space, respectively, follow

$$\partial_0 = i\hat{\partial}_4, \quad \partial_i = \hat{\partial}_i. \quad (\text{A.2})$$

We use the definition of gamma matrices in Minkowski space γ_μ following Peaking

and Schroeder's textbook.

$$\gamma^\mu = \begin{pmatrix} 0 & \tau^\mu \\ \bar{\tau}^\mu & 0 \end{pmatrix}, \quad \gamma_5 = i\gamma^0\gamma^1\gamma^2\gamma^3 = \begin{pmatrix} -1_{2\times 2} & 0 \\ 0 & 1_{2\times 2} \end{pmatrix}, \quad (\text{A.3})$$

where we introduce the quartanion

$$\tau^\mu = \{1_{2\times 2}, \tau^a\}, \quad \bar{\tau}^\mu = \{1_{2\times 2}, -\tau^a\}, \quad (\text{A.4})$$

where $\{\tau^a\}$ ($a = 1, 2, 3$) is Pauli matrices.

We define the gamma matrices in Euclidean space $\hat{\gamma}_\mu$ as

$$\gamma^0 = -\hat{\gamma}_4, \quad \gamma^a = i\hat{\gamma}_a \quad (a = 1, 2, 3), \quad (\text{A.5})$$

$$\{\hat{\gamma}_\mu, \hat{\gamma}_\nu\} = 2\delta_{\mu\nu}, \quad (\hat{\gamma}_\mu)^\dagger = \hat{\gamma}_\mu, \quad (\text{A.6})$$

$$\hat{\gamma}_5 = \hat{\gamma}_1\hat{\gamma}_2\hat{\gamma}_3\hat{\gamma}_4 = -\gamma_5. \quad (\text{A.7})$$

This is equivalent to

$$\hat{\gamma}_\mu = \begin{pmatrix} 0 & -i\tau_\mu^- \\ i\tau_\mu^+ & 0 \end{pmatrix}, \quad \hat{\gamma}_5 = \begin{pmatrix} 1_{2\times 2} & 0 \\ 0 & -1_{2\times 2} \end{pmatrix}, \quad (\text{A.8})$$

where we use

$$\tau_\mu^+ = \{\tau^a, i1_{2\times 2}\}, \quad \tau_\mu^- = \{\tau^a, -i1_{2\times 2}\} \quad (a = 1, 2, 3). \quad (\text{A.9})$$

The projection operators is written as

$$P_L = \frac{1 - \gamma_5}{2} = \frac{1 + \hat{\gamma}_5}{2} = \begin{pmatrix} 1_{2\times 2} & 0 \\ 0 & 0 \end{pmatrix}, \quad (\text{A.10})$$

$$P_R = \frac{1 + \gamma_5}{2} = \frac{1 - \hat{\gamma}_5}{2} = \begin{pmatrix} 0 & 0 \\ 0 & 1_{2\times 2} \end{pmatrix}. \quad (\text{A.11})$$

A.2 Thermal field theory

The thermodynamic property of the theory with Hamiltonian \hat{H} is obtained by the partition function

$$Z = \text{Tr}(e^{-\beta\hat{H}}), \quad (\text{A.12})$$

and the expectation value of the operator

$$\langle \mathcal{O} \rangle = \frac{1}{Z} \text{Tr}(e^{-\beta\hat{H}} \mathcal{O}), \quad (\text{A.13})$$

where $\beta = 1/k_B T$.

The finite temperature field theory with temperature T is obtained by the quantum field theory in Euclidean space which has periodic boundary condition along the time direction $\tau \in [0, \beta]$. In the scalar field theory, the partition function Z with temperature T is written as

$$Z = \int [d\phi] \exp\left(-\int_0^\beta d\tau \int d^3x \mathcal{L}(\phi, \partial_\mu \phi)\right), \quad (\text{A.14})$$

where the scalar field $\phi(\mathbf{x}, \tau)$ is the expectation value in terms of the canonical ensemble of the Heisenberg operator $\hat{\phi}(\mathbf{x}, \tau) = e^{\hat{H}\tau} \hat{\phi}(\mathbf{x}) e^{-\hat{H}\tau}$,

$$\phi(\mathbf{x}, \tau) = \frac{\text{Tr} e^{-\beta\hat{H}} \hat{\phi}(\mathbf{x}, \tau)}{\text{Tr} e^{-\beta\hat{H}}}. \quad (\text{A.15})$$

Thus the field has periodicity $\phi(\mathbf{x}, \tau) = \phi(\mathbf{x}, \tau + \beta)$. Likewise the scalar field theory at finite temperature, the thermal gauge field theory also has the periodicity,

$$A_\mu(\mathbf{x}, \tau) = A_\mu(\mathbf{x}, \tau + \beta), \quad U(\mathbf{x}, \tau) = U(\mathbf{x}, \tau + \beta). \quad (\text{A.16})$$

Bibliography

- [1] A. I. Vainshtein, Valentin I. Zakharov, V. A. Novikov, and Mikhail A. Shifman. ABC's of Instantons. *Sov. Phys. Usp.*, 25:195, 1982. [Usp. Fiz. Nauk136,553(1982)].
- [2] R. D. Peccei and Helen R. Quinn. CP Conservation in the Presence of Instantons. *Phys. Rev. Lett.*, 38:1440–1443, 1977.
- [3] R. D. Peccei and Helen R. Quinn. Constraints Imposed by CP Conservation in the Presence of Instantons. *Phys. Rev.*, D16:1791–1797, 1977.
- [4] Steven Weinberg. A New Light Boson? *Phys. Rev. Lett.*, 40:223–226, 1978.
- [5] Frank Wilczek. Axions and Family Symmetry Breaking. *Phys. Rev. Lett.*, 49:1549–1552, 1982.
- [6] Jihn E. Kim. Weak Interaction Singlet and Strong CP Invariance. *Phys. Rev. Lett.*, 43:103, 1979.
- [7] Mikhail A. Shifman, A. I. Vainshtein, and Valentin I. Zakharov. Can Confinement Ensure Natural CP Invariance of Strong Interactions? *Nucl. Phys.*, B166:493–506, 1980.
- [8] Michael Dine, Willy Fischler, and Mark Srednicki. A Simple Solution to the Strong CP Problem with a Harmless Axion. *Phys. Lett.*, 104B:199–202, 1981.
- [9] A. R. Zhitnitsky. On Possible Suppression of the Axion Hadron Interactions. (In Russian). *Sov. J. Nucl. Phys.*, 31:260, 1980. [Yad. Fiz.31,497(1980)].
- [10] John Preskill, Mark B. Wise, and Frank Wilczek. Cosmology of the Invisible Axion. *Phys. Lett.*, 120B:127–132, 1983.

- [11] L. F. Abbott and P. Sikivie. A Cosmological Bound on the Invisible Axion. *Phys. Lett.*, 120B:133–136, 1983.
- [12] Michael Dine and Willy Fischler. The Not So Harmless Axion. *Phys. Lett.*, 120B:137–141, 1983.
- [13] A. A. Belavin, Alexander M. Polyakov, A. S. Schwartz, and Yu. S. Tyupkin. Pseudoparticle Solutions of the Yang-Mills Equations. *Phys. Lett.*, 59B:85–87, 1975.
- [14] Barry J. Harrington and Harvey K. Shepard. Periodic Euclidean Solutions and the Finite Temperature Yang-Mills Gas. *Phys. Rev.*, D17:2122, 1978.
- [15] Thomas C. Kraan and Pierre van Baal. Exact T duality between calorons and Taub-NUT spaces. *Phys. Lett.*, B428:268–276, 1998.
- [16] Thomas C. Kraan and Pierre van Baal. Monopole constituents inside $SU(n)$ calorons. *Phys. Lett.*, B435:389–395, 1998.
- [17] Ki-Myeong Lee and Chang-hai Lu. $SU(2)$ calorons and magnetic monopoles. *Phys. Rev.*, D58:025011, 1998.
- [18] M. Luscher. A Semiclassical Formula for the Topological Susceptibility in a Finite Space-time Volume. *Nucl. Phys.*, B205:483–503, 1982.
- [19] Gerard 't Hooft. Computation of the Quantum Effects Due to a Four-Dimensional Pseudoparticle. *Phys. Rev.*, D14:3432–3450, 1976. [Erratum: *Phys. Rev.* D18,2199(1978)].
- [20] David J. Gross, Robert D. Pisarski, and Laurence G. Yaffe. QCD and Instantons at Finite Temperature. *Rev. Mod. Phys.*, 53:43, 1981.
- [21] Curtis G. Callan, Jr., R. F. Dashen, and David J. Gross. The Structure of the Gauge Theory Vacuum. *Phys. Lett.*, 63B:334–340, 1976.
- [22] R. D. Pisarski and L. G. Yaffe. THE DENSITY OF INSTANTONS AT FINITE TEMPERATURE. *Phys. Lett.*, 97B:110–112, 1980.
- [23] Olivier Wantz and E. P. S. Shellard. Axion Cosmology Revisited. *Phys. Rev.*, D82:123508, 2010.

- [24] Sinya Aoki, Hidenori Fukaya, and Yusuke Taniguchi. Chiral symmetry restoration, eigenvalue density of Dirac operator and axial U(1) anomaly at finite temperature. *Phys. Rev.*, D86:114512, 2012.
- [25] Hidenori Fukaya. Can axial U(1) anomaly disappear at high temperature? In *35th International Symposium on Lattice Field Theory (Lattice 2017) Granada, Spain, June 18-24, 2017*, 2017.
- [26] Takuya Kanazawa and Naoki Yamamoto. U (1) axial symmetry and Dirac spectra in QCD at high temperature. *JHEP*, 01:141, 2016.
- [27] Ryuichiro Kitano and Norikazu Yamada. Topology in QCD and the axion abundance. *JHEP*, 10:136, 2015.
- [28] Evan Berkowitz, Michael I. Buchoff, and Enrico Rinaldi. Lattice QCD input for axion cosmology. *Phys. Rev.*, D92(3):034507, 2015.
- [29] S. Borsanyi, M. Dierigl, Z. Fodor, S. D. Katz, S. W. Mages, D. Nogradi, J. Redondo, A. Ringwald, and K. K. Szabo. Axion cosmology, lattice QCD and the dilute instanton gas. *Phys. Lett.*, B752:175–181, 2016.
- [30] Claudio Bonati, Massimo D’Elia, Marco Mariti, Guido Martinelli, Michele Mesiti, Francesco Negro, Francesco Sanfilippo, and Giovanni Villadoro. Axion phenomenology and θ -dependence from $N_f = 2 + 1$ lattice QCD. *JHEP*, 03:155, 2016.
- [31] Peter Petreczky, Hans-Peter Schadler, and Sayantan Sharma. The topological susceptibility in finite temperature QCD and axion cosmology. *Phys. Lett.*, B762:498–505, 2016.
- [32] Alessandro Laio, Guido Martinelli, and Francesco Sanfilippo. Metadynamics surfing on topology barriers: the CP^{N-1} case. *JHEP*, 07:089, 2016.
- [33] Hilmar Forkel. Direct instantons, topological charge screening and QCD glueball sum rules. *Phys. Rev.*, D71:054008, 2005.
- [34] Michael Dine, Patrick Draper, and Guido Festuccia. Instanton Effects in Three Flavor QCD. *Phys. Rev.*, D92(5):054004, 2015.

- [35] Jihn E. Kim and Gianpaolo Carosi. Axions and the Strong CP Problem. *Rev. Mod. Phys.*, 82:557–602, 2010.
- [36] C. Patrignani et al. Review of Particle Physics. *Chin. Phys.*, C40(10):100001, 2016.
- [37] Giovanni Grilli di Cortona, Edward Hardy, Javier Pardo Vega, and Giovanni Villadoro. The QCD axion, precisely. *JHEP*, 01:034, 2016.
- [38] Gregory Gabadadze and M. Shifman. QCD vacuum and axions: What’s happening? *Int. J. Mod. Phys.*, A17:3689–3728, 2002. [,521(2002)].
- [39] J. M. Pendlebury et al. Revised experimental upper limit on the electric dipole moment of the neutron. *Phys. Rev.*, D92(9):092003, 2015.
- [40] Z. Fodor, C. Hoelbling, S. Krieg, L. Lellouch, Th. Lippert, A. Portelli, A. Sastre, K. K. Szabo, and L. Varnhorst. Up and down quark masses and corrections to Dashen’s theorem from lattice QCD and quenched QED. *Phys. Rev. Lett.*, 117(8):082001, 2016.
- [41] David B. Kaplan and Aneesh V. Manohar. Current Mass Ratios of the Light Quarks. *Phys. Rev. Lett.*, 56:2004, 1986.
- [42] Michael Creutz. Quark mass dependence of two-flavor QCD. *Phys. Rev.*, D83:016005, 2011.
- [43] Michael Creutz. The ’t Hooft vertex revisited. *Annals Phys.*, 323:2349–2365, 2008.
- [44] Julien Frison, Ryuichiro Kitano, and Norikazu Yamada. $N_f = 1 + 2$ mass dependence of the topological susceptibility. *PoS, LATTICE2016:323*, 2016.
- [45] Frank Wilczek. Problem of Strong p and t Invariance in the Presence of Instantons. *Phys. Rev. Lett.*, 40:279–282, 1978.
- [46] Cumrun Vafa and Edward Witten. Parity Conservation in QCD. *Phys. Rev. Lett.*, 53:535, 1984.
- [47] Howard Georgi and Lisa Randall. Flavor Conserving CP Violation in Invisible Axion Models. *Nucl. Phys.*, B276:241–252, 1986.

- [48] Howard Georgi, David B. Kaplan, and Lisa Randall. Manifesting the Invisible Axion at Low-energies. *Phys. Lett.*, 169B:73–78, 1986.
- [49] R. J. Crewther. Chirality Selection Rules and the U(1) Problem. *Phys. Lett.*, 70B:349–354, 1977.
- [50] P. Di Vecchia and G. Veneziano. Chiral Dynamics in the Large n Limit. *Nucl. Phys.*, B171:253–272, 1980.
- [51] T. W. Donnelly, S. J. Freedman, R. S. Lytel, R. D. Peccei, and M. Schwartz. Do Axions Exist? *Phys. Rev.*, D18:1607, 1978.
- [52] S. Barshay, H. Faissner, R. Rodenberg, and H. De Witt. Coherent Conversion of Very Light Pseudoscalar Bosons. *Phys. Rev. Lett.*, 46:1361–1364, 1981.
- [53] Augusto Barroso and Nimai C. Mukhopadhyay. AXIONS: TO BE OR NOT TO BE? *Phys. Lett.*, 106B:91–94, 1981.
- [54] Lawrence M. Krauss and Frank Wilczek. A SHORTLIVED AXION VARIANT. *Phys. Lett.*, B173:189–192, 1986.
- [55] Georg G. Raffelt. Particle physics from stars. *Ann. Rev. Nucl. Part. Sci.*, 49:163–216, 1999.
- [56] Sz. Borsanyi et al. Calculation of the axion mass based on high-temperature lattice quantum chromodynamics. *Nature*, 539(7627):69–71, 2016.
- [57] Claudio Bonati, Massimo D’Elia, Marco Mariti, Guido Martinelli, Michele Mesiti, Francesco Negro, Francesco Sanfilippo, and Giovanni Villadoro. Recent progress on QCD inputs for axion phenomenology. *EPJ Web Conf.*, 137:08004, 2017.
- [58] Michael Dine, Patrick Draper, Laurel Stephenson-Haskins, and Di Xu. Axions, Instantons, and the Lattice. *Phys. Rev.*, D96(9):095001, 2017.
- [59] M. Shifman. *Advanced topics in quantum field theory*. Cambridge Univ. Press, Cambridge, UK, 2012.
- [60] Michael E. Peskin and Daniel V. Schroeder. *An Introduction to quantum field theory*. Addison-Wesley, Reading, USA, 1995.

- [61] Claude W. Bernard. Gauge Zero Modes, Instanton Determinants, and QCD Calculations. *Phys. Rev.*, D19:3013, 1979.
- [62] Gerald V. Dunne, Jin Hur, Choonkyu Lee, and Hyunsoo Min. Calculation of QCD instanton determinant with arbitrary mass. *Phys. Rev.*, D71:085019, 2005.
- [63] Barry J. Harrington and Harvey K. Shepard. Euclidean Solutions and Finite Temperature Gauge Theory. *Nucl. Phys.*, B124:409–412, 1977.
- [64] O-Kab Kwon, Choon-kyu Lee, and Hyunsoo Min. Massive field contributions to the QCD vacuum tunneling amplitude. *Phys. Rev.*, D62:114022, 2000.
- [65] V. A. Novikov, Mikhail A. Shifman, A. I. Vainshtein, and Valentin I. Zakharov. Calculations in External Fields in Quantum Chromodynamics. Technical Review. *Fortsch. Phys.*, 32:585, 1984.
- [66] Robert D. Carlitz and Dennis B. Creamer. Light Quarks and Instantons. *Annals Phys.*, 118:429, 1979.
- [67] M. Luscher. Dimensional Regularization in the Presence of Large Background Fields. *Annals Phys.*, 142:359, 1982.
- [68] T. R. Morris, D. A. Ross, and Christopher T. Sachrajda. Higher Order Quantum Corrections in the Presence of an Instanton Background Field. *Nucl. Phys.*, B255:115–148, 1985.
- [69] K. G. Chetyrkin, Bernd A. Kniehl, and M. Steinhauser. Decoupling relations to $O(\alpha_s^3)$ and their connection to low-energy theorems. *Nucl. Phys.*, B510:61–87, 1998.
- [70] Sinya Aoki. Field Theory on the lattice. (*Springer Verlag Japan*).
- [71] J. Frison, R. Kitano, H. Matsufuru, S. Mori, and N. Yamada. Topological susceptibility at high temperature on the lattice. *JHEP*, 09:021, 2016.
- [72] Kenneth G. Wilson. Confinement of Quarks. *Phys. Rev.*, D10:2445–2459, 1974. [,45(1974)].

- [73] Philippe de Forcrand, Margarita Garcia Perez, and Ion-Olimpiu Stamatescu. Topology of the SU(2) vacuum: A Lattice study using improved cooling. *Nucl. Phys.*, B499:409–449, 1997.
- [74] K. Symanzik. Continuum Limit and Improved Action in Lattice Theories. 2. O(N) Nonlinear Sigma Model in Perturbation Theory. *Nucl. Phys.*, B226:205–227, 1983.
- [75] K. Symanzik. Continuum Limit and Improved Action in Lattice Theories. 1. Principles and ϕ^4 Theory. *Nucl. Phys.*, B226:187–204, 1983.
- [76] P. Weisz and R. Wohlert. Continuum Limit Improved Lattice Action for Pure Yang-Mills Theory. 2. *Nucl. Phys.*, B236:397, 1984. [Erratum: *Nucl. Phys.*B247,544(1984)].
- [77] Herbert Neuberger. More about exactly massless quarks on the lattice. *Phys. Lett.*, B427:353–355, 1998.
- [78] Hidenori Fukaya, Shoji Hashimoto, Ken-Ichi Ishikawa, Takashi Kaneko, Hideo Matsufuru, Tetsuya Onogi, and Norikazu Yamada. Lattice gauge action suppressing near-zero modes of H(W). *Phys. Rev.*, D74:094505, 2006.
- [79] M. Okamoto et al. Equation of state for pure SU(3) gauge theory with renormalization group improved action. *Phys. Rev.*, D60:094510, 1999.
- [80] J. J. Giombi and K. D. Rothe. Regular n Instanton Fields and Singular Gauge Transformations. *Nucl. Phys.*, B129:111–124, 1977.
- [81] Bridge++ project website. <http://bridge.kek.jp/Lattice-code/>.
- [82] J. Engels, F. Karsch, and K. Redlich. Scaling properties of the energy density in SU(2) lattice gauge theory. *Nucl. Phys.*, B435:295–310, 1995.
- [83] Martin Lüscher. Properties and uses of the Wilson flow in lattice QCD. *JHEP*, 08:071, 2010. [Erratum: *JHEP*03,092(2014)].
- [84] Martin Luscher and Peter Weisz. Perturbative analysis of the gradient flow in non-abelian gauge theories. *JHEP*, 02:051, 2011.